

**EVALUATION AND UTILIZATION OF  
AIRPLANE FLIGHT LOADS DATA  
PART II. DATA ACQUISITION EQUIPMENT  
PERFORMANCE AND ACCURACY**

*PETER E. RENTZ*

*Measurement Analysis Corporation*

\*\*\* Export controls have been removed \*\*\*

This document is subject to special export controls and each transmittal to foreign governments or foreign nationals may be made only with prior approval of the Air Force Flight Dynamics Laboratory, FDTR, Wright-Patterson AFB, Ohio 45433.

FOREWORD

This final report was prepared by Measurement Analysis Corporation, Los Angeles, California, under Contract AF33(615)-67-C-1033. The contract was initiated under Project Number 1367, "Structural Design Criteria," Task No. 136716, "Techniques for the Evaluation of Vehicle Loads Data." The work was administered under the direction of the Air Force Flight Dynamics Laboratory, Wright-Patterson AFB, Ohio. Mr. E. Titus was the program monitor. Research performed under this contract has been part of a continuing effort to improve the evaluation and utilization of loads applied to the vehicle design and fatigue problem.

This report is published in two parts — Part I, "Techniques and Uncertainties," and Part II, "Data Acquisition Equipment Performance and Accuracy." Manuscripts for both parts were submitted by the authors in April 1968.

The author gratefully acknowledges the assistance of C. L. Gray and R. D. Kelly of the Measurement Analysis Corporation, and the cooperation of Messrs. C. Schmid and D. Simpkins of the Theoretical Mechanics Branch, Air Force Flight Dynamics Laboratory.

This technical report has been reviewed and is approved.



Francis J. Janik, Jr.  
Chief, Theoretical Mechanics Branch  
Structures Division  
Air Force Flight Dynamics Laboratory

## ABSTRACT

This report discusses the principles of operation and the various machine errors of airborne flight loads measuring equipment. The categories of equipment covered are angle of attack sensors, gyroscopes, accelerometers, strain gages, pressure transducers, signal conditioning equipment, and magnetic tape recorders. Machine errors are classified as being either intrinsic, environmentally induced, or attributable to usage or application. The errors are further classified in accordance with their effect on the measured data. The principles of operation and errors are expressed either with mathematical formulae or by indicating the state-of-the-art performance. Methods for minimizing both the errors and the effect of the errors are indicated.

# Contrails

## CONTENTS

1.	Introduction	1
2.	Instrumentation System and Error Classification	4
2.1	Data Acquisition System - General	4
2.1.1	Instrumentation Transducers	6
2.1.2	Analog Signal Conditioners	7
2.1.3	Recorder - Reproducers	7
2.2	Specific Instrumentation Systems	8
2.3	Error Classifications	14
3.	Pickoff Devices	17
3.1	General	17
3.2	Potentiometers	22
3.2.1	Intrinsic Errors, Potentiometers	22
3.2.2	Environmental Errors, Potentiometers	24
3.2.3	Usage Errors, Potentiometers	24
3.3	Variable Reluctance Pickoff	27
3.4	Differential Transformers	30
3.4.1	Intrinsic Errors, Differential Transforms	31
3.4.2	Usage Errors, Differential Transforms	32
3.5	Synchros	33
3.5.1	Intrinsic Errors, Synchros	33
3.6	Resolver	34
3.7	Microsyn	34
3.8	Variable Capacitance Pickoff	35
4.	Gust Input Measurement Transducers	36
4.1	Vanes and Probes	38
4.1.1	Moveable Vanes	38
4.1.2	Differential Pressure Probes	43
4.1.3	Fixed Vane Probes	49
4.2	Mounting Booms	51

## CONTENTS (Continued)

5.	Attitude and Angular Rate Measurement Transducers . . . . .	53
5.1	Gyroscope Errors . . . . .	54
5.1.1	Gyroscope Drift . . . . .	57
5.1.2	Nutation . . . . .	57
5.1.3	Nonlinearity . . . . .	58
5.1.4	Hysteresis and Resolution . . . . .	58
5.1.5	Gimbal Errors . . . . .	58
5.1.6	Gimbal Lock and Tumbling . . . . .	60
5.2	Free Gyroscopes . . . . .	60
5.3	Vertical Gyroscopes . . . . .	61
5.3.1	Intrinsic Errors, Vertical Gyroscopes . . . . .	61
5.3.2	Environmental Errors, Vertical Gyroscopes . . . . .	61
5.4	Rate Gyros . . . . .	62
5.4.1	Intrinsic Errors, Rate Gyroscopes . . . . .	64
5.4.2	Environmental Errors, Rate Gyroscopes . . . . .	65
5.4.3	Usage Errors, Rate Gyroscopes . . . . .	65
5.5	Rate Integrating Gyroscopes . . . . .	66
5.6	Stable Platforms . . . . .	67
6.	Accelerometers . . . . .	69
6.1	Variable Reluctance, Potentiometer, Strain Gage, and Piezoresistive Accelerometers . . . . .	73
6.1.1	Intrinsic Errors — Variable Reluctance, Potentiometer, Strain Gage, and Piezoresistive Accelerometers . . . . .	76
6.1.2	Environmental Errors — Variable Reluctance, Potentiometer, Strain Gage, and Piezoresistive Accelerometers . . . . .	79
6.1.3	Usage Errors — Variable Reluctance, Potentiometer, Strain Gage, and Piezoresistive, Servo and Piezoelectric Accelerometers . . . . .	81

CONTENTS (Continued)

6.2	Servo Accelerometers	88
6.2.1	Intrinsic Errors, Servo Accelerometers	90
6.2.2	Environmental Errors, Servo Accelerometers	91
6.2.3	Usage Errors, Servo Accelerometers	92
6.3	Piezoelectric (Quartz) Accelerometers	92
7.	Strain Gages	96
7.1	Conventional Strain Gages	97
7.1.1	Intrinsic Errors, Conventional Strain Gages	104
7.1.2	Environmental Errors, Conventional Strain Gages	109
7.1.3	Usage Errors, Conventional Strain Gages	112
7.2	Semiconductor Strain Gages	116
7.2.1	Intrinsic Errors, Semiconductor Strain Gages	117
7.2.2	Environmental Errors, Semiconductor Strain Gages	119
7.2.3	Usage Errors, Semiconductor Strain Gages	121
8.	Pressure Transducers	122
8.1	Intrinsic Errors, Pressure Transducers	125
8.2	Environmental Errors, Pressure Transducers	128
8.3	Usage Errors, Pressure Transducers	129
9.	Signal Conditioning Equipment	131
9.1	Excitation Supplies	131
9.2	Cabling	133
9.3	Demodulators	135
9.4	Low Pass Filters	136
9.4.1	Intrinsic Errors, Low Pass Filters	137

## CONTENTS (Continued)

9.5	Wheatstone Bridge Circuit . . . . .	137
9.5.1	Intrinsic Errors, Wheatstone Bridge Circuit . . . . .	138
9.5.2	Usage Errors, Wheatstone Bridge Circuits . . . . .	142
9.5.3	Environmental Errors, Wheatstone Bridge Circuit . . . . .	148
9.6	AC Bridges . . . . .	149
9.7	Amplifiers . . . . .	149
9.7.1	Amplifier Errors . . . . .	151
9.8	Other Strain Gage Circuits . . . . .	151
9.8.1	Dual Voltage Source . . . . .	152
9.8.2	Dual Current Source . . . . .	152
9.8.3	Wheatstone Bridge — Constant Gage Current . . . . .	154
9.8.4	Common Excitation . . . . .	154
10.	Magnetic Tape Recorders . . . . .	156
10.1	Classification of Recorders . . . . .	156
10.1.1	Analog and Digital . . . . .	156
10.1.2	Tape Motion . . . . .	158
10.1.3	Modulation . . . . .	158
10.1.4	Commutation . . . . .	158
10.1.5	Formatting . . . . .	159
10.2	Relative Advantages . . . . .	162
10.3	Tape Recorder Components . . . . .	167
10.4	Record and Readout Subsystem . . . . .	167
10.4.1	Errors, Record and Readout Subsystem . . . . .	171

CONTENTS (Continued)

10.5	Tape Transport Subsystem .....	175
10.5.1	Intrinsic Errors, Tape Transport Subsystem .....	177
10.5.2	Environmental Errors, Tape Transport Subsystem .....	180
10.5.3	Usage Errors, Tape Transport Subsystem ...	181
10.6	Modulation-Demodulation Subsystem .....	182
10.6.1	Pulse Amplitude Modulation .....	184
10.6.2	Frequency Modulation .....	185
10.6.3	Pulse Duration Modulation .....	185
10.6.4	Pulse Code Modulation .....	187
10.6.5	Errors in Modulation .....	187
10.7	Analog-To-Digital Converters .....	187
References	.....	189
Appendix - Frequency Response of Single Degree-of-Freedom Transducers		197



## LIST OF SYMBOLS

$a_v$	relative acceleration, vane—accelerometer, feet/sec <sup>2</sup>
$A$	area, feet <sup>2</sup>
$b$	dimension
$c$	coefficient of viscous damping, lbs-sec/feet
$C_a$	accelerometer capacitance, picofarads
$C_c$	cable capacitance, picofarads
$C_i$	input capacitance, picofarads
$C_t$	total capacitance, picofarads
$C_f$	feedback capacitance, picofarads
$C$	constant
$C_L$	coefficient of lift
$C_{FR}$	figure of merit relating frequency and full scale range
$d$	diameter, inch
$e_{cm}$	ground loop or common mode potential, volts
$e_i$	excitation potential, volts
$e_o$	output potential, volts
$e_r$	reference potential, volts
$E$	Young's modulus of elasticity, pounds/inch <sup>2</sup>

## LIST OF SYMBOLS (Continued)

$f_c$	carrier frequency, Hertz
$f_d$	data frequency, Hertz
$f_n$	undamped natural frequency, Hertz
F	force
g	acceleration of gravity, 32.14 feet/sec <sup>2</sup>
$g_{FS}$	full scale range, "g's"
h	dimension
H	angular momentum, foot pound second/radian
H(f)	frequency response function
$i_i$	excitation current, ampere
$i_r$	reference current, ampere
$I_o$	moment of inertia about output axis, slug/feet <sup>2</sup>
$I_s$	moment of inertia about spinaxis, slug/feet <sup>2</sup>
$I_{ig}$	moment of inertia of inner gimbal and gyro about inner axis, slug/feet <sup>2</sup>
$I_{og}$	moment of inertia of inner gimbal, gyro, and outer gimbal about outer axis, slug/feet <sup>2</sup>
j	$\sqrt{-1}$
K	strain sensitivity or gage factor, dimensionless

## LIST OF SYMBOLS (Continued)

$K_a$	amplifier transfer function, dimensionless
$K_e$	accelerometer voltage sensitivity, volts/g
$K_f$	force coil transfer function, pounds/ampere
$K_p$	pickoff transfer function, dimensionless
$K_q$	accelerometer charge sensitivity, picocoulombs/g
$k$	potentiometer fractional deflection
$k$	spring constant, lbs/feet
$L$	inductance, henrys
$l_i$	primary inductance, henrys
$l_x$	constant length between acceleration measurement and angle of attack measurement, feet
$l$	moment arm length, feet
$l$	dimension
$l_1$	zero strain length or original length
$l_2$	length after strain applied
$m$	mass, slugs
$m$	modulation index, dimensionless
$M$	mach number
$M$	mutual inductance, henrys

## LIST OF SYMBOLS (Continued)

$n$	number of potentiometer windings
$n$	number of code symbols per data input
$N$	hysteresis expressed in terms of full scale
$n$	number of active gages
$p$	Laplace operator, $A + jB$
$P$	pressure, pounds/inch <sup>2</sup>
$P_s$	static pressure, pounds/inch <sup>2</sup>
$q$	dynamic pressure, pounds/feet <sup>2</sup>
$R_a R_b$	partial potentiometer resistances, ohms
$R_B$	bridge balance series resistor resistance, ohms
$R_C$	standardization or calibration resistor resistance, ohms
$R_D$	voltage dropping resistor resistance, ohms
$R_f$	feedback resistance, ohms
$R_g$	gage resistance, ohms
$R_{gl}$	ground loop resistance, ohms
$R_h$	gage resistance, no load, after three complete cycles of plus and minus strain, ohms
$R_i$	input resistance, ohms
$R_i$	primary resistance, ohms

## LIST OF SYMBOLS (Continued)

$R_{iw}$	wire resistance, input ohms
$R_l$	load resistor resistance, ohms
$R_L$	lead wire resistance, ohms
$R_m$	modulus compensation resistor resistance, ohms
$R_{max}$	gage resistance, full scale strain, ohms
$R_o$	wire resistance, output, ohms
$R_0$	upstrained gage resistance, ohms
$R_p$	potentiometer resistance, ohms
$R_s$	shunt resistor resistance, ohms
$S$	stress, psi
$t$	time, seconds
$T$	temperature, $^{\circ}F$
TCR	temperature coefficient of resistance, $1/^{\circ}G$
TCGF	temperature coefficient of gage factor
$v$	volume, feet <sup>3</sup>
$V$	velocity, feet/sec
$V_s$	sound velocity, feet/sec
$w_g$	gust velocity (vertical), feet/sec

## LIST OF SYMBOLS (Continued)

x	displacement
y	displacement
z	displacement
$\alpha$	angle of attack, radians
$\beta$	angle, radians
$\gamma$	angular displacement, radians
$\Delta ( )$	change in a parameter or variable ( )
$\Delta$	output
$\delta_s$	coefficient of thermal expansion of test specimen, $1/^\circ\text{F}$
$\delta_g$	coefficient of thermal expansion of the gage, $1/^\circ\text{G}$
$\epsilon$	strain or unit deformation, nondimensional
$\epsilon_T$	strain transverse to the sensitive axis
$\zeta$	damping factor, dimensionless
$\theta$	angle, radians
$\Theta$	aircraft attitude, referenced to earth, radians
$\lambda$	percent response to transverse inputs
$\lambda$	wavelength, inches
$\mu$	Poisson's ratio
$\mu$	viscosity, slug/feet-sec

## LIST OF SYMBOLS (Continued)

$\rho$	resistivity, ohms-inch
$\rho$	air density, slugs/feet <sup>3</sup>
$\eta$	angular displacement, radians
$\tau$	time delay, seconds
T	torque, feet-pound
$\phi$	input angle, radians
$\phi$	misalignment angle, radians
$\phi(f)$	phase lag, radians
$\Omega$	angular velocity, radians/sec
$\psi$	constant

### Operations

F(f)	Function of frequency
F(t)	Function of time or instantaneous value of F
$\dot{\quad}$	Time derivative
$\hat{\quad}$	Total or summation
F(p)	Laplace Transform of F(t)

# *Contrails*



## 1. INTRODUCTION

The measurement of actual flight and ground loads data has traditionally been an integral part of aircraft structural development programs. Loads measurements usually begin with an early experimental prototype of a new design and continue well into the operational phase of development. During this time, a variety of data acquisition equipment is required to satisfy continually changing measurement objectives. This report is concerned with many of the basic types of instruments suitable for use in flight loads data acquisition, and the various aspects of their performance and accuracy.

Structural loads for an aircraft are usually interpreted by the designer as the bending moments, shears, and torques which result from aerodynamic and inertia forces. In this context, the loads are considered a response to a variety of inputs. However, to other analysts, the inertia and aerodynamic forces are themselves called loads. In view of the many facets of this problem, the term "loads" is applied broadly throughout this report, and interpretation of the meaning for specific applications is left to the reader.

The scope of this report has been limited to discussions of those instrumentation systems used for the acquisition of steady and unsteady aerodynamic environmental data, and aircraft static and dynamic response data. These data represent essentially low frequency phenomena which can be evaluated effectively within the range 0 to 50 Hz. Therefore, discussions of general performance and specific machine errors of the measurement equipment will refer to this low frequency range.

# Contrails

The report is also limited to those instrumentation systems which record the data onboard the aircraft. However, much of the material concerning tape recorder technology is applicable to telemetry.

The purpose of this report is to review the principles of operation and present expressions for the machine errors of flight loads measuring and recording equipment. The scope of flight loads recording is covered in the preceding paragraphs. Machine errors are defined as errors in a measurement of any function which can be attributed to imperfections in the design, manufacturing, or use of equipment. This excludes human errors such as improper reading or interpretation of measurements and statistical errors resulting from analyzing finite samples of random processes. Where feasible, mathematical expressions have been used to describe or give an upper bound to the particular error. In those cases where the error expression is unknown or too complex to be useful, the state-of-the-art performance is indicated. An example is accelerometer cross axis sensitivity.

The application of the given error expressions depends on the amount of information available. If all the variables in a bias error expression are known, an error correction to the measurement can be made. However, if only the distribution of the magnitudes of the variables in a bias error expression are known or if the errors are random, an uncertainty in the measurement exists and only error bounds or confidence intervals can be determined. Another use of the error expressions is to determine necessary equipment performance required to attain a given overall measurement accuracy.

The report is organized by equipment type. Section 2 discusses the types of systems used for flight loads measurement and the classification

# *Contrails*

of errors. Section 3 covers pickoff devices which are common to various transducers. Sections 4 through 8 analyze the types of transducers used. Section 9 covers signal conditioners. Section 10 discusses tape recorders. Appendix A develops the frequency response expressions for the various transducers.

## 2. INSTRUMENTATION SYSTEM AND ERROR CLASSIFICATION

### 2.1 DATA ACQUISITION SYSTEMS - GENERAL

A flight loads measurement instrumentation or data acquisition system may be represented, in general, as being composed of three types of components, as follows:

1. Instrumentation Transducer
2. Signal Conditioner
3. Recorder - Reproducer

These components are shown in block diagram in Figure 2-1. This figure also shows instrumentation transducers and recorders represented as two series of subcomponents. The reason for dividing these components into smaller functional elements is that various performance limitations and errors are attributable to particular subcomponents. Therefore, a better understanding of the error process is achieved when the error is assigned to the process involved. For example, when considering instrumentation transducers, deviations from ideal frequency response are usually attributable to the conversion from the physical quantity being measured to an intermediate mechanical quantity. For magnetic tape recording, the upper frequency limitation is dependent primarily upon a number of parameters associated with the three elements of the magnetization-reproduction process.

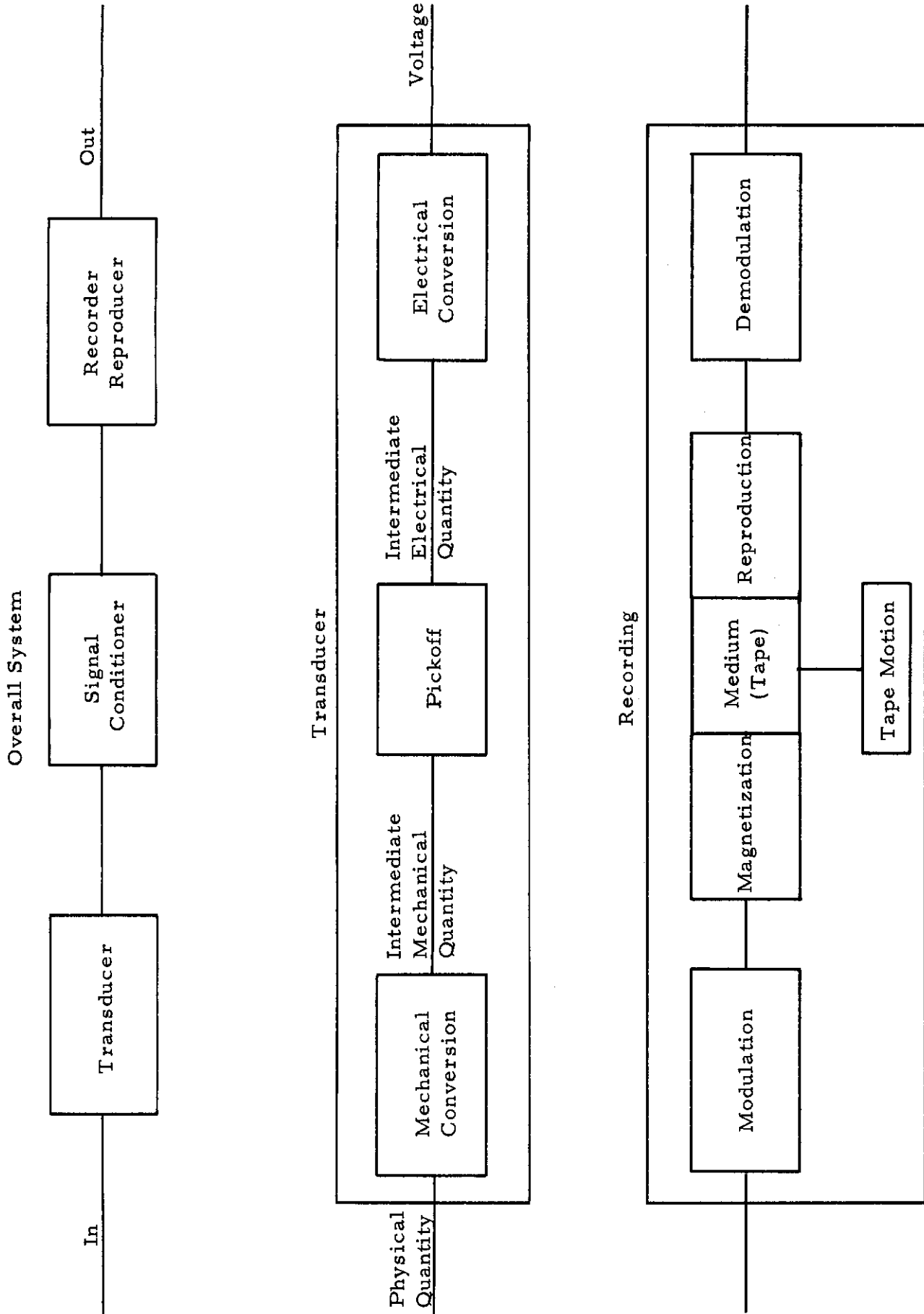


Figure 2.1. General Data Acquisition System Block Diagram

## 2.1.1 Instrumentation Transducers

Instrumentation transducers can be defined as devices which convert physical phenomena into electrical signals for the purpose of measurement. This implies that a definable, useful relationship or proportionality exists between the property being measured and the electrical signal. In order to make this conversion, the transducing element may utilize either an active energy converting principle such as the thermoelectric effect of thermocouples or an energy controlling effect such as thermoresistance. Over twenty such physical effects are utilized in instrumentation transducers (Reference 1, page 8). However, some physical properties, such as acceleration and angular rate, are not easily converted directly into electrical signals. In these instances, the typical transducer functions by first converting the quantity to be measured (acceleration, pressure, etc.) to a measurable quantity such as relative displacement or force (see Figure 2-1). The relative displacement or force is converted to a change in an intermediate electrical quantity (resistance, capacitance, etc.) by a pickoff. Typical pickoff devices are potentiometers, strain gages, and variable inductors. Since the different types of pickoff devices are common to transducers covered in this report, their principles of operation and associated errors are discussed separately in Section 3. The final conversion is to an electrical voltage which has a calibrated relationship with the original physical quantity and, if the transducer is ideal, is independent of all other physical inputs. Some transducers are designed to operate without performing all three steps. Electrodynamic transducers generate a voltage proportional to relative velocity, thus combining the pickoff and electrical conversion. Thermocouples produce a voltage proportional to a temperature difference and therefore combine all three steps into one.

## 2.1.2 Analog Signal Conditioners

In this report, components between the transducer and recording units are considered analog signal conditioning equipment. Auxiliary equipment is included. For example, power supplies for amplifiers and electric motors have been categorized as signal conditioning equipment. Signal conditioning equipment usually performs a single particular function and no breakdown into subcomponents is proposed (see Figure 2-1).

## 2.1.3 Recorder - Reproducers

Recorders are those devices used to store data, usually for subsequent analysis. The types or classes of recorders covered in this report are limited to analog and digital magnetic tape recording devices. Reproduction of the data signal is covered in the same section as recording. The subcomponents of a recorder are categorized as indicated in Figure 2-1, as follows:

1. Modulation and Demodulation
2. Magnetization and Reproduction
3. Tape Motion

A detailed discussion of these elements is presented in Section 10. Briefly, the underlying magnetization and reproduction process is common to all types of recording. This process employs a record head, ferromagnetic tape and a reproduce head. The tape motion element or subsystem provides the means of recording a signal as a function of time. The basic recording process usually has unacceptable frequency response and signal to noise specifications. In these instances, the signal is coded or modulated. The result is improved performance at the expense of data bandwidth. In this report, commutators and analog-to-digital recorders are grouped with digital recorders because of the similarity and interdependence of the equipment errors.



## 2.2 SPECIFIC INSTRUMENTATION SYSTEMS

The instrumentation systems employed for the determination of aircraft flight loads may be broken down into those required for the following measurements:

1. Gust velocity measurement
2. Attitude and angular rate measurement
3. Acceleration measurement
4. Strain measurement
5. Static and fluctuating pressure measurement
6. Aircraft flight parameter measurement  
(altitude, airspeed, Mach number)

Typical block diagrams of systems for performing measurements (1) through (5) above are presented in Figures 2-2 through 2-6, respectively. The components of each of the systems are categorized as either transducing, signal conditioning, or recording elements. Some components are used for more than one measurement system. Most analog signal conditioning elements and all recording elements are identical for all of the measurement systems. Their principles of operation and associated errors are covered separately.

Instruments which are unique to aircraft flight parameter measurement (pitot tubes, altimeters, air data computers) are not covered. Some flight parameter measurement components (pressure transducers, signal conditioning and recording equipment) are common to other systems which are covered.



Recorders

Analog Signal Conditioners

Transducers

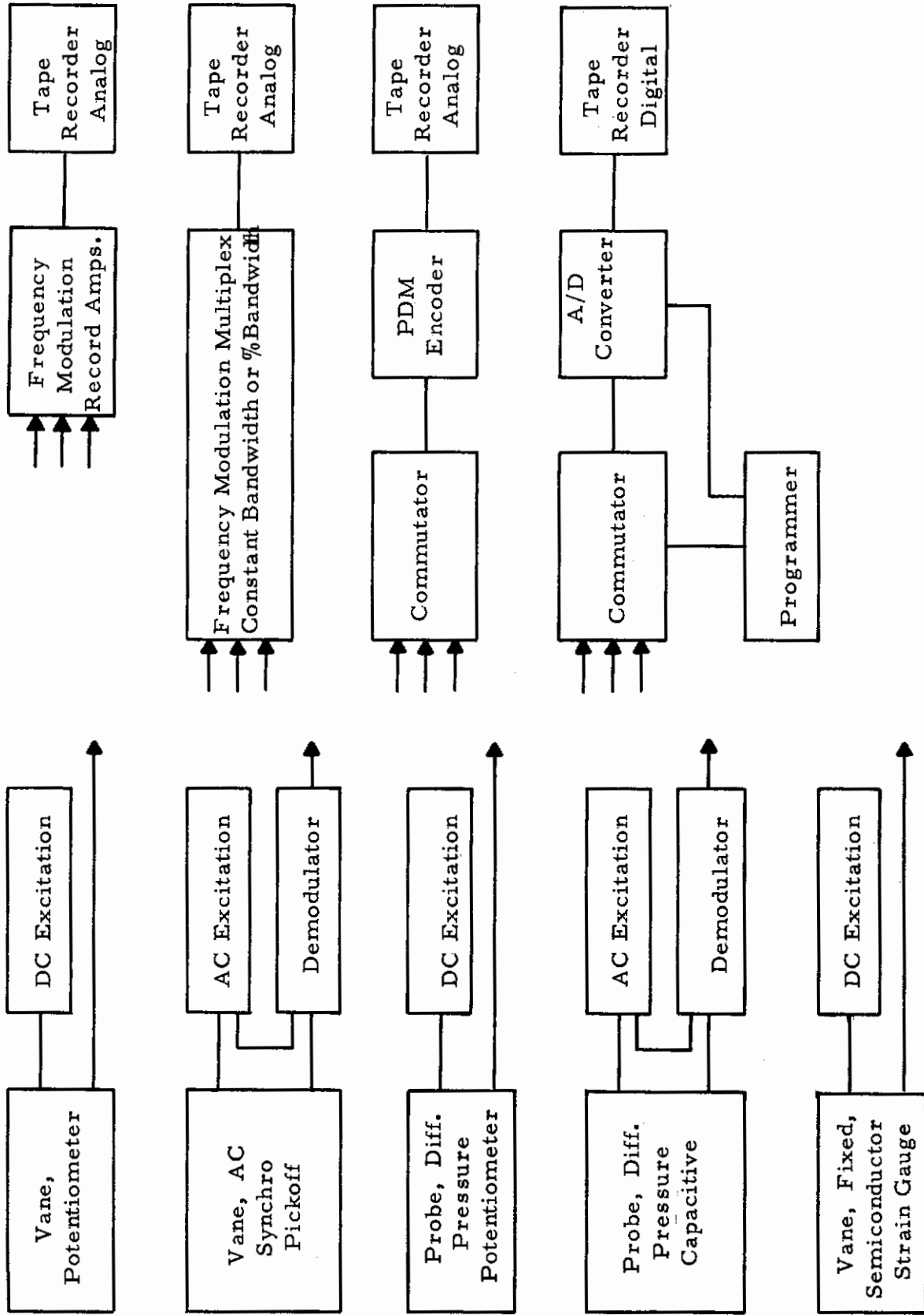


Figure 2-2. Angle of Attack Measurement and Recording Systems

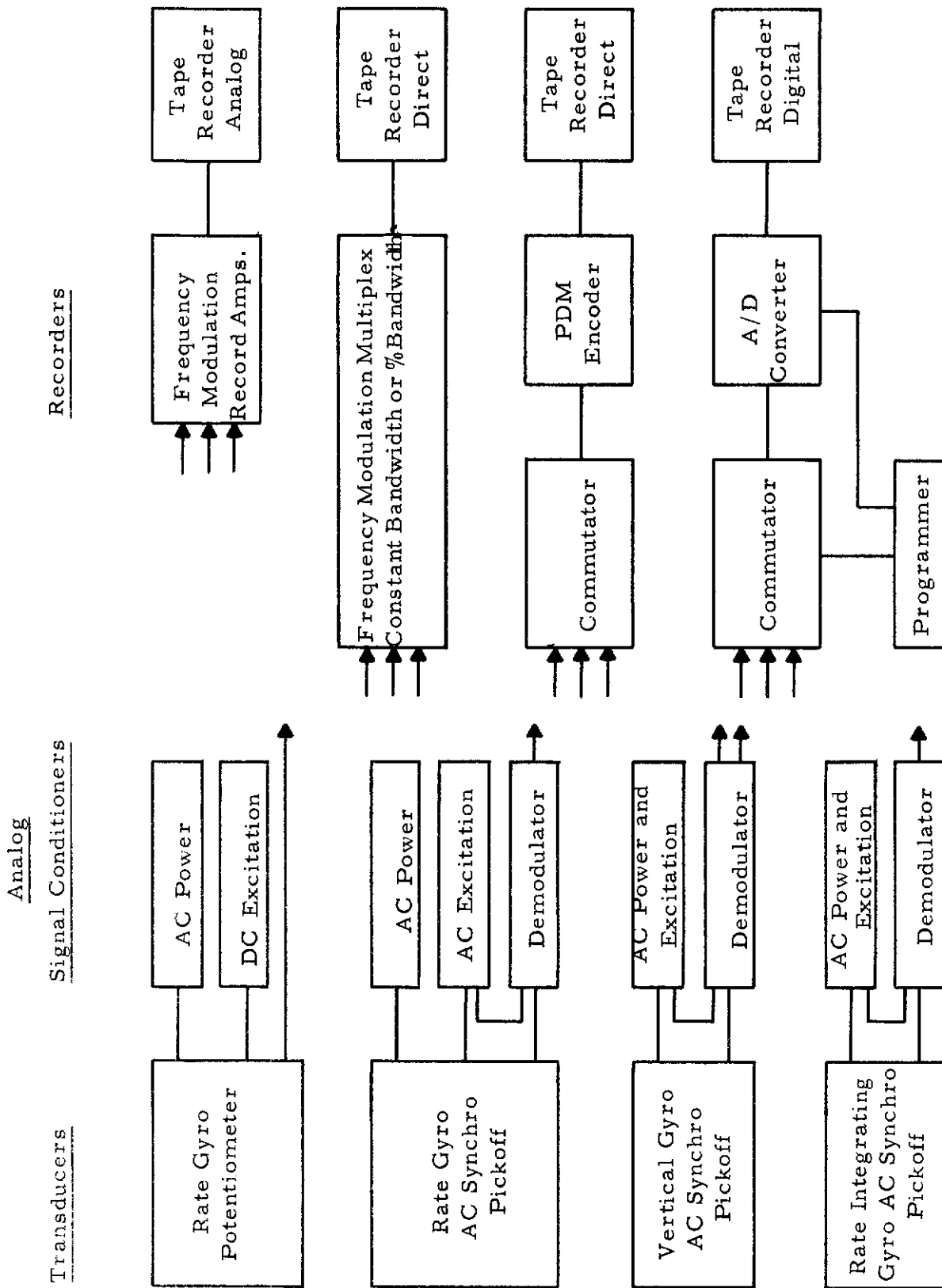


Figure 2-3. Attitude and Angular Rate Measurement and Recording Systems

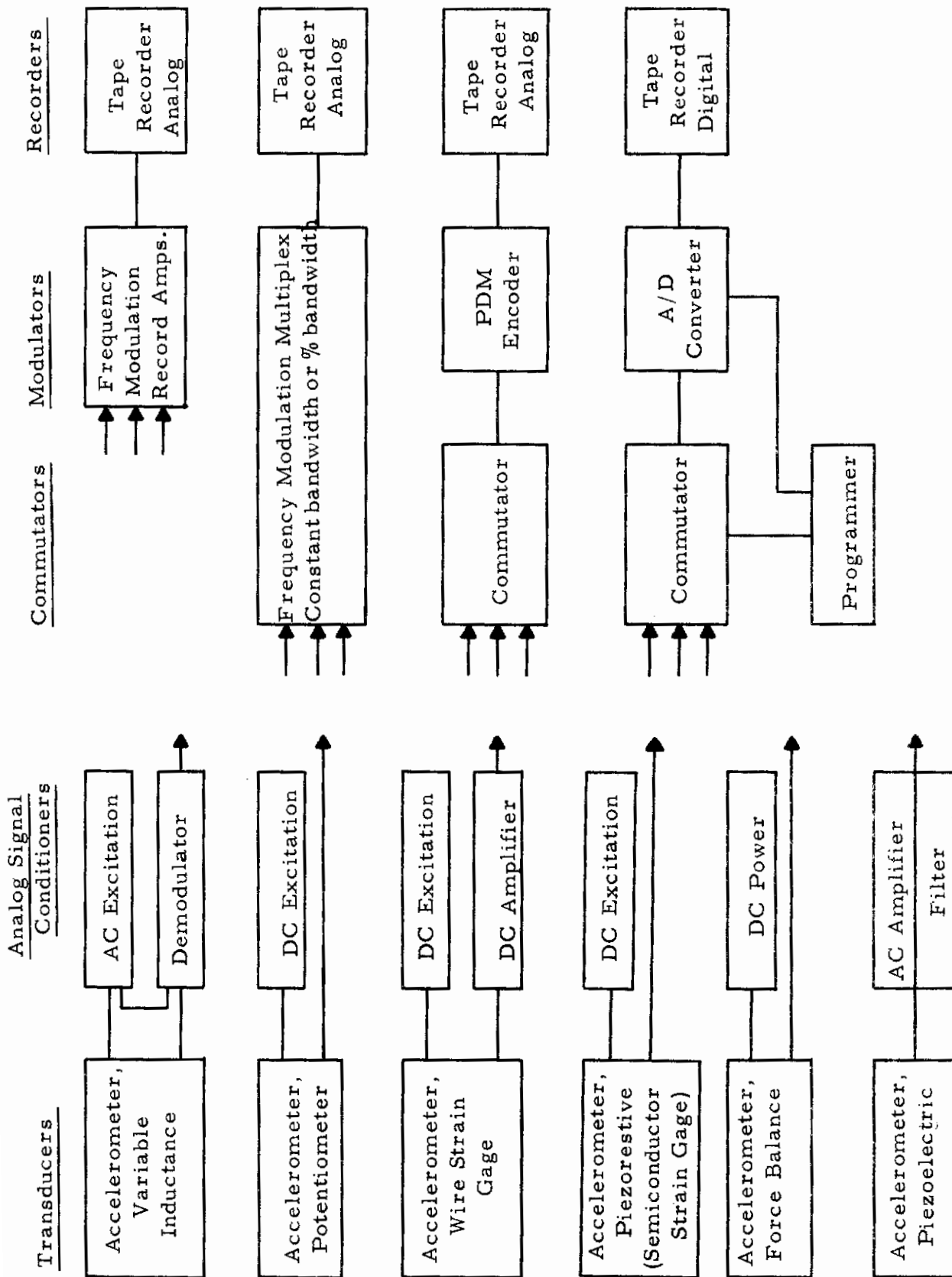


Figure 2-4. Acceleration Measurement and Recording Systems

Recorders

Analog Signal Conditioners

Transducers

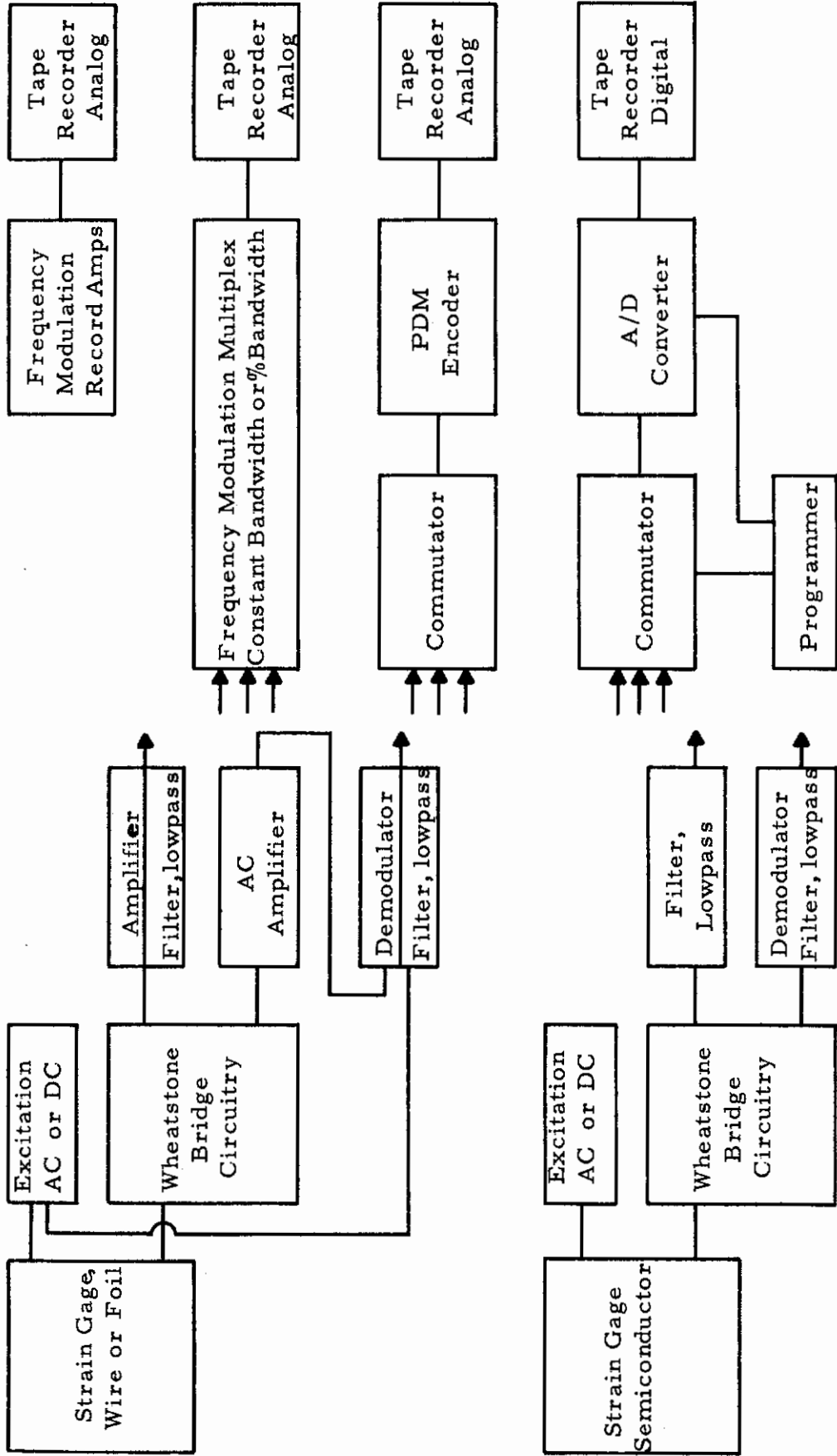


Figure 2-5. Strain Measurement and Recording Systems

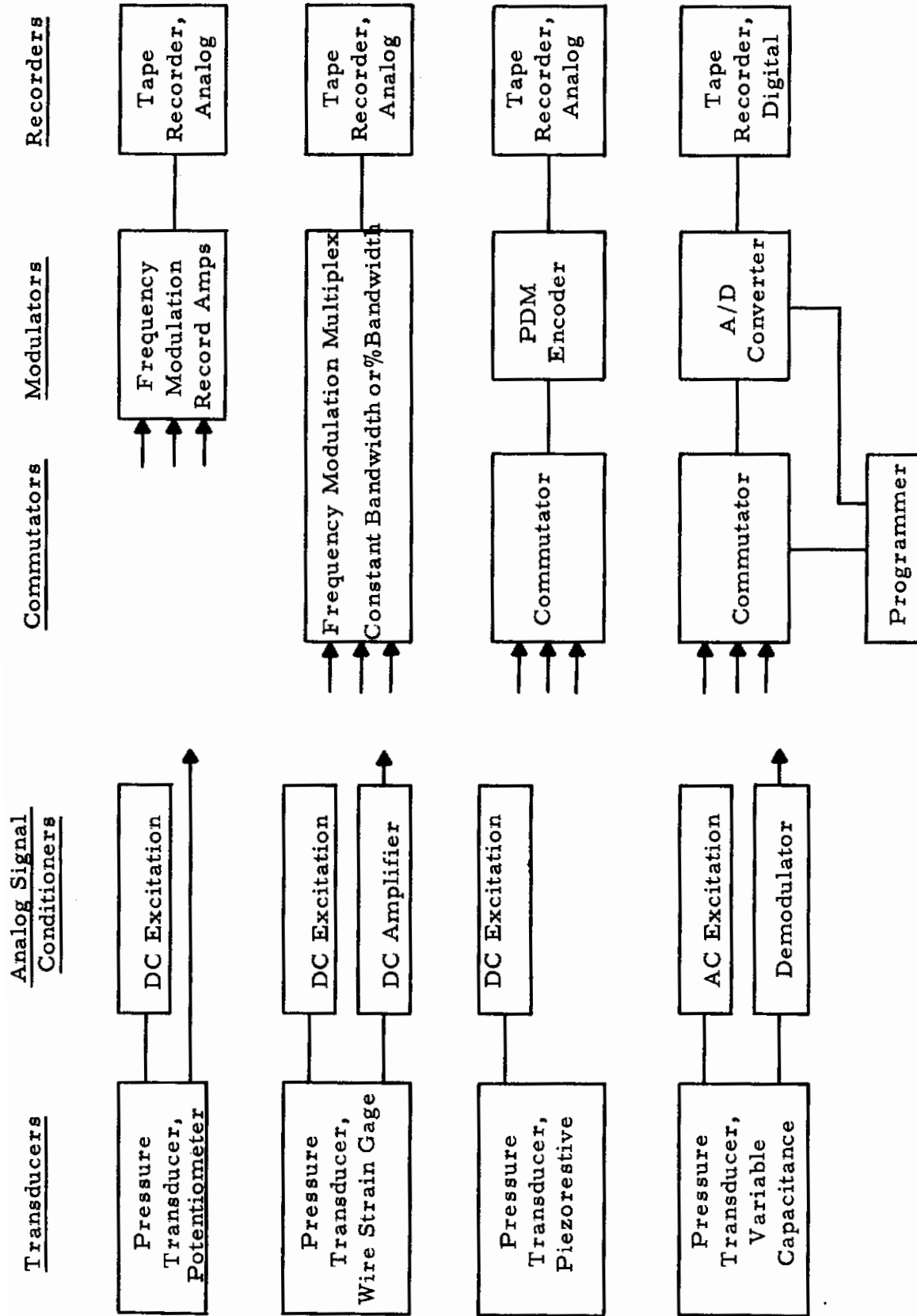


Figure 2-6. Pressure Measurement and Recording Systems

## 2.3 ERROR CLASSIFICATIONS

In order to systematically approach the problem of describing machine errors, various classifications of errors are useful. In this report, machine errors are first classified as either intrinsic, environmental, or usage (see Figure 2-7). Intrinsic errors are those which are inherent in the design of the particular equipment. A typical intrinsic error is the deviation from a constant frequency response of a transducer in ideal environmental conditions. Environmental errors are those variations from nominal performance which are attributable to a change in the environment from the ideal. A typical environmental error is the change in frequency response due to the temperature dependent variation of viscosity of the damping fluid of transducers. Usage errors are those which are attributable to improper application of a particular equipment. Calibration errors are included as usage errors. Another typical usage error is the incorrect response of an accelerometer due to installation on a relatively flimsy structure.

Errors may be also broadly classed as being either bias errors or random errors (see Figure 2-7). Bias errors are those which have a constant or systematic effect on measurement. For example, it can be said that extraneous noise will always tend to increase the power of a data signal. Random errors are those which can cause variations in data that can only be predicted on the basis of probability. Thus, the instantaneous voltage of a data signal which includes extraneous noise will have a random error tending either to increase or decrease the voltage. In this report, those errors which are clearly either random or bias are not identified.

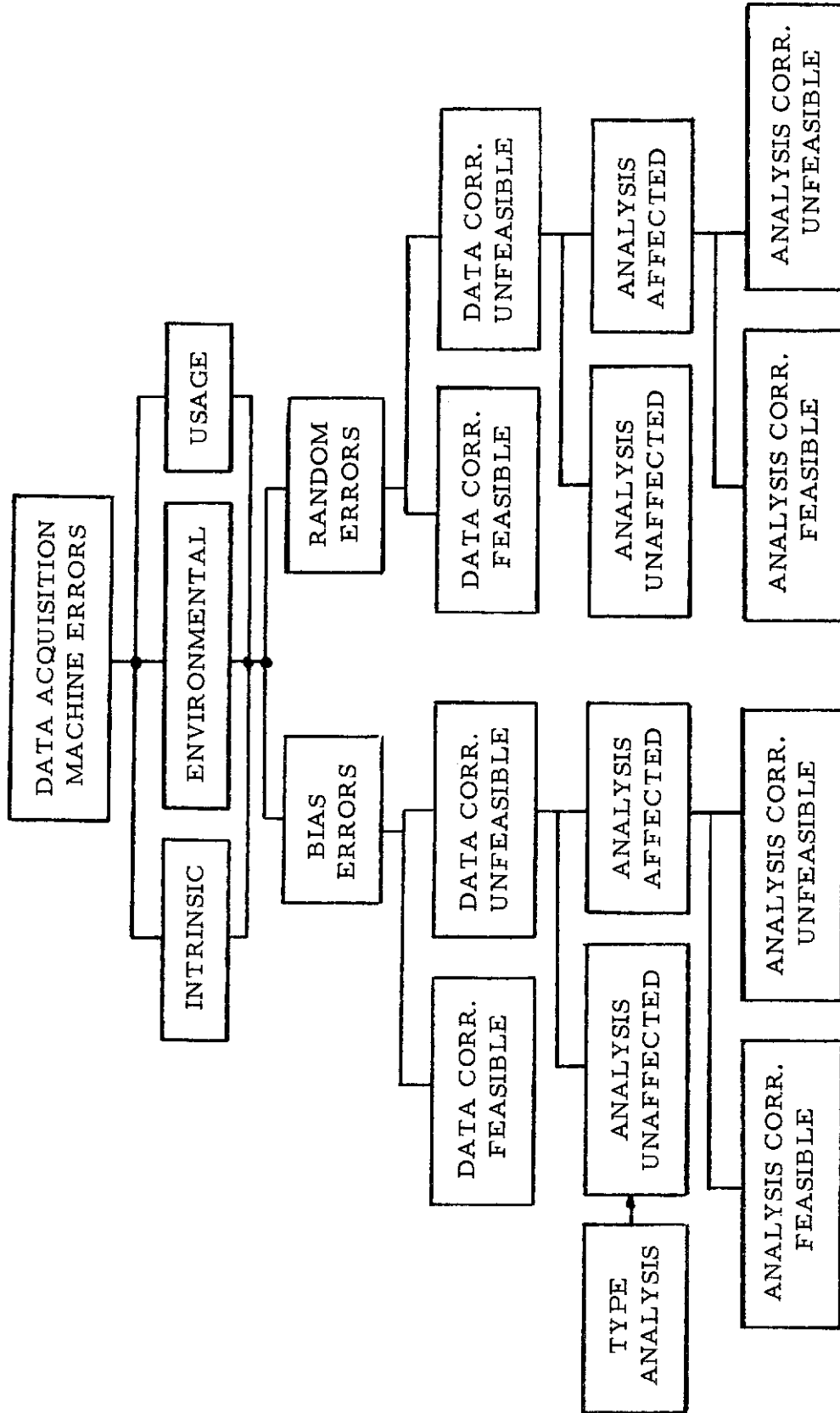


Figure 2-7. Classification of Machine Errors Depending on Type Analysis

# Contrails

A final criterion for evaluating an error is related to the effect it has on the analyzed results of the measurement. Therefore, to complete the classification of machine errors, two categories have been added which differentiate between errors that can be corrected after analysis and those which cannot. An example of the classification of an error is as follows:

The temperature effect on the sensitivity of a strain gage is an environmental bias error. If the temperature is known as well as the effect of temperature on sensitivity, the data time history may be corrected. If the temperature is unknown, data correction is unfeasible and the effect depends on the analysis to be performed. If probability density of the temperature record is to be determined, the analysis is unaffected by a constant sensitivity variation. However, the power spectral density is directly affected. The uncertainty about the effect of temperature on the strain measurement is then a random error. Because of the quantity of combinations involved, the complete classification of even this one simple error is not feasible. However, when analyzing a particular instrumentation system, the errors should be classified in accordance with the type of analysis performed.



## 3. PICKOFF DEVICES

### 3.1 GENERAL

Many transducers function by converting the physical quantity to be measured to a relative displacement which may be sensed with a pickoff device. Different types of pickoff devices are employed to sense either angular or linear relative displacement. Since these devices are common to a number of transducers, their principles of operation and machine errors have been grouped or arranged in this section.

The types of transducers covered, along with their wiring schematics, their input-output relationships, and their major advantages and disadvantages, are listed in Table 3-1. Some special types which are commonly used are covered in other sections. The piezoelectric effect is discussed briefly in the section on accelerometers. Strain gages are covered in Section 7 of this report.

For a comprehensive review of the design considerations of various pickoff devices, see Reference 1. References 2 and 3 contain thorough discussions of the various types of pickoff devices, including many practical aspects. For a discussion of the principles of operation of synchros, resolvers, and microsyns, see References 15 and 16. Reference 4, page 51, presents a practical review of differential transformers, synchros, and resolvers. The applications of these pickoff devices in transducers for experimental flight loads measurement programs are indicated in Table 3-2. This table also presents minimum and maximum full scale displacement ranges for typical units. The pickoff full scale range strongly influences the size and natural frequency of the resulting transducer.

Table 3-1. Comparison of Pickoff Characteristics

Type Pickoff	Schematic	Output Characteristics	Major Advantages	Major Disadvantages
Potentiometer Wirewound			Simplicity Linear, unmodulated output with dc excitation High sensitivity Large range	Wiper friction Wiper wear Wiper bounce Poor resolution
Variable Reluctance			High resolution No brushes Low friction	Nonlinear at large displacements Low sensitivity Large moving mass Modulated output with ac excitation
Differential Transformer or "E Transformer"			Good resolution No brushes Low friction	Nonlinear at large displacements Nonpolarized Large moving mass Modulated output

Table 3-1. Comparison of Pickoff Characteristics (continued)

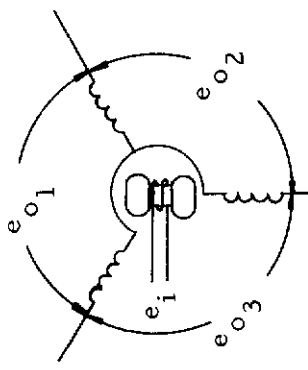
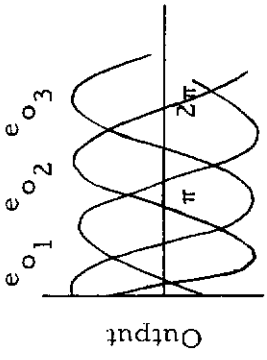
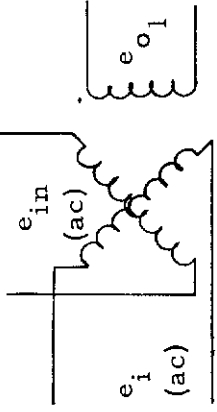
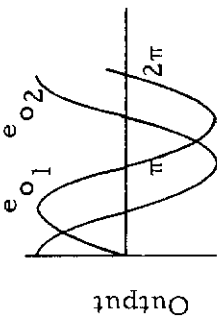
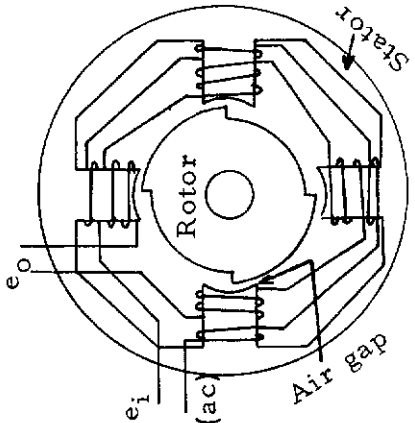
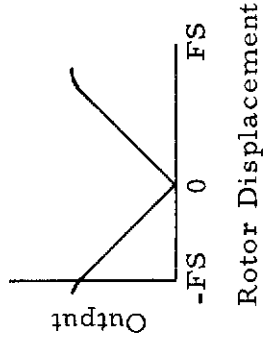
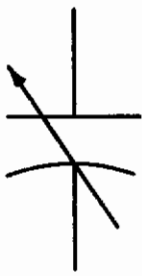
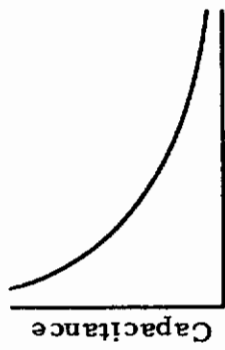
Type Pickoff	Schematic	Output Characteristics	Advantages	Disadvantages
Synchro		 <p style="text-align: center;">Rotor Displacement</p>	Large displacements	Demodulation reqd. Brushes reqd. Output $\approx \sin \theta$ , not $\theta$ Modulated output with ac excitation
Resolver		 <p style="text-align: center;">Rotor Displacement</p>	Large displacements	Brushes required Output $\approx \sin \theta$ , $\cos \theta$ , not $\theta$ Modulated output with ac excitation
Microsyn		 <p style="text-align: center;">Rotor Displacement</p>	High sensitivity Excellent linearity No brushes	Nonlinear at large displacements Nonpolarized Complex Modulated output with ac excitation

Table 3-1. Comparison of Pickoff Characteristics (continued)

Type Pickoff	Schematic	Output Characteristics	Advantages	Disadvantages
Variable Capacitance			<p>Non-contacting High sensitivity Small moving mass High resolution</p>	<p>Nonlinear Demodulation req'd. if ac excitation is used, no dc response if dc excitation used Small range</p>

*Continued*

Table 3-2. Applications of Relative Displacement Pickoff Devices

Type Pickoff	Full Scale Range	Transducer Application						
		Movable Vanes	Free Gyro	Vertical Gyro	Rate Gyro	Rate Integrating Gyro	Accel.	Pressure Transducer
Potentiometer	0.1 - 200 in.	✓	✓	✓	✓	✓	✓	✓
Variable Reluctance	0.1 - 200 in.						✓	✓
Differential Transformer	0.005-3in, $\pm 40-60^\circ$				✓		✓	
Synchro	$\pm 60 - 90^\circ$	✓	✓	✓			✓	
Resolver	$\pm 45^\circ$			✓				
Microsyn	$\pm 7 - 10^\circ$						✓	
Variable Capacitance	$0.5 \times 10^{-4} - 0.5\text{in.}$							✓
Strain Gages	$10^{-4} - 10^{-3}$ in.							✓

## 3.2 POTENTIOMETERS

Instrumentation quality potentiometer pickoffs usually consist of wire wound around an insulated support or bobbin and a wiper arm (see Table 3-1). When an excitation voltage is applied to the windings, the voltage at the wiper arm will be proportional to the position of the wiper. The primary advantages are simplicity and the direct analog output with dc excitation. The main disadvantages are the limited resolution and environmental effects on the wiper.

### 3.2.1 Intrinsic Errors, Potentiometers

The primary intrinsic errors of potentiometers are as follows:

1. Resolution
2. Nonlinearity
3. Noise

Frequency response errors are a function of the transducer using the potentiometer pickoff. All pickoff devices have finite resolution. In the case of the wirewound potentiometer, the resolution uncertainty or random error can be expressed as a function of the signal level and the number of turns or windings, as follows:

$$\% \text{ error} = \pm \frac{\Delta_{FS}}{\Delta} \frac{1}{2n} \quad (100) \quad (3.1)$$

where

$\Delta_{FS}$  = full scale output

$\Delta$  = the data signal level

n = number of windings on the potentiometer

# Contrails

This is the maximum possible resolution error. This error is identical to the quantification error associated with digitizing. The standard deviation of this error is approximately  $(0.29)(\Delta_{FS}/n)$  (see Reference 56, page 281). This rms error expressed as a percentage is as follows:

$$\% \text{ error}_{\text{rms}} = \pm \frac{\Delta_{FS}}{\Delta} \frac{0.29}{n} (100) \quad (3.2)$$

A continuous resistance element such as carbon film or conducting plastic may be employed, but environmental sensitivity is usually degraded and the potentiometer resistance becomes large (see Section 3.2.3).

Intrinsic linearity errors are attributable to manufacturing imperfections. A discussion of manufacturing techniques of potentiometers is beyond the scope of this report. The specifications of currently available transducers indicate that the maximum linearity error for transducer potentiometers is less than  $\pm 1\%$  of full range.

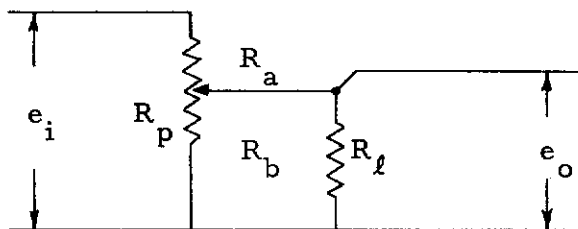
Potentiometer noise originates from the wiper travelling across the wires and usually includes resolution errors. The other sources of noise include dirt and wiper bounce. Many design techniques are employed to minimize these effects. Potentiometer noise may increase with wear. However, carefully designed and manufactured commercially available instrumentation potentiometers can be expected to function satisfactorily for over 20 million cycles (Reference 3, page 224).

### 3.2.2 Environmental Errors, Potentiometers

Various environmental errors are associated with the potentiometer wiper. Contact may be lost if the wiper vibrates. One technique of minimizing wiper bounce is to employ a wiper with two elements with different natural frequencies. Care should be exercised to choose a potentiometer device which has been designed and qualified for the vibration environment anticipated. The resistance of the potentiometer winding will change with temperature changes, but this will not affect the measurement accuracy if the load resistance is high (see Section 3.2.3).

### 3.2.3 Usage Errors, Potentiometers

A common usage error is to load the potentiometer with the resistance of the next unit. If this load resistance is low, the wiper deflection-output voltage relationship will become nonlinear. A potentiometer with a load resistance is shown in schematic below.



$e_i$  - excitation potential, volts

$e_o$  - output potential, volts

$R_l$  - load resistance, ohms

$R_p$  - potentiometer resistance, ohms

$R_a, R_b$  - partial potentiometer resistances, ohms

$k = R_b / R_p$  - wiper deflection



# Contrails

The ideal output is

$$e_o = e_i k \quad (3.3)$$

The output with the load resistor is

$$e_o = e_i k \frac{R_l}{R_l + kR_p - k^2 R_p} \quad (3.4)$$

If the effect of the load resistor is neglected, the resulting error is given by Eq. (3.5).

$$\% \text{ error} = \frac{\text{Actual} - \text{Ideal}}{\text{Ideal}} (100)$$

$$\% \text{ error} = k(k - 1) \frac{R_p}{R_p k(1 - k) + R_l} (100)$$

$$\approx k(k - 1) \frac{R_p}{R_l} (100) \quad (3.5)$$

This expression is plotted in Figure 3-1. Note that even for load resistances as great as ten times the potentiometer resistance, the error at mid-span ( $k = 0.5$ ) is  $-2.5\%$ . In actual practice, the particular transducer may be calibrated with the actual load resistance, and the calibration relationship obtained using the least squares criterion. The maximum error is then less than  $\pm(0.5)$  (maximum error, Figure 3-1). If high accuracy is desired, a nonlinear potentiometer which is designed to compensate for the effect of a particular load resistance may be used (Reference 1, page 117). Using a low resistance potentiometer is an obvious method for minimizing this error, but this conflicts with reso-

lution and power criteria. Another technique is to use resistors in series with the potentiometer (Reference 55, page 59). However, this decreases the basic sensitivity and calibration should be performed to obtain the best straight line fit relating output to input.

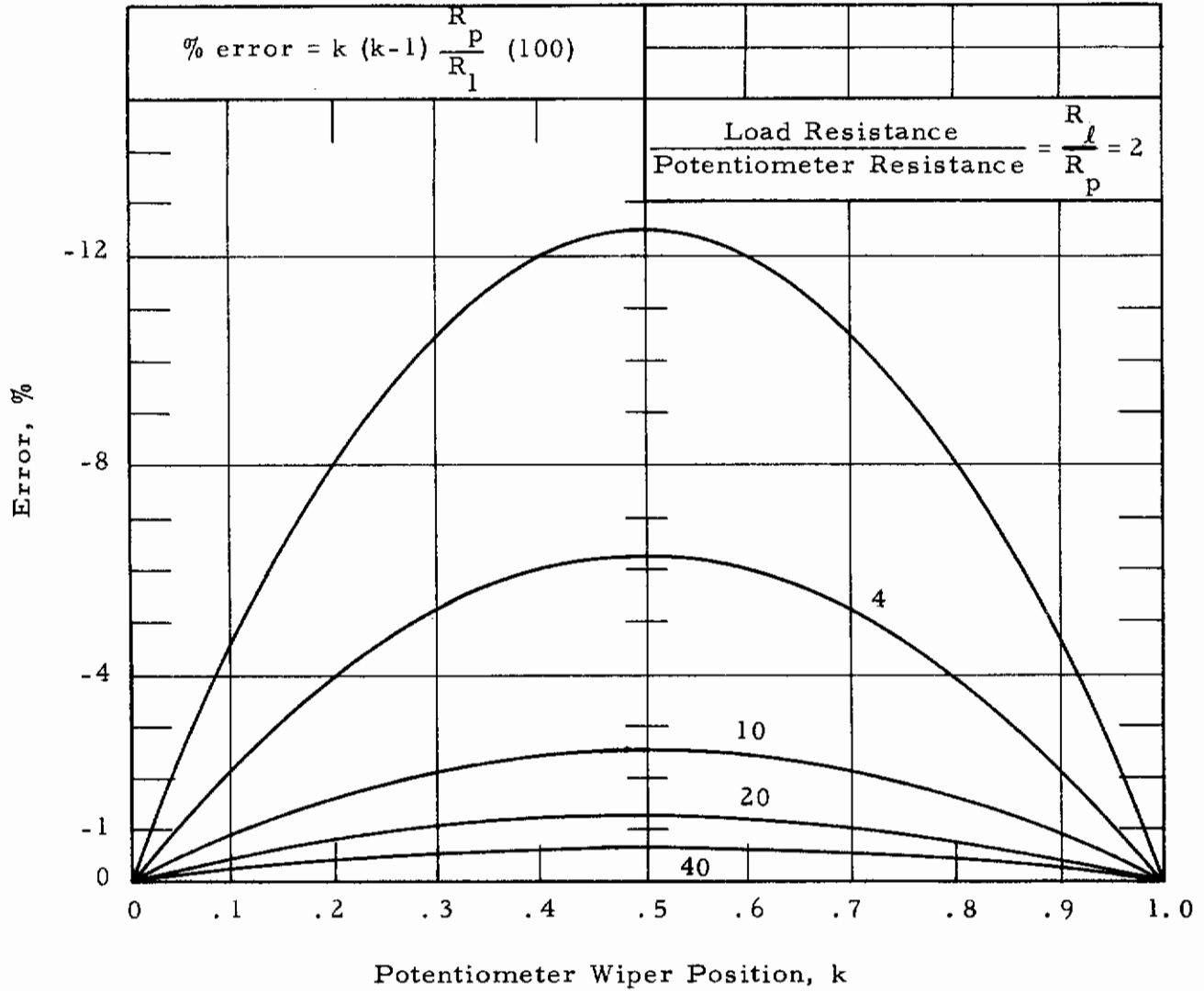


Figure 3-1. Potentiometer Nonlinearity Loading Error

### 3.3 VARIABLE RELUCTANCE PICKOFF

A number of pickoff devices such as differential transformers, synchros, and resolvers are all based on the change of inductance of a coil caused by the motion of an iron core. The designation of the variable reluctance pickoff is therefore somewhat arbitrary. A device with a movable iron core and a dual coil output winding (see Table 3-1) is usually defined as a variable reluctance pickoff. Motion of the iron core changes the inductance of the two output coils, one increasing and the other decreasing. If the resistance of the circuit is neglected, the change in inductance causes the voltage division across the two inductors to change and the output becomes

$$e_o = e_i(t) \frac{j2\pi f_c L_2}{j2\pi f_c L_1 + j2\pi f_c L_2} = e_i(t) \frac{L_2}{L_1 + L_2} \quad (3.6)$$

where  $L_1, L_2$  - inductances of variable reluctance pickoff, Henrys  
 $f_c$  - carrier frequency, Hz

If  $L_1 = L_2$  and the change in  $L_1$ ,  $\Delta L_1$ , is equal and opposite to the change in  $L_2$ ,  $\Delta L_2$ , then

$$e_o = e_i(t) \left[ \frac{1}{2} + \frac{\Delta L}{2L} \right] \quad (3.7)$$

This applies to a slowly varying input and therefore a slowly varying change of inductance. However, it should be noted that variable inductance as well as potentiometer pickoffs constitute systems with time varying parameters.

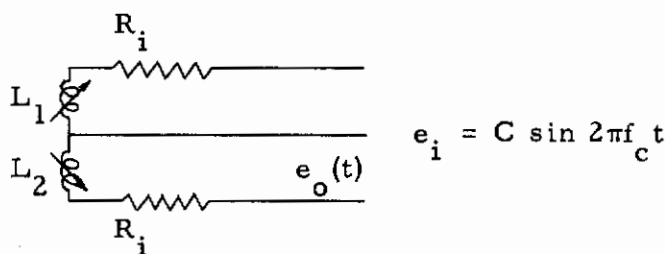
# Contrails

Fortunately, under certain conditions, the change in output has a linear relationship with the change in parameter over the data frequency range, and the system behaves as a linear system with constant parameters. If the pickoff is symmetrical and equal and opposite changes occur in the variable elements, the magnitude of the current does not change. In this situation, a linear input-output relationship exists which is independent of the data frequency. For example, if the time varying change in inductance equals  $\Delta_L \cos 2\pi f_d t$  and the excitation  $e_i(t)$  equals  $C \sin 2\pi f_c t$ , Eq. (3.7) becomes

$$e_o(t) = \frac{e_i(t)}{2} + C \frac{\Delta_L}{2L} \sin 2\pi f_c t \cos 2\pi f_d t$$

$$e_o(t) = \frac{e_i(t)}{2} + C \frac{\Delta_L}{4L} \left[ \sin 2\pi(f_c + f_d)t + \sin 2\pi(f_c - f_d)t \right] \quad (3.8)$$

The output voltage is simply one-half the input voltage plus amplitude modulation components which appear at sum and difference frequencies and are proportional to the maximum change in inductance  $\Delta_L$ . If the resistance of the inductors and lead wires is considered, the circuit and resulting output are



$$e_o(t) = \frac{e_i(t)}{2} + \Delta_L \frac{C j \pi f_c (\sin 2\pi f_c t) (\cos 2\pi f_d t)}{(R_i + j 2\pi f_c L)} \quad (3.9)$$

The output voltage in this situation is one-half the input voltage plus amplitude modulation terms. The coefficient of the second term is a function of the change in inductance and a constant which represents an amplitude and phase angle. Note that in this case the sensitivity is a function of the carrier frequency,  $f_c$ .

A variable inductance pickoff may be used either potentiometrically as indicated in Figure 3-1, or in an inductance bridge. AC inductance bridges are discussed briefly in Section 9 and covered at length in Reference 1, page 225, and in various books on basic electronic circuits. If the device is used as a potentiometer, the output will vary from minimum to maximum, and a simple rectifier-low pass filter demodulator may be used.

The selection of the filter becomes a trade-off between carrier ripple suppression and data frequency response. Reference 3, page 240, points out that a two-section filter with 5% carrier ripple will have only 2% data attenuation at the highest data frequency. For good ripple suppression, it is common practice to use a frequency ratio  $f_c/f_d$  of 10.0 or greater. If the pickoff is used in a bridge, the modulated output will increase for a displacement in either direction and a phase sensitive demodulator is required.

The main advantage of this type of pickoff is that it is noncontacting, that is, it has no electrical leads or brushes attached to the moving element. The main disadvantages are that demodulation of the amplitude modulated output signal is required and that the sensitivity is low compared with a differential transformer type pickoff. Environmental sensitivity is minimum and is best evaluated for the particular transducer.

## 3.4 DIFFERENTIAL TRANSFORMERS

A differential transformer pickoff consists of an input winding, a moveable iron core, and a dual series-wound output coil (see Table 3-1). The output coils are in series, but wound in opposite directions. When the iron core is in the center or null position, the outputs of the two coils are equal and opposite, and the net output is zero. When the iron core is displaced, the voltage on one coil is decreased while the voltage on the other coil increases.

The open circuit output of the circuit indicated in Table 3-1 is given in Reference 3, page 236, and is

$$e_o = e_i \frac{2\pi f_c (M_1 - M_2)}{R_i \sqrt{(2\pi f_c \tau)^2 + 1}} e^{-j\phi(f)} \quad (3.10)$$

$$\phi(f) = 90^\circ - \tan^{-1} 2\pi f_c \tau$$

where

$\tau = L_i/R_i$  - characteristic time of primary circuit

$L_q$  - primary inductance

$M_1$  - mutual inductance, primary to first output inductance, Henrys

$M_2$  - mutual inductance, primary to second output inductance, Henrys

$f_c$  - carrier frequency, Hz

$\phi(f)$  - phase lag, radians

$R_i$  - primary resistance, ohms

Note that the sensitivity indicated in Eq. (3.10) is a function of the carrier frequency. The design frequency for a particular pickoff is always specified. Also note that a phase shift between the input and output carrier signals occurs. This phase shift is  $+90^\circ$  at low frequencies and  $-90^\circ$  at high frequencies. The phase shift for a particular transducer is usually indicated for the design frequency  $f_c$ . The main advantages of this type of pickoff are excellent resolution and linearity over small ranges and the noncontacting design feature. The main disadvantage is that AC excitation and phase sensitive demodulation are required. A simple circuit for phase sensitive demodulation is described in Reference 3, page 239, and is also indicated in Section 9 of this report. This circuit requires both leads from both output inductors.

### 3.4.1 Intrinsic Errors, Differential Transformers

Three types of intrinsic errors are as follows:

1. Nonlinearity
2. Drag
3. Phase shift

Nonlinearity due to end effects for large displacements is the major limitation on amplitude of the differential transformer pickoff. However, with proper design and instrumentation, differential transformers may have nonlinearities as small as 1% for large travel. In the rotary configuration, a 1% error for  $40^\circ$  travel, or 3% for  $60^\circ$  travel, is feasible (Reference 3, page 242). The nonlinearities are due primarily to manufacturing imperfections and nonlinearities of the iron. Even though the differential transformer is a noncontacting device, magnetic effects do produce a finite amount of drag between the moveable core and the case.



This type of drag would probably appear as hysteresis in the transducer in which it is used. The phase shift between the input voltage and the carrier signal in the output signal is a significant problem only if it causes errors in the demodulation. Some carrier systems require small phase shifts to function properly. If required, phase advance and phase retarding circuits may be employed (References 57 and 58). The frequency response errors are usually dependent on the demodulator and other elements of the using transducer. Environmental errors are usually small.

### 3.4.2 Usage Errors, Differential Transformers

Two common types of usage errors of differential transformers are

1. Excitation frequency error
2. Loading error

As previously indicated, the sensitivity of differential transformers is a function of the excitation frequency. Variation of this frequency in usage will cause a corresponding output error as follows:

$$\% \text{ error}_{e_o} = \% \text{ error}_{f_c} \quad (3.11)$$

The impedance of the next stage or unit will affect the output. This error is similar to the potentiometer loading error, Eq. (3.5), but the particular circuit should be analyzed.



## 3.5 SYNCHROS

Synchros are devices which are widely used in servo techniques to sense shaft position. They consist of an input coil wound on a rotor and three output coils. As the shaft rotates, each of the output coils produces an output proportional to the sine of the angle of rotation, but  $120^\circ$  apart (see Table 3-1). In servo work, these outputs are commonly connected to another synchro, usually called a synchro receiver. The shaft position of the synchro receiver will track the shaft position of the position sensing or transmitting synchro. For applications where the displacement signal is to be recorded, synchros are not recommended because the output is not directly proportional to the displacement. However, for small angles, the sine of the angle is essentially equal to the angle and the output may be used directly. For both small and large angles, a DC output may be obtained by electrically connecting a synchro to a synchro receiver which is mechanically connected to a potentiometer. This technique may be useful if the particular measurement must be made with an existing or onboard transducer which has only a synchro pickoff.

### 3.5.1 Intrinsic Errors, Synchros

Synchros have errors which correspond to the errors of potentiometers. The accuracy is limited by manufacturing tolerances on the alignment of the rotor, the uniformity of the laminations, etc. This is analogous to the resolution error of potentiometers but is not definable in reasonable equation form. These angular errors are typically of the magnitude of from five to twenty minutes. In addition, harmonic voltages are generated in the synchro as a result of nonlinearities of

the iron. These residual voltages are attributable to manufacturing imperfections and have the same effect as the resolution error. The synchro type pickoff requires brushes or connecting wires which cause hysteresis or other errors in the particular transducer.

### 3.6 RESOLVER

Resolvers are similar to synchros in that one set of coils is installed on the rotor and one set on the body (see Table 3-1). However, for a resolver, the output coils, not the input coil, are on the rotor. These coils are  $45^{\circ}$  apart and the resulting output signals are proportional to the sine and cosine of the angle of rotation. As with synchros, this output is not in a desirable form for recording and potentiometers are commonly used.

### 3.7 MICROSYN

The microsYN consists of a rotor and a four pole stator on which both input and output coils are wound (see Table 3-1). The output coils are wound in series but connected such that voltages in poles 2 and 4 oppose voltages in poles 1 and 3. When the rotor is at the neutral position, the net output is zero. Essentially, the microsYN is a differential transformer in a rotary configuration. The main advantage of this type pickoff is its high resolution and high accuracy for small displacements. The main disadvantages are the limited displacement, up to only  $\pm 10\%$ , and lack of polarity. As with a differential transformer, a phase-sensitive circuit is required to produce a signal which has polarity.

## 3.8 VARIABLE CAPACITANCE PICKOFF

The variable capacitance pickoff utilizes the variation in capacity with distance to transduce or measure displacements. Capacitance between two parallel plates varies inversely and therefore nonlinearly with distance (see Table 3-1). This basic design problem is overcome in a number of ways. One method is to place the variable capacitor in the feedback loop of an operational amplifier (Reference 3, page 253).

The advantages of this pickoff device are that it is noncontacting and, if DC excitation is used, the resulting signal is in analog form. However, the frequency response when DC excitation or polarization is employed falls off as zero frequency is approached.

One environmental error attributable entirely to capacitance pickoff is the effect of ambient pressure changing the dielectric constant between the plates. Humidity will also have an effect, but it will usually produce an identifiable short.

## 4. GUST INPUT MEASUREMENT TRANSDUCERS

Gusts or free air fluctuating velocities create significant input forces and, therefore, aircraft responses. The absolute free air velocity cannot be determined directly with one measurement on an aircraft because the aircraft is a moving platform in space. In addition, measurement of the profile of the gust velocity at various points on the aircraft is virtually impossible because the aircraft disturbs the free air.

However, if certain assumptions are made, the relative time varying velocity of the airflow at a single point on the aircraft may be used to compute a valid input forcing function. The gust wavelength is assumed to be large compared to the aircraft dimensions. Also, the gust is assumed to have a washboard character. That is, even though the aircraft moves vertically or laterally due to the gust, the gust velocity measured is assumed to be the same as would be measured if the aircraft flew perfectly straight.

Present techniques for gust velocity measurements calculate the gust velocity from the aircraft angle of attack measurement multiplied by the aircraft velocity. The angle of attack sensor for this purpose is usually mounted at the end of a boom on the nose of the aircraft to place it in the undisturbed airstream. Since the aircraft may not have zero attitude and will probably have acceleration and angular velocities, gust velocity corrections are required. References 5 and 6 indicate that vertical gust velocity is calculated by the relationship:

$$w_g(t) = Va(t) - V\theta(t) + \int \ddot{z}(t) dt + l_x \dot{\theta}(t) \quad (4.1)$$

# Contrails

where  $w_g(t)$  = gust velocity (vertical), feet/sec  
 $V$  = aircraft velocity, feet/sec  
 $\alpha(t)$  = angle of attack, radians  
 $\theta(t)$  = aircraft attitude, referenced to earth, radians  
 $\ddot{z}(t)$  = aircraft vertical acceleration, feet/sec<sup>2</sup>  
 $\ell_x$  = length between acceleration measurement and angle of attack measurement, feet  
 $\dot{\theta}(t)$  = aircraft pitch rate, radians/sec

Gust velocities in the orthogonal directions are calculated in a similar fashion. In actual practice, the running average or trend for each of these parameters being measured is determined and subtracted from the instantaneous value to minimize the accumulation of drift and bias errors. This is indicated in Eq. (4.2)

$$w_g = V[\alpha(t) - \bar{\alpha}] - V[\theta(t) - \bar{\theta}] + \int [\ddot{z}(t) - \bar{\ddot{z}}] dt + \ell_x [\dot{\theta}(t) - \bar{\dot{\theta}}] \quad (4.2)$$

A significant problem encountered when employing this relationship is the required resolution of the attitude pitch rate and acceleration measurements. Tests reported in Reference 88 exhibited low level, low frequency pitch rate and acceleration signals,  $\pm 0.082$  degree per second and  $0.041$  g, respectively, which produced gust velocity corrections greater than the uncorrected gust velocity term,  $V\alpha(t)$ . The measurement of the attitude term data, the pitch rate, and the aircraft acceleration are covered in the sections on vertical gyros, rate gyros, and accelerometers, respectively. The balance of this section will be devoted to angle of attack sensors, and problems associated with the boom on which the angle of attack sensor is mounted to place it in the free undisturbed air stream in front of the aircraft.

## 4.1 VANES AND PROBES

Three different basic types of angle of attack and/or sideslip sensors are presently commercially available and used for gust velocity determination. These basic types of sensors are as follows:

1. Moveable vanes
2. Differential pressure probes
3. Fixed vane probes

These three types of angle of attack sensors are shown schematically in Figure 4-1. The moveable vane type aligns itself with the air flow and therefore measures the angle of attack directly. The differential pressure probe senses the difference in pressure between two points on the end of a blunt boom. This difference in pressure is related directly to the angle of attack and the dynamic pressure. The fixed vane probe senses the lift on a fixed vane. This lift is related directly to the angle of attack and the dynamic pressure.

### 4.1.1 Moveable Vanes

Moveable vanes are used extensively to sense the angle of attack. This type transducer functions by aligning itself with the airstream. The angle formed between the shaft of the vane and the mounting structure, usually the aircraft fuselage, is sensed by a potentiometer or a synchro. The vanes are usually dynamically balanced and the response to acceleration or inertia forces is therefore minimized. The advantage of this type of sensor is basic simplicity of design which permits measurement of angle of attack directly. The main disadvantage is susceptibility to environmental and usage errors.

# Contrails

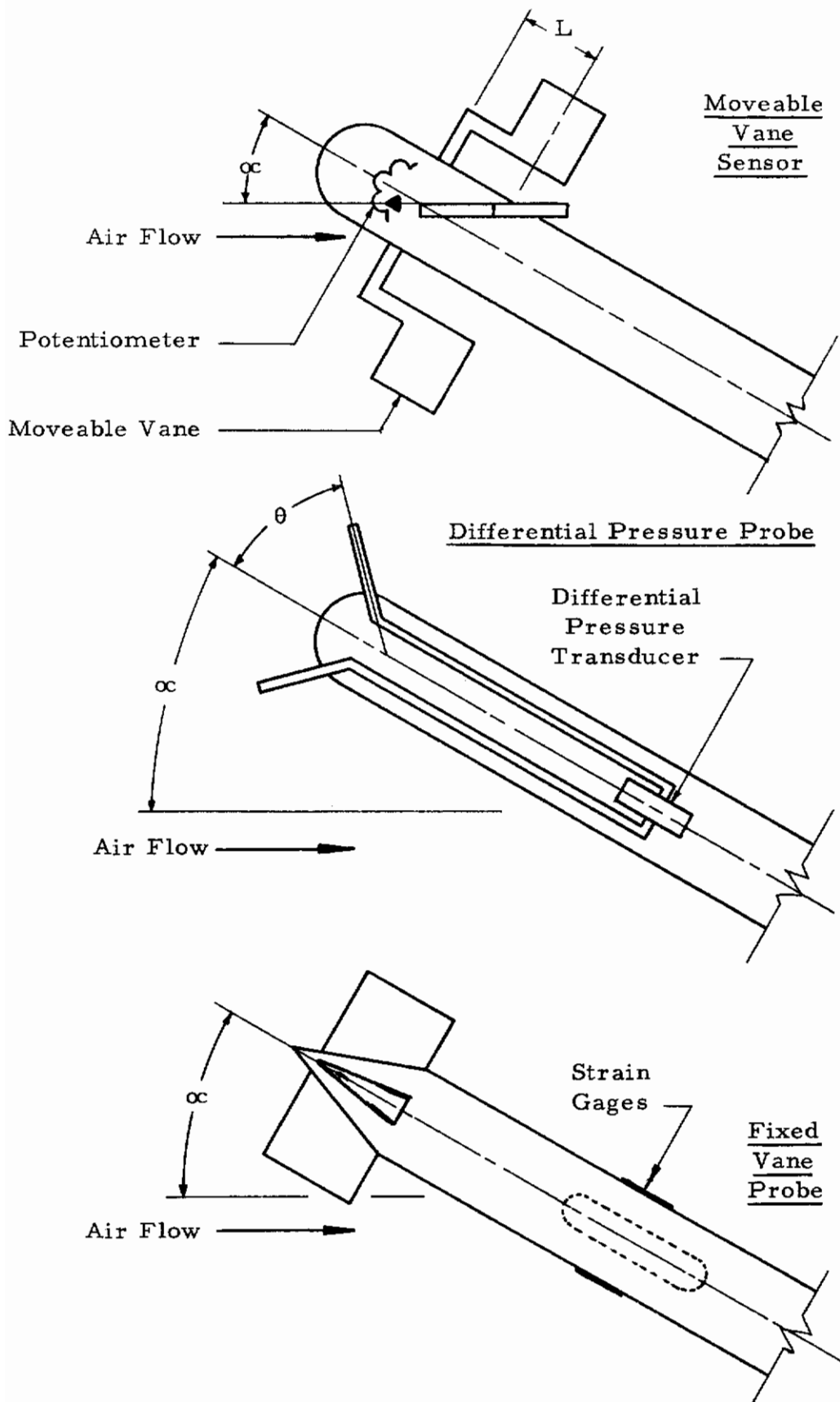


Figure 4.1. Angle of Attack Sensors



# Contrails

The natural frequency is derived by considering the restoring torque when the vane is not aligned with the airstream.

$$T = (\text{lift}) (\text{moment arm})$$

$$T = \left[ C_L A \frac{\rho V^2}{2} \right] l \quad (4.3)$$

where

$C_L$  - coefficient of lift

$A$  - vane area, feet<sup>2</sup>

$\rho$  - density of airstream air, slugs/feet<sup>3</sup>

$V$  - aircraft velocity, feet/sec

$l$  - distance center line shaft to center vane, feet (see Figure 4-1)

$T$  - torque, feet-pound

The sectional coefficient of lift for a thin airfoil for small angles of attack is given by Reference 11, page 81 as

$$C_L = 2\pi\alpha \quad (4.4)$$

where

$\alpha_v = \alpha - \phi$  = vane angle of attack, radians

$\alpha$  - aircraft angle of attack, radians

$\phi$  - relative angular displacement, aircraft-vane, radians

The restoring torque per unit angle of attack is therefore

$$k_{\text{eff}} = T/\alpha_v = \left[ 2\pi A \left( \frac{\rho V^2}{2} \right) \right] l \quad (4.5)$$

where  $T/\alpha_v$  is the effective spring constant, inch lb/radian.

The undamped natural frequency of a single degree-of-freedom torsion system is given by



# Contrails

$$f_n = \frac{1}{2\pi} \sqrt{\frac{k}{I}} = \frac{1}{2\pi} \sqrt{\frac{k}{mr^2}} \quad (4.6)$$

where

k - spring constant, foot pounds/radian

I - moment of inertia, slug feet<sup>2</sup>

m - mass, slugs

r - radius of gyration, feet

Therefore, for the conditions stated (thin airfoil, small angles of attack), the undamped natural frequency of a moveable vane in an airstream is approximately

$$f_n = \sqrt{\frac{lA}{2\pi mr^2} \left( \frac{\rho V^2}{2} \right)} \quad (4.7)$$

Note that the natural frequency is a linear function of the aircraft velocity.

#### 4.1.1.1 Intrinsic Errors, Moveable Vanes

Two types of intrinsic errors are as follows:

1. The amplitude and phase inaccuracies due to response of a single degree-of-freedom system (bias error)
2. Resolution errors in the pickoff device (random error)

The expressions for amplitude and phase errors due to the frequency response of a moveable vane are developed in Appendix A. If the input is due only to airstream variation with the aircraft attitude remaining constant, the normalized frequency response of open loop accelerometers applies (Figures A-2, A-3, and A-4). With aircraft attitude variation, the frequency response is greatly different (Figure A-14). In an application, the contributions from each source should be investigated and the response combined.

# Contrails

As an example, consider a typical vane.

$$l = r = 3/12 \text{ feet}$$

$$m = \frac{0.3 \text{ lb sec}^2}{32.2 \text{ feet}}$$

The natural frequencies at typical flight conditions are as follows:

Case	1	2	3
Mach No.	.3	.6	.7
Altitude, feet	sea level	3,000	40,000
$f_n$ Hz	16.1	31.4	16.9

Since these frequencies approach typical gust frequencies, extremely light weight vanes with higher natural frequencies have been used (see Reference 7).

If the vane shaft angle is sensed with a wire wound potentiometer pickoff, a resolution error results. This error is given in Section 3 and repeated below:

$$\% \text{ error}_{\text{rms}} = \pm \frac{\alpha_{\text{fs}}}{\alpha} \frac{0.29}{n} (100) \quad (4.8)$$

where  $\alpha_{\text{fs}}$  = total full scale range, radians  
 $n$  = number of potentiometer windings

For example, with a full scale of  $\pm 20^\circ$  and  $n = 2000$ , the rms error in the measurement of  $0.5^\circ$  is  $\pm 1.16\%$ . This random error is significant because

the angle of attack variation due to gust velocities is usually small compared to the range of absolute angle of attack measurement.

#### 4. 1. 1. 2 Environmental Errors, Moveable Vane Sensors

Since the vane is of necessity mounted in the airstream, it is subject to temperature variations and humidity phenomena including icing. This icing may be avoided or minimized in effect by installing de-icing heaters in the assembly. Variations in temperature may affect the damping provided within the unit. If damping varies as a function of temperature, the errors described in Appendix A are applicable. Another environmental error is its potential susceptibility to vibration. This defect may be eliminated only if the device is balanced, and sufficiently stiff so that the vane itself has no bending natural frequencies in the frequency region of interest, zero to 20 Hz.

#### 4. 1. 1. 3 Usage Errors, Moveable Vane Sensors

Moveable vanes are inherently fragile devices installed in exposed external locations. As a result, the major usage errors are attributable to damage due to mishandling and exposure to adverse environments.

#### 4. 1. 2 Differential Pressure Probes

Differential pressure probes function by measuring the difference in pressure on two points of a blunt object as indicated in Figure 4. 1. The subsonic pressure distribution around a sphere is given by Reference 8, page 413, as follows:

# Contrails

$$P = \frac{1}{2} \rho V^2 \left(1 - \frac{9}{4} \sin^2 \theta\right) + P_s \quad (4.9)$$

where

$P$  = pressure at point on sphere, lbs/feet<sup>2</sup>

$\theta$  = angular position of point, ref Figure 5, degrees

$P_s$  = static pressure, lbs/feet<sup>2</sup>

If the two pressure taps are mounted 45° from the center line, the difference in pressure will then be as follows:

$$\begin{aligned} P_1 - P_2 = \Delta P &= \frac{1}{2} \rho V^2 \frac{9}{4} \left[ -\sin^2 (45^\circ + \alpha) + \sin^2 (-45^\circ + \alpha) \right] \\ &= \frac{1}{2} \rho V^2 \frac{9}{4} \left[ \sin (\alpha - 45^\circ + \alpha + 45^\circ) \sin (\alpha - 45^\circ - \alpha - 45^\circ) \right] \quad (4.10) \\ &= -\frac{1}{2} \rho V^2 \frac{9}{4} \sin 2\alpha \end{aligned}$$

If this quantity is then normalized by dividing by the dynamic pressure and evaluated for small angles, the difference in pressure is related to the angle of attack by the equation:

$$\frac{\Delta P}{q} = - (0.079) \alpha = -k\alpha \quad (4.11)$$

where

$k$  - constant

$q = \frac{\rho V^2}{2}$  - dynamic pressure, lbs/ft<sup>2</sup>

Indeed, wind tunnel tests (Reference 9) indicate that the constant is 0.0819 compared with the ideal 0.079. Calibrations of a probe with protruding tubes instead of flush ports (Reference 10) gives a nominal value of the constant as 0.1.

#### 4.1.2.1 Intrinsic Errors, Differential Pressure Probes

The major intrinsic errors of differential pressure probes are as follows:

1. Errors due to the measurement of the dynamic pressure
2. Variation of the calibration constant with Mach number

The measurement of the angle of attack,  $\alpha$ , requires the determination of the dynamic pressure,  $q$  (Eq. 4.11). For small errors, the errors are related by:

$$\% \text{ error }_{\alpha} = - \% \text{ error }_q \quad (4.12)$$

The relationship between angles of attack and differential pressures as expressed in Eq. (4.11) is reasonably accurate between Mach 0.1 and 0.6. However, in the transonic and supersonic region, the physics of drag change and one would expect the relationship between differential pressure and angle of attack to subsequently change. Indeed, this is the case. References 9 and 10 present test data showing the variations in the constant with Mach number. The data from Reference 9 is presented as Figure 4-1. In order to scale the data properly, an accurate measure of the aircraft Mach number must be made and the appropriate scale factor applied. Frequency response is a function of the tubing, pressure transducer, and mounting boom, not the basic transducer.

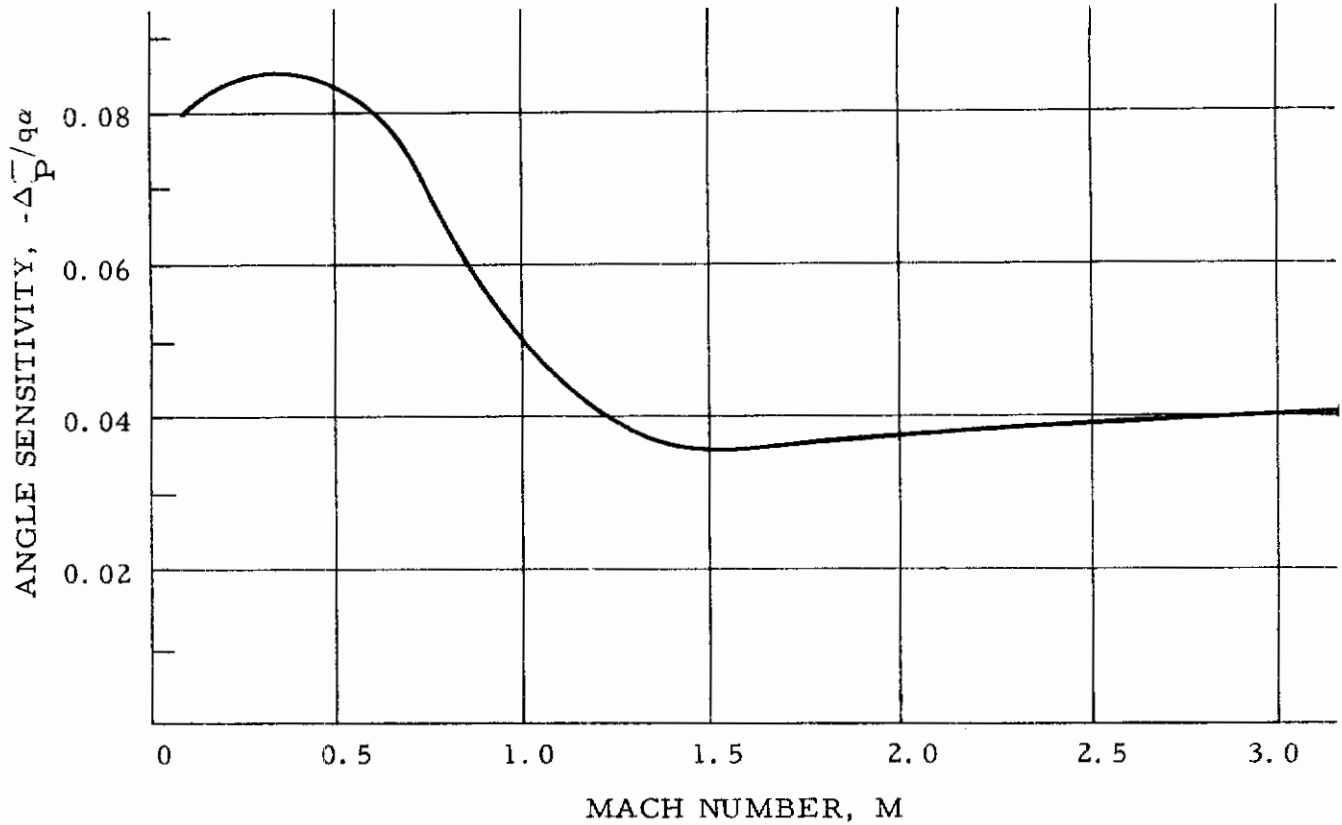


Figure 4-1. Sensitivity of Differential Pressure Angle of Attack Sensor versus Mach Number

#### 4.1.2.2 Environmental Errors, Differential Pressure Probes

The most significant environmental error is associated with ice formation on the probe. The aerodynamic characteristics will change and the probe ports may become blocked. This may be avoided by adequate de-icing provisions. Another type of environmental error concerns the differential pressure transducer. Typically a strain gage or

capacitive device with fluid damping is used for this application. The damping provided by the fluid may change with temperature. In addition, the transducer should be designed to withstand any anticipated vibration environment. Pressure transducers are discussed in Section 8.

#### 4.1.2.3 Usage Errors, Differential Pressure Probes

The usage errors of differential pressure probes are as follows:

1. Frequency response errors due to tubing
2. Calibration
3. Damage

The frequency response of the differential pressure type angle of attack sensor is dependent on the dimensions of the tubes to the pressure transducer and the natural frequency of the transducer itself. The expressions for natural frequency and damping of the gas in the tube are given in Section 8.

The error may be extremely large for small tube diameters. For example, consider a case at standard atmospheric conditions at 10,000 feet altitude with a long, small diameter tube.

Tube diameter,  $d$  - 0.02 inch

Tube length,  $l$  - 100 inches

Vol, pressure transducer,  $v$  - 0.314 inch<sup>3</sup>

Sound velocity,  $V_s$  - 1078 feet/second

Air density,  $\rho$  - 0.001756 slug/feet<sup>3</sup>

Air viscosity,  $\mu$  -  $3.515 \times 10^{-7}$  slug/feet-second

Substituting in Eqs. (8.6) and (8.7)

$$\text{Natural frequency, } f_n = 6.34 \text{ Hz}$$

$$\text{Damping factor, } \zeta = 28.9$$

The corresponding frequency response function is unacceptable. However, the characteristics improve rapidly with increased tube diameter. If tube diameter = 0.1 inch,

$$f_n = 21.7 \text{ Hz}$$

$$\zeta = 0.338$$

Since the response characteristics of this type of probe are nonlinear with Mach number, the probe must be calibrated to provide an accurate readout. Wind tunnel calibration of these devices should be made for the entire Mach number range of interest. The method employed will depend on the type of pressure transducer used. A method of referring the measured data to the wind tunnel calibration which is independent of any excitation voltages, lead wire length, and other extraneous effects should be provided for as discussed in Section 9 under usage errors of Wheatstone bridges.

Another usage error results if the probe is damaged. If the effective angle between the probe ports is changed from  $90^\circ$  by bending the protruding tubes, the sensitivity will change by a factor of the sine of the new angle. If the airflow is changed by damage to the probe, no valid expression may be used to describe the error. The probe should then be repaired and/or recalibrated.



## 4. 1. 3 Fixed Vane Probes

This type of angle of attack sensor functions by measuring the aerodynamic lifting force on a vane and relating this measurement to the angle of attack. A variation of the fixed vane probe uses a feedback loop to provide restoring force for a movable vane. The expressions for ideal subsonic and supersonic lift on a symmetrical body are given by Reference 11 and presented in Eqs. (4. 13) and (4. 14).

$$\begin{aligned} \text{Subsonic lift} = F &= C_L A \frac{\rho V^2}{2} \\ &= 2\pi\alpha A \frac{\rho V^2}{2} \end{aligned} \quad (4. 13)$$

$$\begin{aligned} \text{Supersonic lift} = F &= C_L A \frac{\rho V^2}{2} \\ &= \frac{4\alpha}{\sqrt{M^2 - 1}} A \frac{\rho V^2}{2} \end{aligned} \quad (4. 14)$$

As with the case of the differential pressure probe, the output is a function of the dynamic pressure. If the above equations are rearranged, the angle of attack is related directly to the lifting force.

$$\alpha = \frac{F}{2\pi A q} \quad \text{subsonic} \quad (4. 15)$$

$$\alpha = \frac{F \sqrt{M^2 - 1}}{4 A q} \quad \text{supersonic} \quad (4. 16)$$

where  $q = \frac{\rho V^2}{2}$  = dynamic pressure, pounds/feet<sup>2</sup>

The natural frequency depends on both the mechanical and aerodynamic restoring springs. The response will approach that of the movable vane if the mechanical spring is soft.

#### 4.1.3.1 Intrinsic Errors, Fixed Vane Probes

Intrinsic errors for fixed vane probes are divided into the following items:

1. Nonlinearities in the general expression for lift on the vane
2. Errors associated with the strain gage measuring device

The relationship between angle of attack and lifting force given by Eqs. (4.15) and (4.16) show the dependence on dynamic pressure and Mach number. Therefore, as with the case of differential pressure probes, these parameters must be measured accurately. Reference 12 gives calibration data for a fixed vane gust probe. Errors associated with strain gage measurement are treated in detail in Section 6.

#### 4.1.3.2 Environmental Errors, Fixed Vane Gust Probes

The main environmental error for the fixed vane gust probes are attributable to temperature effects on the strain gages measuring the bending force. These errors are described in detail in the section on either conventional strain gages or semi-conductor strain gages. As with the other types of angle of attack sensors, ice formation on the vane is a potential source of error. As with movable vanes, the sensitivity to vibration is minimized if the vane is balanced and stiff.

#### 4.1.3.3 Usage Errors, Fixed Vane Gust Probes

The calibration errors associated with differential pressure probes apply to fixed vane probes because the nonlinearities due to Mach number apply or are similar. Since the sensing is done with strain gages, all the usage errors for strain gages in Section 7 apply.

## 4.2 MOUNTING BOOMS

The boom used to place the angle of attack sensor in the undisturbed airstream can contribute errors to the angle of attack measurement. This occurs when the aircraft acceleration and pitch rate correction measurements are not made at the end of the boom where the angle of attack sensor is located. Therefore the gust velocity determination, Eq. (4-2), is in error.

$$w_g(t)_m = w_g(t) - V\phi(t) - \int a_v(t) dt \quad (4.17)$$

where  $w_g(t)_m$  — measured gust velocity  
 $V$  — aircraft velocity  
 $\phi(t)$  — angle between end of boom and attitude gyro  
 $a_v(t)$  — relative acceleration, vane - accelerometer

The error is therefore:

$$\% \text{ error} = \frac{-V\phi(t) - \int a_v(t) dt}{w_g(t)} (100) \quad (4.18)$$

Sample calculations for booms with simple geometry indicate that the error due to the angular deflection of the boom is one to two orders of magnitude greater than the error due to the boom tip relative velocity. The error expression is therefore

$$\% \text{ error} \approx \frac{-V\phi(t)}{\omega_g(t)} (100) \quad (4.19)$$

The evaluation of this error for different combinations of boom geometry, aircraft vibration and gust velocity spectra is beyond the scope of this report.

One method for correcting for boom deflection is to measure the boom bending moment with strain gages, compute the corresponding angular deflection at the tip, and apply an appropriate correction, Reference 99, page 205.

## 5. ATTITUDE AND ANGULAR RATE MEASUREMENT TRANSDUCERS

The measurement of the angular motion parameters is an integral and important part in flight loads determination. The types of measurements that are commonly made and their applications are as follows:

- 1) angular position or attitude
  - a) gust velocity calculation
  - b) correlation with other responses and inputs
- 2) angular rate
  - a) describing touchdown
  - b) describing a maneuver

The angular motion measurements which are desired are those of the rigid body aircraft. Localized motion which describes the aircraft modal response is usually determined with accelerometers. Therefore, the frequency range of interest for angular motion measurement is from 0 to approximately 6 Hz.

A number of different types of gyroscopic devices are suitable for the measurement of the desired parameters. The five different types of attitude and rate sensing devices considered are as follows:

- 1) free gyroscope
- 2) vertical gyroscope
- 3) rate gyroscope
- 4) rate integrating gyroscope
- 5) stable platforms

The schematics, the type of measurements which these devices are capable of making, and the advantages and disadvantages of each are presented in Table 5-1. The stable platform has a variety of configurations and its schematic is not indicated. Reference 13 presents a thorough introductory discussion of all types of gyroscopic devices, as well as state-of-the-art specifications. References 14 and 15 also present introductory gyroscopic principles. A comprehensive collection of publications on gyroscopic principles and applications exists; however, the primary use of gyroscopes is for navigation and control and the literature is not oriented towards flight parameter measurement.

## 5.1 GYROSCOPE ERRORS

Since gyroscopic devices have a reasonable amount of similarity between one another, they have a number of common errors. These common errors are discussed separately in the following text. The errors unique to each gyroscopic device are discussed under the particular gyroscope sections. The primary errors associated with each type of gyroscopic device are listed in Table 5-2. The common errors which are discussed separately are noted. The major differentiation between the types of devices is the number of degrees of freedom which the gyro possesses. This is usually equivalent to the number of gimbals. As seen in Table 5-1, the housings of free gyros and vertical gyros are free to move in two directions with respect to the gyroscopic wheel. Rate gyros and rate integrating gyros are single degree-of-freedom devices, and are restrained to one type of motion. The major errors tend to be divided into those common to all gyroscopes, single degree-of-freedom gyroscopes, and multiple degree-of-freedom gyroscopes.

Table 5-1. Comparison of Gyroscopic Devices for Flight Loads Measurements

Type Device	Schematic	Type Measurement	Major Advantages	Major Disadvantages
Free Gyro	<p>The diagram shows a gyroscope with two torque inputs labeled 'TORQUE' and two pickoff points labeled 'PICKOFF ROLL ANGLE' and 'PICKOFF PITCH ANGLE'.</p>	Angular position; Pitch and Roll or Pitch, Yaw and Roll	Independent of gyro speed Large range	Large drift Subject to nutation
Vertical Gyro	<p>The diagram shows a gyroscope with a vertical reference line labeled 'VERTICAL REFERENCE' and two pickoff points labeled 'PICKOFF ROLL ANGLE' and 'PICKOFF PITCH ANGLE'.</p>	Angular position; Pitch and Roll	Vertical reference Independent of gyro speed Large range	Vertical reference errors Subject to nutation
Rate Gyro	<p>The diagram shows a gyroscope with two damping inputs labeled 'DAMPING' and two pickoff points labeled 'PICKOFF PITCH RATE' and 'PICKOFF PITCH ANGLE'.</p>	Angular rate	Small displacements allow variable reluctance pickoff Measures angular rate directly Small size	Dependent on spring characteristics Dependent on gyro speed
Rate Integrating Gyro	<p>The diagram shows a gyroscope with two damping inputs labeled 'DAMPING' and one pickoff point labeled 'PICKOFF PITCH ANGLE'.</p>	Angular position	High accuracy	Small range Dependent on gyro speed and on damping Poor frequency response function
Stable Platform		Angular position and rate	High accuracy	Complex



Table 5-2. Gyroscope Errors

Type Gyroscope	Intrinsic Errors	Environmental Errors	Usage Errors
Free Gyros	Drift* Nutation* Linearity* Hysteresis and Resolution* Gimbal errors*	Vibration effects on drift*	Gimbal lock and tumbling
Vertical Gyros	Drift* Nutation* Vertical repeatability Hysteresis and Resolution* Linearity* Gimbal errors*	Vibration effects on drift* Lateral acceleration effects on erection Temperature effects	Erection cutout Gimbal lock and tumbling
Rate Gyros	Frequency Response Gyro speed Hysteresis and Resolution* Linearity*	Vibration effects* Temperature effects on damping	Calibration Mounting
Rate Integrating Gyroscope	Frequency Response Gyro Speed Hysteresis and Resolution* Linearity* Drift*	Vibration effects Temperature effects on damping	Exceed range

\* Common Errors



## 5.1.1 Gyroscope Drift

Probably the most common and well-known gyro error is drift. Small friction torques cause gyro precession in unrestrained devices, that is, free gyros, vertical gyros and rate integrating gyros. The amount of this drift limits the usefulness of the free gyroscope, making it essentially a short-term device. Drift is a primary specification parameter which is well defined for each particular gyroscope. The environmental effect of vibration increasing drift is not so well defined. A considerable amount of technical work has been devoted to describing the mechanics of vibration creating drift (References 13, 60 and 61). Reference 22 presents the results of a study to relate gyro drift with vibration acceleration. The general conclusion of this work is that insufficient correlation existed to describe gyroscope vibration coefficients.

## 5.1.2 Nutation

Nutation is an error or unwanted phenomenon of two degree-of-freedom gyroscopes. Basically, nutation is an exchange of energy between one degree of freedom and another. This motion requires no external energy or force to sustain it. The natural frequency of this phenomenon is as follows:

$$f_n = \frac{1}{2\pi} \frac{H}{\sqrt{I_{og} I_{ig}}} \quad (5.1)$$

where

$I_{ig}$  - moment of inertia of inner gimbal and gyro about inner axis

$I_{og}$  - moment of inertia of inner gimbal, gyro, and outer gimbal about outer axis

$H = I_s \Omega$  - momentum of gyro wheel, foot pound second/radian

Proper gyroscope design will keep this nutation frequency above the frequency of interest. This is done by maintaining a large angular momentum for the gyroscope wheel compared with the gimbal moments of inertia. If that is not possible, knowledge of the nutation frequency should be used when analyzing resulting data. In most gyroscope designs, the bearing friction serves to damp out nutation and it is not a serious problem.

### 5.1.3 Nonlinearity

Nonlinearity is an error which manifests itself in all types of transducers, and is a function of the transducer design. The nonlinearity and loading effects of potentiometers are discussed in Section 3. Typical values of nonlinearity for commercially available gyroscopes are less than +1%.

### 5.1.4 Hysteresis and Resolution

As with linearity, hysteresis and resolution are quantities which are a function of the detail design of the gyroscope. The resolution errors of potentiometers are discussed in Section 3. Hysteresis is usually combined in specifications with linearity because the two parameters are difficult to separate by practical tests. Typical values for linearity and hysteresis are +1% for free and vertical gyroscopes, and ±.25% for rate gyroscopes and rate integrating gyroscopes.

### 5.1.5 Gimbal Errors

In free and vertical gyroscopes, the pitch angle pickoff device measures the relative angle between the inner and outer gimbal. This

is the same as the angle between the aircraft center line and the local horizontal plane or horizon. If a large roll angle is being measured simultaneously, the pitch angle measurement is in error. This is because the pitch angle is usually defined as vertical motion about the wings instead of about the local horizontal (see Figure 5-1). This is a specific type of gimbal error. Correction for this error involves computations using spherical geometry. In some types of gyroscopes, three or four gimbals are employed in order to measure the third degree of motion, yaw. Gimbal errors are more complex in these units.

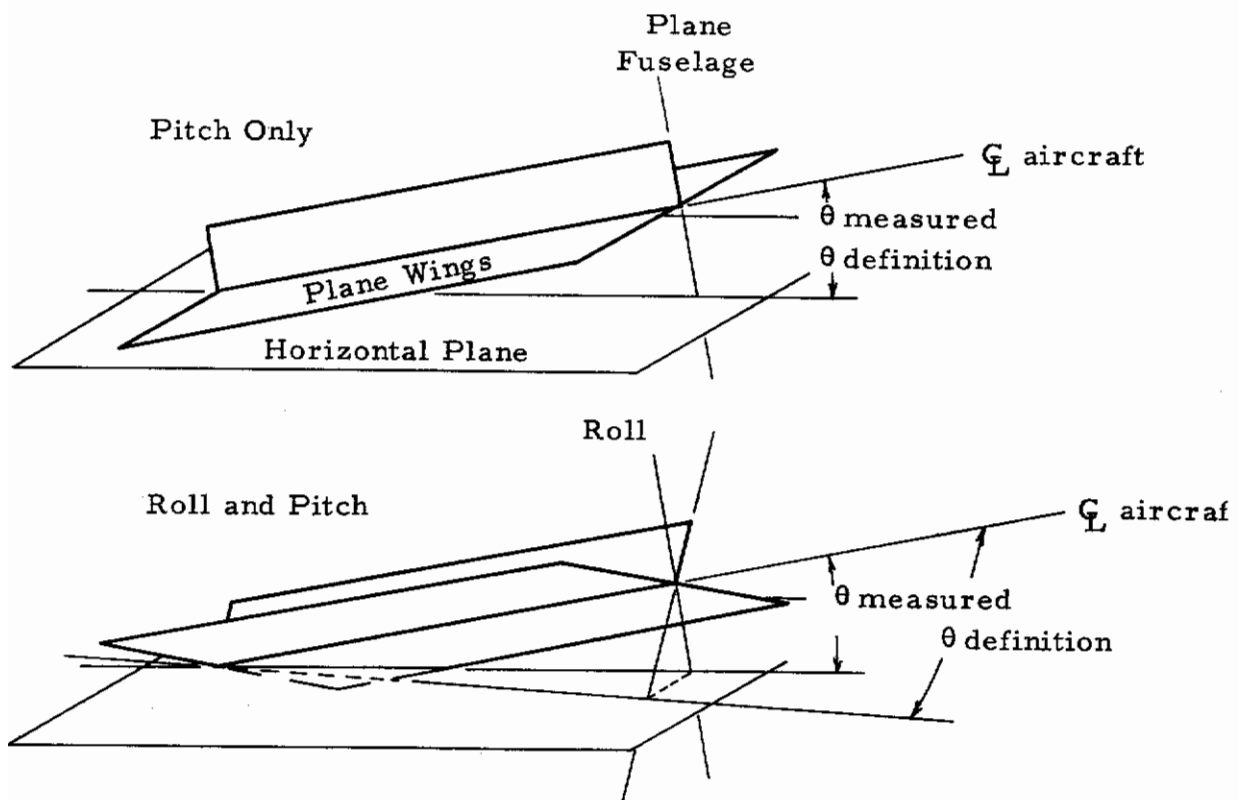


Figure 5-1. Gimbal Error Due to Definition of Pitch Angle

## 5.1.6 Gimbal Lock and Tumbling

If a free or vertical gyroscope is used beyond the angular deflection limits, usually in pitch, mechanical stops are encountered. The outer gimbal turns through 180 degrees about its own or roll axis. This is called gimbal tumbling. If the stops are not employed, the gyro spin axis coincides with the roll axis and the whole assembly begins to spin about the roll axis. Once this has begun, the spin axis remains locked to the roll axis regardless of the aircraft attitude, thus gimbal lock.

## 5.2 FREE GYROSCOPES

A free gyroscope is a two (or three) degree-of-freedom device with gimbals which allow the outer case to rotate with respect to the gyroscope wheel (see Figure 5-1). Conventionally, free gyros have  $360^\circ$  of angular motion about the outer gimbal axis, and slightly less than  $\pm 90^\circ$  of angular motion about the inner gimbal axis. The angular position is sensed with a potentiometer pickoff or three phase synchros located on the outer axis of the gyro. Free gyros exhibit drift phenomena, typically 0.5 degree per minute. Free gyros, therefore, are basically short-term devices. Most models are furnished with torquers to orient the gyroscopic wheel to some desired position. A typical procedure would be to torque the gyro until it was oriented with the aircraft while the aircraft was on the ground. The main advantage of free gyros for experimental flight test use is that large pitch and roll angular displacements can be measured directly. All the major errors of free gyroscopes are covered in the previous discussion, Section 5.1.

## 5.3 VERTICAL GYROSCOPES

Vertical gyroscopes are special free gyroscopes with a gravity sensing device used to continuously or frequently refer the gyroscope back to a known reference. A vertical gyroscope usually has  $360^{\circ}$  of angular motion about the roll axis, and  $\pm 85^{\circ}$  of angular motion about the pitch axis. Vertical gyroscopes are positioned in the vertical axis from signals from the vertical reference sensor by torquers, as indicated in Figure 5-1. The vertical reference is, of course, sensitive to lateral and longitudinal aircraft accelerations. When experiencing maneuvering, the vertical reference sensor is normally disconnected or compensated for. With this restriction in mind, the vertical gyro is a useful tool for experimental flight measurement. The design considerations of vertical gyros are discussed in Reference 15, page 131.

### 5.3.1 Intrinsic Errors, Vertical Gyroscopes

The only significant intrinsic error not covered in Section 5.1 is the vertical reference repeatability. However, in commercially available units which have been designed for navigational purposes, this error is quite small (on the order of 0.2 degrees).

### 5.3.2 Environmental Errors, Vertical Gyroscopes

The environmental errors of vertical gyros are listed in Table 5-2 and are repeated below.

1. Vibration and temperature effects on accuracy
2. Lateral acceleration effects on erection

Temperature variations tend to increase the accuracy error. This error, which is the total effect of nonlinearity errors, hysteresis errors, and resolution errors, is not conveniently expressible as a function of the environment. Vibration effects on drift are covered in Section 5.1.1. The unit employed should be evaluated in the vibration environment anticipated.

Lateral acceleration errors are unique to vertical gyros. The vertical reference pendulum cannot distinguish between earth's gravity and lateral accelerations. A solution would be to design the erection servo loop with a long time constant in order to prevent the gyro from responding to anticipated maneuvers. However, this would make the initial erection time unsatisfactorily long. In addition, the gyroscope should be able to track and correct for the angular rate of change of the earth, 0.2507 degrees per minute. A solution is to employ an erection cutout switch which senses low frequency lateral acceleration. Units of this type can maintain vertical reference within 0.25°. For higher frequency acceleration such as vibration, the response of the servo loop should be investigated (see Reference 23).

## 5.4 RATE GYROS

A rate gyro is a single degree-of-freedom spinning wheel which is restrained. The rate gyro utilizes the precession phenomenon; that is, an input angular velocity produces an output torque which is sensed by measuring the angular displacement of the spin axis perpendicular to the input axis. The main advantages of rate gyros are their small size and ability to measure angular rate directly. The only other commonly used angular rate transducers are stable platforms. The main disadvantage of

rate gyros is that their sensitivity is dependent on the spring constant and gyro speed. The frequency response is developed in Appendix A and is repeated below:

$$H'_{\theta-e_o}(f) = \frac{I_s \Omega K_p}{I_o (2\pi f_n)^2} \frac{1}{\sqrt{\left[1 - \left(\frac{f}{f_n}\right)^2\right]^2 + \left[2\zeta \frac{f}{f_n}\right]^2}} e^{-j\phi(f)} \quad (5.2)$$

$$\phi(f) = \tan^{-1} \frac{2\zeta \frac{f}{f_n}}{1 - \left(\frac{f}{f_n}\right)^2} \quad (5.3)$$

where

$I_s$  - moment of inertia about gyro spin axis, slug feet<sup>2</sup>

$I_s \Omega = H$  - momentum of gyro wheel, foot pound second/radian

$\Omega$  - angular velocity, rotating wheel, radians/second

$K_p$  - pickoff transfer function, volts/radian

$I_o$  - moment of inertia about output axis, slug feet<sup>2</sup>

$f_n = \frac{1}{2\pi} \sqrt{\frac{k}{I_o}}$  - natural frequency, Hz

From inspection of these equations, the following items should be noted:

1. The sensitivity of a particular rate gyroscope with the same pickoff sensitivity,  $K_p$ , is inversely proportional to the natural frequency squared. The sensitivity is inversely proportional



to the full scale range. Therefore, full scale range and natural frequency are related by

$$f_n = C_{FR} \dot{\theta}_{FS}^{1/2} \quad (5.4)$$

The constant  $C_{FR}$  may be considered a figure of merit. The ranges for this constant for commercially available rate gyroscopes are given in Table 5-3.

2. The magnitude of the frequency response function has positive and negative terms and may therefore be essentially constant for certain ranges of damping and frequency. Indeed, from inspection of Figures A-2 through A-4, the frequency response is flat within  $\pm 2\%$  for a damping ratio of 0.64 up to  $f/f_n = 0.6$ .
3. The phase factor is a nonlinear function. See Sections 6.1 and 6.1.1 for further discussion of the variation of time delay with damping and frequency.

Table 5-3. Rate Gyroscopes, Range and Natural Frequency Characteristics

Range of Natural Frequencies, Hz	Full Scale Ranges, Degrees/Sec	Figure of Merit $C_{FR} = f_n / \dot{\theta}_{FS}^{1/2}$
10-150	10-1000	2.0-7.0

#### 5.4.1 Intrinsic Errors, Rate Gyroscopes

Gyroscope errors are listed in Table 5-2. Frequency response and gyro speed variation are error sources which are not covered as common gyroscope errors. The frequency response, when normalized, is identical to that of an open loop accelerometer (Section 6.1.1). The error which re-



sults if a constant sensitivity is assumed is plotted in Figure A-4.

If a constant time delay,  $\tau = 1/4f_n$ , is assumed, an error results. This error is presented in Figure A-5. Accurate knowledge of the time delay characteristics is of prime importance in cross correlation and cross spectra analyses.

The gain factor error is directly related to gyro speed error.

$$\% \text{ error } |H(f)| = \% \text{ error }_{\Omega} \quad (5.5)$$

#### 5.4.2 Environmental Errors, Rate Gyroscopes

Vibration effects are discussed in Section 5.1.1. Temperature variations cause changes in the viscosity of the damping medium. These errors are covered at length in Section 6.1.2. A method for compensating for variation in the damping viscosity is to employ a nylon cylinder as the moving element in the damping device (Reference 3, page 36). As temperature increases, the viscosity decreases, but the nylon expands more rapidly than the case material, closing the narrow damping gap. By proper choice of materials and geometry, the damping variation error may essentially be eliminated over the operating range of the gyroscope.

#### 5.4.3 Usage Errors, Rate Gyroscopes

Typical rate gyroscope usage errors result from

1. Mounting
2. Calibration

If the rotational natural frequency of the gyroscope mounting approaches the frequency range of interest, errors result. However, this should never be a significant error source because of the frequency range of rigid body motion, 0 - 6Hz.

Calibration of rate gyroscopes is performed by aligning the gyro input axis parallel to the axis of rotation of a rate table. The output of the rate gyro is recorded as the rate table input is varied. All parameters of static calibration can be maintained and measured to accuracies much smaller than other errors. The natural frequency, damping, and frequency response are determined either by applying rotational vibration about the input axis or by applying a step input and measuring the gyro output. If the step input technique is employed, the frequency response is inferred from the natural frequency and damping. The best accuracy obtainable for frequency response calibration with state-of-the-art techniques is approximately  $\pm 2\%$ .

## 5.5 RATE INTEGRATING GYROSCOPES

Rate integrating gyros are similar to rate gyros, the difference between the two being in the nature of their respective precession axis restraints. As indicated in Figure 5-1 and discussed in Appendix A, the spring restraint for rate integrating gyros is kept as small as is possible. The major problem with the use of rate integrating gyroscopes for flight loads measurement is the lack of range. Typical units developed for stable platform applications have only one or two degrees full range. However, more recent models designed for strap-down applications have ranges which are as great as  $\pm 20$  degrees. For cases where this limited range would be satisfactory, such as gust response measurement, this type of gyroscope has superior performance characteristics

when compared with free gyroscopes and vertical gyroscopes. The primary performance parameter in this case is the drift rate. Published specifications indicate drift rates as low as 0.01 degree per hour. The frequency response of the rate integrating gyroscope device is developed in Appendix A. The gain factor and phase factor are repeated below for reference.

$$H_{\theta-e_o} = \frac{K H}{c} \frac{1}{\sqrt{1 + \left(\frac{2\pi f I_o}{c}\right)^2}} e^{-j\phi(f)} \quad (5.6)$$

$$\phi(f) = \tan^{-1} 2\pi \frac{I_o}{c} \quad (5.7)$$

where  $c$  - coefficient of viscous damping, inch pound second/radian

The response indicated above is that of a first-order type system. The frequency response is plotted in Figures A-7 and A-8, Appendix A. As can be seen, there is always a gain factor error with frequency when compared with zero frequency response. Typical commercially available units with ranges up to  $\pm 10^{\circ}$  have characteristic times of 0.0006 to 0.004 seconds. Therefore, for the frequency range of interest, 0 to 6Hz, the maximum gain factor error is -1%.

## 5.6 STABLE PLATFORMS

Stable platforms are gyroscopic instruments which incorporate a triad of gyroscopes and accelerometers. The outputs of the gyroscopes

# *Contrails*

and accelerometers are operated upon and used to position or control the gimbals which support the platform on which the gyros and accelerometers are mounted. Different schemes or configurations are used to correct for the rotation of the earth and to produce output signals of azimuth, pitch, and roll. Stable platforms are characteristically very high accuracy devices with drift rates from  $.001^{\circ}$  per hour to  $.5^{\circ}$  per hour.

## 6. ACCELEROMETERS

In experimental flight loads determination, accelerometers are used for the measurement of four classes of aircraft motion. These are as follows:

1. localized and rigid body velocities (for gust velocity correction)
2. rigid body aircraft response accelerations
3. aircraft modal response accelerations
4. localized aircraft vibration accelerations

The different measurements impose slightly different requirements on accelerometer characteristics. An accelerometer used for the gust velocity should be located in the boom near the angle of attack sensor. A small, light-weight accelerometer is advantageous for this application. The approximate frequency range is from 0 to 20 Hz. In addition, the accelerometer mounted in the boom will probably experience a more hostile temperature environment than experienced by an accelerometer mounted within the aircraft fuselage.

An accelerometer used to measure aircraft rigid body response accelerations should be mounted as close as is feasible to the aircraft center of gravity. The size of this accelerometer is limited only by the available space, the mounting natural frequency, and the load carrying capacity of the aircraft. The approximate frequency range of interest is from 0 to 6 Hz.

For the measurement of modal response accelerations, a small unit is desirable, mainly because of space limitations of the remote areas of aircraft. The frequency range of interest is from 0 Hz to approximately 50 Hz.

Accelerometers used for the fourth class of aircraft motion measurement, localized vibration, are necessarily small compared with the part being monitored and have useful frequency ranges from 5 Hz up to as high as 3K Hz. The instrumentation for these types of measurements is similar to and in some cases identical to the instrumentation employed for the other applications. However, the study of the unique requirements, problems, and errors of "vibration" instrumentation is beyond the scope of this report.

A number of different types of accelerometers are suitable for experimental flight test programs. These types are as follows:

1. variable inductance (variable inductance and differential transformer)
2. potentiometer
3. strain gage (wire)
4. piezoresistive (semiconductor strain gage)
5. servo or force balance
6. piezoelectric (quartz)

All six types of accelerometers function in a similar manner. An inertial mass is suspended within the case of the unit. Accelerations of the case cause forces and relative motions between the case and the mass. These forces and/or motions can be converted to electrical signals; whereas no simple, practical methods exist for converting acceleration to electrical signals directly. The variable inductance, potentiometer, unbounded

# Contrails

strain gage, and piezoresistive accelerometers are essentially identical in principle, and merely employ different relative displacement pickoff devices. The servo or force balance type accelerometer produces an electrical current proportional to the force necessary to restore the inertial mass to the zero or no-displacement position. This current is proportional to the applied acceleration. The piezoelectric type accelerometer employs a crystal as the spring supporting the inertial mass. The crystal generates an electrical charge proportional to the applied force. A comparison of the advantages and disadvantages of the different types of accelerometers for flight loads measurement is presented in Table 6-1. In addition to the type of relative displacement pickoff device, accelerometers are classified by the type of damping employed. The advantages and disadvantages of various damping methods are discussed in Section 6.1.2.

Other types of accelerometers have been developed, usually for specific uses, but have not been generally adopted for flight loads measurement. Two such types are the variable capacitance and vibrating string accelerometers. The variable capacitance type is similar to the potentiometer, etc., using a variable capacitance pickoff. The vibrating string accelerometer utilizes a mass suspended by a pair of taut strings. Acceleration of the mass causes a change in the difference of the frequencies of the strings. Counting the cycles gives a digital readout. This type of accelerometer has many advantages for inertial navigation, but manufacturing difficulties and low frequency response make it undesirable for flight loads measurement (see Reference 13).

In addition to accelerometers, velocity transducers may be used to measure aircraft motion. Two such devices are the inertial, self-generating velocity probe and the pendulus integrating gyroscope accelerometer, or PIGA. The main disadvantage of the self-generating or dynamic velocity transducer is that the frequency response is approximately constant



Table 6-1. Comparison of Types of Accelerometers for Dynamic Measurements

Type of Accelerometer	Major Advantages	Major Disadvantages
Variable inductance (variable reluctance and differential transformer)	High resolution Rugged	Large size Precision AC source required Demodulation required Damping temperature sensitive
Potentiometer	Large DC output (no amplifier required) Rugged Simplicity	Finite resolution Low natural frequency Damping temperature sensitive Wiper vibration sensitive Precision DC or AC source required
Strain gage (wire)	High natural frequency Small size Continuous resolution	Precision DC or AC source required DC amplifier or demodulation required Damping temp. sensitive
Piezoresistive (semiconductor strain gage)	High output High natural frequency	Precision DC or AC source required
Servo (force balance)	High accuracy Continuous resolution High output Self test feature	Low natural frequency Frequency response poor Complex
Piezoelectric (quartz)	High frequency response Small size and weight Self-generating Rugged	No DC response Low sensitivity Special amplifier required



only for frequencies above the natural frequency (Reference 1, p. 81). The PIGA is a single axis gyro with a mass unbalance. Acceleration of the mass causes a gyro precession velocity. Integration shows precession displacement to be proportional to applied linear velocity (see Reference 13). This high accuracy device would be suitable for flight loads measurement but, because of limited general application, is not considered an off-the-shelf item. The schematics of the various types of accelerometers are shown in Figure 6-1. The various elements are defined and discussed in the following text and in Appendix A.

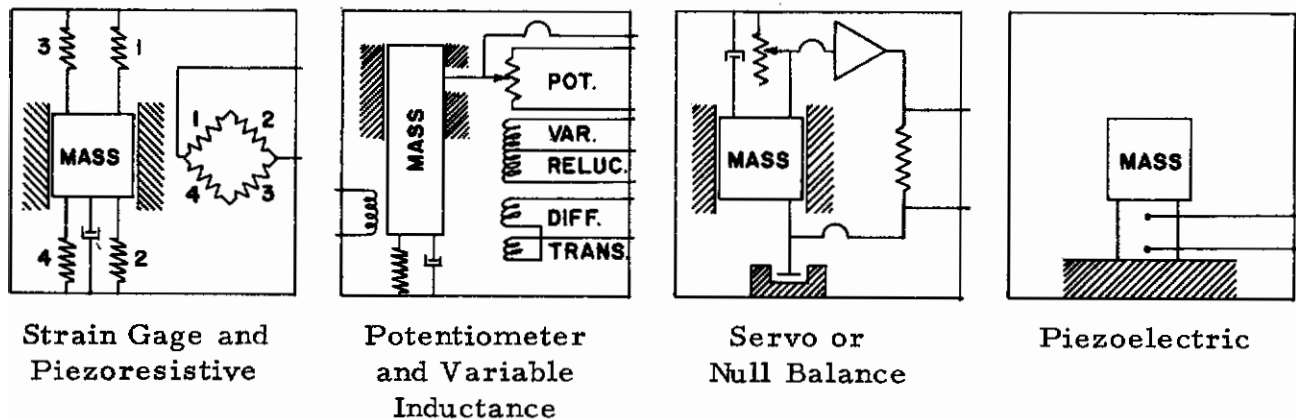


Figure 6-1. Accelerometer Schematics

## 6.1 VARIABLE RELUCTANCE, POTENTIOMETER, STRAIN GAGE, AND PIEZORESISTIVE ACCELEROMETERS

These four different types of accelerometers function in essentially the same manner. The main difference between the four different types is, as previously indicated, the type of pickoff device employed. The amount of relative motion between the mass and the case is determined by the nature of the pickoff device. For example, piezoresistive and strain gage types require only a few thousandths of an inch displacement to obtain full scale output. On the other hand, the potentiometer type requires a much larger displacement, on the order of a tenth of an inch, for full scale (see Table 3.2).

# Contrails

The frequency response function for all four types of accelerometers is given in Appendix A. This equation is repeated below for reference.

$$H(f)_{a-e_o} = K_p \frac{1}{(2\pi f_n)^2} \frac{1}{\sqrt{\left[1 - \left(\frac{f}{f_n}\right)^2\right]^2 + \left[2\zeta\left(\frac{f}{f_n}\right)\right]^2}} e^{-j\phi(f)} \quad (6.1)$$

$$\phi(f) = \tan^{-1} \frac{2\zeta \frac{f}{f_n}}{1 - \left(\frac{f}{f_n}\right)^2} \quad (6.2)$$

where  $H(f)_{a-e_o}$  — frequency response function  
base acceleration to output  
 $K_p$  — pickoff transfer function, volts/feet  
 $\phi(f)$  — phase lag, output voltage to applied acceleration

From inspection of these equations, the following items should be noted.

1. The sensitivity of a particular accelerometer with the same pickoff sensitivity,  $K_p$ , is inversely proportional to the natural frequency squared. The full scale acceleration range will be inversely proportional to sensitivity; the less sensitive the accelerometer the greater the acceleration level required to obtain full scale output. Therefore, full scale range and natural frequency are related by

$$f_n = C_{FR} g_{FS}^{1/2}$$

The constant  $C_{FR}$  may be considered a figure of merit. The ranges of this constant for the various types of commercially available accelerometers are given in Table 6-2.

# Contrails

2. The magnitude of the frequency response function has positive and negative terms and may therefore be essentially constant for certain ranges of damping and frequency. Indeed, from inspection of Figures A-2 - A-4, the frequency response is flat within +2% for a damping ratio of 0.64 up to  $f/f_n = 0.6$ .
3. The phase factor is a nonlinear, arctangent function of the frequency ratio. Reference 18, page 22, points out that the requirement for linear phase factor would be that  $d\phi / d(f/f_n)$  be a constant

$$\frac{d\phi(f)}{d(f/f_n)} = \frac{2\zeta[1 + (f/f_n)^2]}{\left(\frac{f}{f_n}\right)^4 + \left(4\zeta^2 - 2\right)\left(\frac{f}{f_n}\right)^2 + 1} = \text{constant} \quad (6.3)$$

The only value for which this is true is  $\zeta = 0$ . However, for a damping ratio of 0.7 the phase factor approaches a linear function. If a linear phase shift of the form  $\phi(f) = \pi f / 2f_n$  is assumed (see Figure A-3), the output of the transducer will be delayed by  $1/4f_n$  seconds from the applied acceleration. That is

$$\tau = \frac{\phi(f)}{2\pi f} = \frac{\pi f}{(2f_n) 2\pi f} = \frac{1}{4f_n} \quad (6.4)$$

where  $\tau$  = time delay, seconds.

Table 6-2. Comparison of Accelerometer Natural Frequency and Range

Type Accelerometer	Range of Natural Frequencies, Hz	Figure of Merit $C_{FR} = f_n / g_{FS}^{1/2}$
Variable reluctance	5.5 - 750	2 - 72
Potentiometer	9 - 130	4.5 - 20
Strain gage	25 - 900	25 - 170
Piezoresistive	2700 - 12,000	540 - 760
Servo	8 - 700	10 - 200

## 6.1.1 Intrinsic Errors — Variable Reluctance, Potentiometer, Strain Gage, and Piezoresistive Accelerometers

The types of intrinsic errors common to these types of accelerometers are as follows:

1. Amplitude and phase frequency response errors
2. Resolution errors in the pickoff device
3. Amplitude linearity
4. Hysteresis
5. Cross axis sensitivity

The deviation of the sensitivity from a constant value as a function of frequency and damping is represented by the frequency response expression, Eq. (6.1). The error which results if a constant sensitivity is assumed is as follows:

$$\% \text{ error} = \frac{1 - \sqrt{\left(1 - \frac{f^2}{f_n^2}\right)^2 + \left(2\zeta \frac{f}{f_n}\right)^2}}{\sqrt{\left(1 - \frac{f^2}{f_n^2}\right)^2 + \left(2\zeta \frac{f}{f_n}\right)^2}} 100 \quad (6.5)$$

This error is plotted as a function of  $\zeta$  and  $(f/f_n)$  in Figure A-4. In order to remain within a specified accuracy, the upper frequency must be restricted and the damping ratio controlled.

The deviation from zero delay between applied acceleration and response as a function of frequency and damping is represented in the phase lag expression, Eq. (6.2). The error which results if a constant time delay,  $\tau = 1/4f_n$ , is assumed as follows:

$$\% \text{ error}_{\tau} = \left[ \frac{2}{\pi} \left( \frac{f}{f_n} \right) \tan^{-1} \frac{2\zeta \frac{f}{f_n}}{1 - \left( \frac{f}{f_n} \right)^2} - 1 \right] 100 \quad (6.6)$$

This error is plotted in Figure A-5. Nonlinear or non constant time delays cause distortion of complex waveforms. Accurate knowledge of the time delay characteristics is of prime importance in cross correlation and cross spectra analyses.

Resolution errors of the pickoff device are covered in Section 3. Resolution errors for commercially available units are small compared with the other types of intrinsic errors.

Amplitude linearity is the deviation from constant sensitivity as a function of amplitude. This error by definition is a bias error because it is systematic or reproducible. Hysteresis is the inability to return to zero output with zero acceleration. For a single cycle, this error appears as an amplitude nonlinearity. Hysteresis is a bias error if it can be reproduced in controlled tests. However, two factors make error correction difficult.

1. With complex motion, the hysteresis correction would be a unique function dependent on the preceding time history.

2. The magnitude of the hysteresis is usually small compared with accuracy of the accelerometer and the calibration device.

For commercially available accelerometers, amplitude nonlinearity and hysteresis are combined. Typical values for the different types of accelerometers are given in Table 6-3.

Table 6-3. Typical Values of Accelerometer Amplitude Nonlinearity and Hysteresis Errors

Type Accelerometer	Combined Amplitude Nonlinearity and Hysteresis Errors
Variable reluctance	$\pm 0.5\% - \pm 2.5\%$ Full scale
Potentiometer	$\pm 0.75\% - \pm 2.5\%$ Full scale
Strain gage	$\pm 0.75\% - \pm 1\%$ Full scale
Piezoresistive	$\pm 1\%$ Full scale

Cross axis sensitivity is the response to acceleration in the axis perpendicular to the sensitive axis. The percent error in the measurement of acceleration along the sensitive axis is given by:

$$\% \text{ error} = \lambda_a \frac{\ddot{x}_T(t)}{\ddot{x}(t)} \quad (6.7)$$

where  $\lambda_a$  = percent response to transverse acceleration. Typical values of  $\lambda_a$  quoted in specifications for these types of accelerometers range

from 0.5% to 3%. The specifications apply to static acceleration. Little work to determine cross axis sensitivity as a function of frequency for these types of accelerometers has been performed. A method for testing at low frequencies is outlined in Reference 1, Section 12.

## 6.1.2 Environmental Errors – Variable Reluctance, Potentiometer, Strain Gage, and Piezoresistive Accelerometers

The types of environmental errors common to these types of accelerometers are as follows:

1. Variation of the damping constant with temperature
2. Variation of the electrical characteristics with temperature
3. Catastrophic failure due to elevated temperature
4. Vibration effects

Damping of these types accelerometers is usually accomplished with a dashpot of some kind using a silicone fluid or a gas. The viscosity characteristics of liquids vary significantly with temperature. Silicone fluid is chosen because its viscosity change is small compared with petroleum oils. The viscosity change affects the damping characteristics and therefore the frequency response. Reference 1, page 45, Reference 2, pages 12-23, and Reference 19 present typical plots of the variations of damping ratio with temperature. Such a plot is presented as Figure 6-2.

If an accelerometer is calibrated at one temperature and used at another temperature, the viscosities of the damping fluid will change

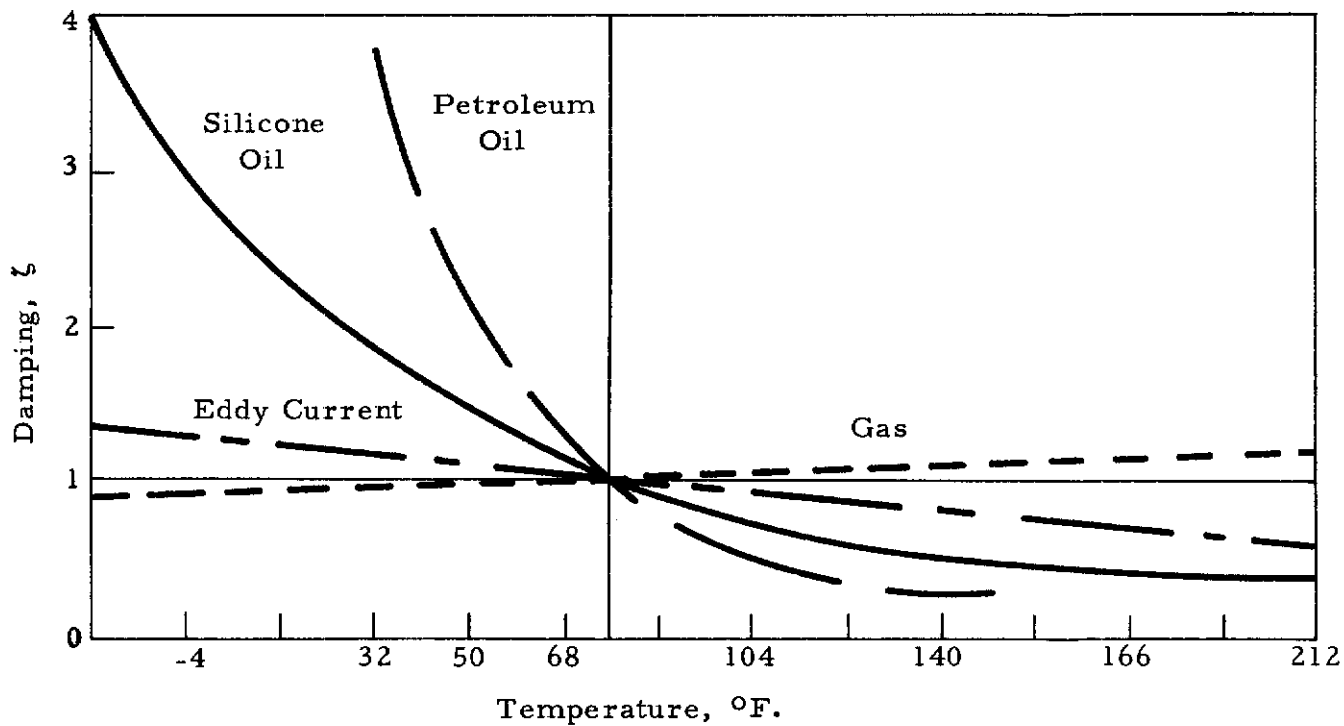


Figure 6-2. Variation of Damping with Temperature Referenced to 77 $^{\circ}\text{F}$ .

and the frequency response will vary. The amplitude error resulting from this temperature change is given by:

$$\% \text{ error} = \frac{|H(f)|_{\zeta_{\text{use}}} - |H(f)|_{\zeta_{\text{cal}}}}{|H(f)|_{\zeta_{\text{cal}}}} \cdot 100 \quad (6.8)$$

When  $\zeta_{\text{cal}} = 0.707$ , the expression for  $\zeta_{\text{use}}$  as a function of frequency and % error becomes

$$\zeta_{\text{use}} = \frac{1}{2} \sqrt{\left[ \frac{1}{1 + \frac{\% \text{ error}}{100}} - 1 \right] \left[ \left( \frac{f}{f_n} \right)^2 - \left( \frac{f_n}{f} \right)^2 \right] + 2}$$



This expression is presented in Figure 6-3. Constant error is plotted against frequency and damping. In addition, the ordinate is scaled in temperature for different types of damping. The frequency response and time delay errors become extremely large at the low temperatures of high altitude flight. For gas damped units the effect of temperature on damping is much smaller than for liquid damped units. In addition to temperature insensitivity, gas damped units may have nominal frequency response characteristics which are more desirable than those of accelerometers with other types of damping (Reference 17). Damping is effected by pumping the gas through a porous plug. As a result, the response is slightly different from that of a simple, single-degree-of-freedom system.

Techniques for minimizing errors in frequency response due to temperature are as follows:

1. Control the temperature of the accelerometer
2. Select an accelerometer with minimum viscosity change with frequency
3. Use the accelerometer up to a frequency which is a small fraction of its natural frequency
4. Measure the temperature of the accelerometer and apply a suitable correction to the measured data

### 6.1.3 Usage Errors - Variable Reluctance, Potentiometer, Strain Gage, and Piezoresistive, Servo and Piezo-electric Accelerometers

The usage errors common to all types of accelerometers are as follows:

1. Misalignment
2. Improper installation
3. Mounting natural frequency
4. Calibration errors

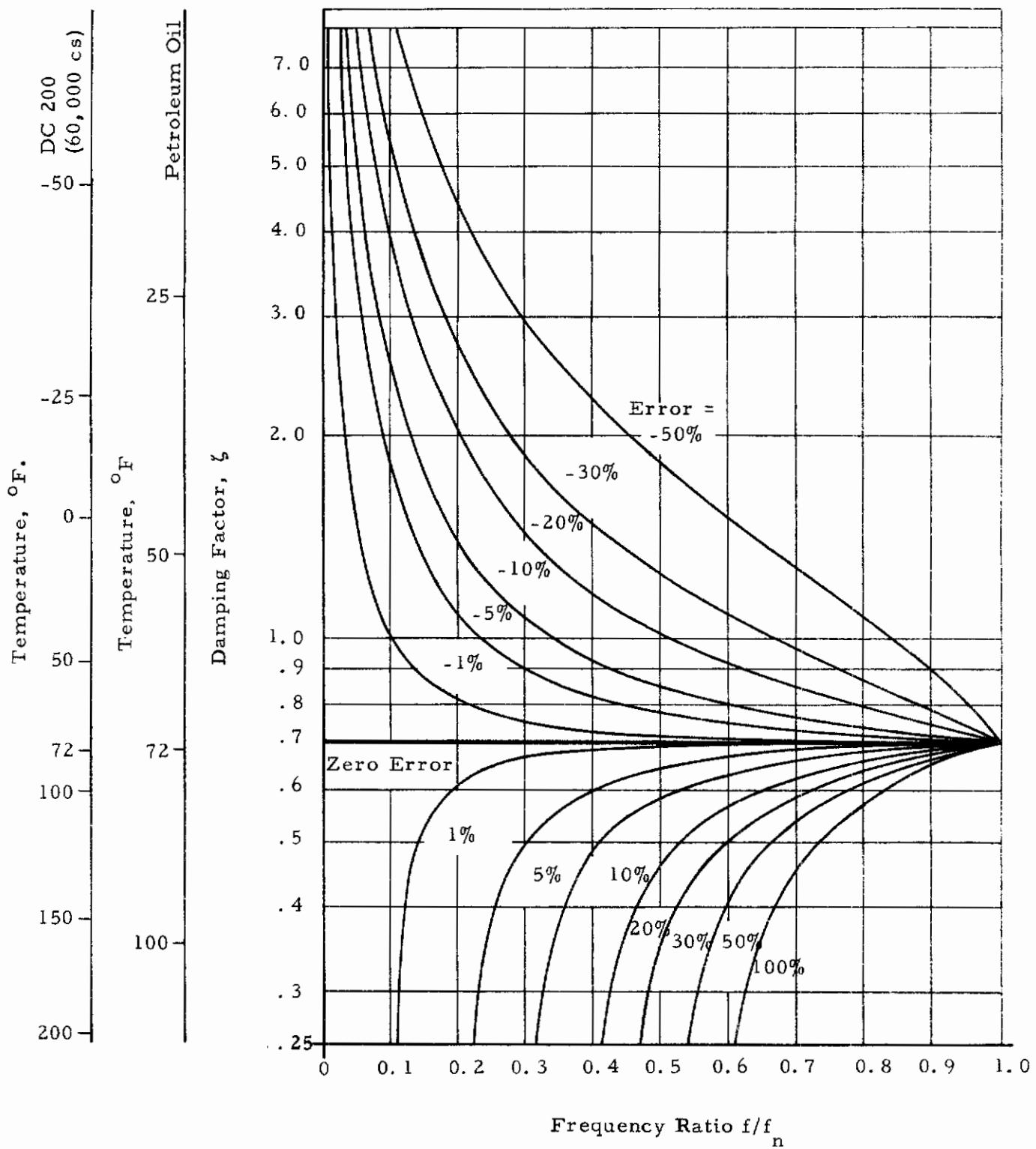


Figure 6-3. Calibrated Accelerometer Frequency Response Error versus Frequency Ratio and Damping Factor

Misalignment between the accelerometer sensitive axis and the desired axis causes an erroneous reading. This error is a function of the acceleration along all three axes and the angles of misalignment. If all these quantities are known, corrections to the measurement can be made using simple geometric relationships.

To compare the magnitude of this error with other errors, consider the common case of misalignment in one plane, Figure 6-4 with the transverse acceleration greater than the acceleration to be measured as indicated in Figure 6-5.

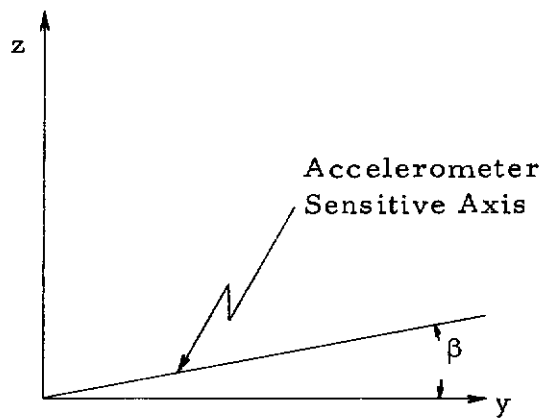


Figure 6.4 Accelerometer Misalignment

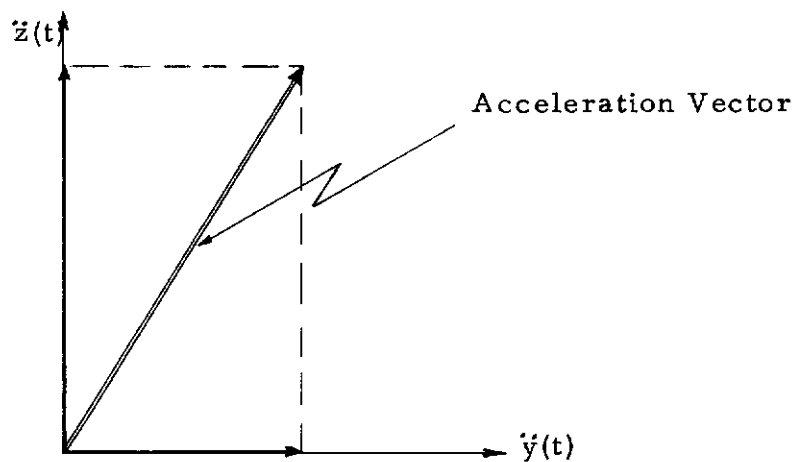


Figure 6.5 Acceleration Vector

The measured acceleration is given by Eq. (6.10) and shown in Figure 6-6.

$$a(t) = \ddot{y}(t) \cos \beta + \ddot{z}(t) \sin \beta \quad (6.10)$$

where

- $a(t)$  - accelerometer sensitive axis acceleration, g's
- $\ddot{y}(t)$  - acceleration to be measured, g's
- $\ddot{z}(t)$  - transverse acceleration, g's
- $\beta$  - misalignment angle, degrees

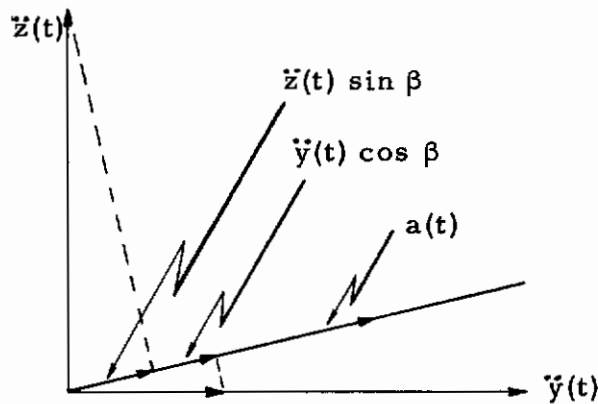


Figure 6.6 Accelerometer Misalignment Error

The error in the measurement of  $\ddot{y}(t)$  is

$$\% \text{ error} = \left[ 1 - \cos \beta + \frac{\ddot{z}(t)}{\ddot{y}(t)} \sin \beta \right] 100 \quad (6.11)$$

for small angles of misalignment and large transverse acceleration, the error may be approximated by

$$\% \text{ error} = \frac{\ddot{z}(t)}{\ddot{y}(t)} \beta \quad (1.75) \quad (6.12)$$

This error may easily be as large or larger than any other error discussed. For example, in maneuvering, the acceleration ratio  $\ddot{z}(t)/\ddot{y}(t)$  may be as great as 15. The error for a small misalignment,  $\beta = 1^\circ$ , then becomes 26.26%. Note that the accelerations are the instantaneous values.

If the accelerometer is improperly installed, relative motion between it and the member to which it is mounted can occur. Installation errors are usually associated with high frequency vibration measurement. The displacements associated with the accelerations and frequencies in loads measurement are much larger than the displacements associated with poor installation. Therefore, improper installation is not a significant error source in this application. The very process of acceleration measurement influences the acceleration being measured.

Two types of acceleration motion are commonly measured, aircraft rigid body motion,  $\dot{\mathbf{x}}_1(t)$  Figure 6-7, and modal response,  $\dot{\mathbf{x}}_2(t)$  Figure 6-7. The installation of the accelerometer can affect these measurements. To minimize the effect of the accelerometer, the following mounting guidelines should be observed.

<u>Type Motion Measurement</u>	<u>Proper Mounting Guideline</u>
Aircraft Rigid Body	Combined Structure - Accelerometer natural frequency well above rigid body frequencies
Modal Response	Accelerometer small compared with mounting structure

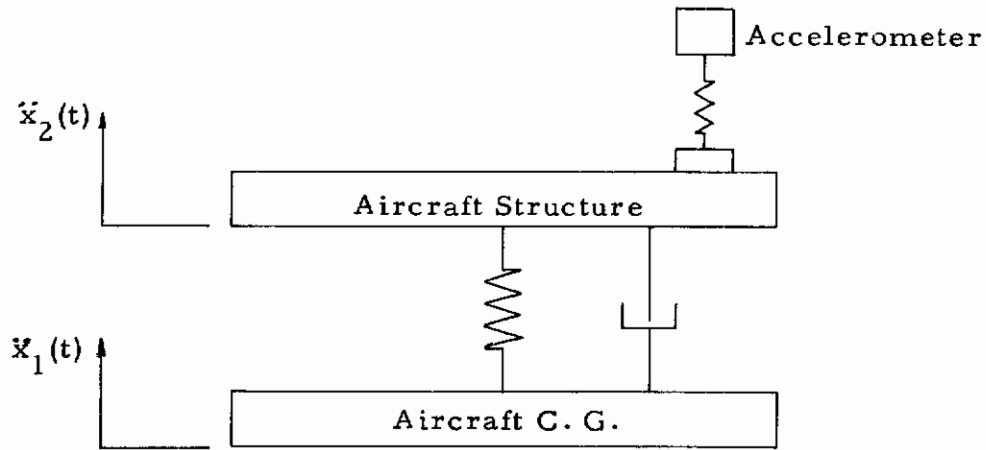


Figure 6.7 Effect of Accelerometer Mounting

The calibration of accelerometers is a subject by itself. A number of basically different techniques or approaches are used. These are as follows:

- (1) two g or intermediate turnover calibration
- (2) comparison with standard accelerometers
- (3) displacement measurement at specific frequency
- (4) infarametric techniques
- (5) reciprocity

For relative low frequency, high sensitivity accelerometers which are used for experimental flight test programs, the turnover or two g calibration is extremely useful and accurate. The primary error

# Contrails

associated with this technique is that the maximum range is  $\pm$  one g, whereas the range of the accelerometer may be up to twenty times that value. The error which results from extrapolation of the one g calibration to a higher level is a function of the accelerometer linearity. In addition, this calibration is applicable only for quasi-static acceleration measurements. An extension of this technique is to put the accelerometer on a horizontal centrifuge and expose it to a higher level static acceleration. The acceleration is proportional to radius. It is important to use the radius to the center of the accelerometer mass to determine applied acceleration. If the centrifuge is oriented vertically, a  $\pm$  one g input is superimposed upon the nominal centripetal acceleration. The most common method for calibrating accelerometers which are used at higher frequencies is the comparison method. The accelerometer to be tested is mounted adjacent to a standard accelerometer, and their outputs compared over a frequency range. The error associated with this technique is of course the error of the standard accelerometer combined with the error of the measuring equipment. Another frequency calibration is performed by measuring the displacement of the sinusoidal motion of the accelerometer and then comparing the accelerometer output with the calculated acceleration. For low frequencies, below 100 Hz, the displacement is usually measured with a microscope with a precision graticule. For frequencies from 2000 to 10,000 Hz, the displacement may be measured using fringe disappearance interferometric techniques. This procedure requires essentially distortion-free sinusoidal excitation. The reciprocal or reciprocity method consists of measuring transfer, admittance, voltage ratio, frequency, and mass, and requires special equipment, see Reference 89. Reference 20 presents a summary of calibration methods and standards.



## 6.2 SERVO ACCELEROMETERS

The servo or force balance accelerometer is a null seeking, closed loop device. It is similar to an open loop type accelerometer where the restoring force or spring is supplied by an electrical feedback loop. Presently available commercial servo accelerometers have been developed primarily for inertial navigation purposes. This application takes advantage of the extremely high accuracy and resolution which are obtainable with a servo type device. A thorough analysis of the force balance accelerometer requires the well developed theory of servo practice. However, for the purposes of this report, it will suffice to discuss the operating principles and to investigate an approximation of the frequency response function. The schematic and functional block diagram for a servo accelerometer is presented in Figure A-6, Appendix A. Accelerations cause relative displacements between the accelerometer case and inertial mass. This displacement is sensed, amplified, and used as a feedback signal to restore the mass to a point of zero displacement. The electrical current used to provide the restoring force is used as the measure of the accelerometer output. The frequency response function for a servo accelerometer is developed in Appendix A and is repeated below for reference.

$$H(f) = \frac{R_l m}{K_f} \frac{\sqrt{1 + \left(2\zeta_2 \frac{f}{f_n}\right)^2}}{\sqrt{\left[1 - \left(\frac{f}{f_n}\right)^2\right]^2 + \left[2\left(\zeta_1 + \zeta_2\right) \frac{f}{f_n}\right]^2}} e^{-j\phi f} \quad (6.14)$$

$$\phi(f) = \tan^{-1} \frac{2\left(\frac{f}{f_n}\right)\zeta_1 + 2\left(\frac{f}{f_n}\right)^2\zeta_2}{1 - \left(\frac{f}{f_n}\right)^2 + 4\left(\frac{f}{f_n}\right)^2\zeta_2(\zeta_1 + \zeta_2)} \quad (6.15)$$



# Contrails

where  $\zeta_1 = \frac{c}{4\pi f_n m} = \text{mechanical damping}$  (6.16)

$$\zeta_2 = \pi f_n \psi = \text{electrical damping} \quad (6.17)$$

$$f_n = \frac{1}{2\pi} \sqrt{\frac{K_f K_p K_a}{R_\ell m}} \quad (6.18)$$

$R_\ell = \text{load resistance, ohms}$

$K_a (\psi p + 1) = \text{feedback amplifier transfer function}$

$K_f = \text{restoring coil transfer function, lbs/ampere}$

$K_p = \text{pickoff transfer function, volts/feet}$

From inspection of these equations, the following items should be noted:

1. Sensitivity is a function of the inertial mass, the force coil transfer function, the load resistance, and the dimensionless gain factor, not the pickoff and amplifier transfer function.
2. If the damping is all mechanical,  $\zeta_2 = 0$ , the frequency response function for open loop accelerometers applies (Figures A-2 through A-5). If the damping is all electrical,  $\zeta_1 = 0$ , the frequency response functions (Figures A-7 and A-8) apply.
3. If the damping is mechanical, the damping is inversely proportional to the natural frequency, whereas if electrical damping is employed, the damping is directly proportional to the natural frequency.
4. If the servo accelerometer is damped as an open loop accelerometer, the relationship between the full scale range and natural frequency is the same as for the open loop accelerometer. The ranges of natural frequency for commercially available units and the corresponding figures of merit are presented in Table 6-2.

The major advantages of servo accelerometers are their high accuracy and resolution achieved by the elimination of the mechanical spring. An additional advantage is that the accelerometer may be excited by an externally applied electrical signal. This self-test feature may be extremely valuable for certain applications. Another advantage is that the natural frequency is a function of the amplifier gain which may be made large with little adverse effect. The servo accelerometer is a basically stable device (Reference 1, page 363). References 3 and 21 present general, descriptive material on servo accelerometers.

## 6.2.1 Intrinsic Errors, Servo Accelerometers

Servo accelerometers have the same type intrinsic errors as closed loop accelerometers. These are as follows:

1. Amplitude and phase frequency response errors
2. Resolution errors
3. Amplitude linearity
4. Hysteresis
5. Cross axis and torsional sensitivity

The amplitude and phase frequency response errors are described in Appendix A. Since damping may be effected in one of two ways with correspondingly different frequency response functions, the particular gain factor and phase factor should be evaluated for each individual accelerometer.

The resolution, amplitude linearity, and hysteresis errors for servo accelerometers are extremely small, on the order of 0.01%,

and may be neglected when compared with other errors.

One inherent error of the servo type accelerometer is the sensitivity to torsional acceleration. Design considerations call for minimum restraint of the mass. One technique for achieving minimum restraint is to suspend the mass pendulously with jewelled bearings. The error if the accelerometer senses angular acceleration as well as normal acceleration is as follows:

$$\text{error} = \frac{2\ddot{\theta}r}{\ddot{x}} \quad (100)$$

where  $\ddot{\theta}$  is the angular acceleration,  $r$  is the radius or length of pendulum, and  $\ddot{x}$  is the normal acceleration. In order to overcome this error, servo accelerometers are designed to be non-pendulous, the inertial mass being supported by a system of flexures which are stiff in the transverse and rotational directions.

### 6.2.2 Environmental Errors, Servo Accelerometers

The major environmental errors are as follows:

1. Variation of the damping constant with temperature
2. Variation of the load resistance with temperature

A major advantage of servo type accelerometers is that the damping may be made independent of temperature. If only electrical damping is used, damping is independent of temperature, and the frequency response functions (Figures A-7 and A-8) apply. Note that a constant gain factor occurs with very high damping ratios. Also note that the

damping is a function of the natural frequency, Eq. (6.18). Therefore, a double benefit is obtained from having the amplifier gain as high as stability and other considerations permit. If damping is mechanical, the frequency response errors of open loop accelerometers (Figure 6-3) apply. However, in this case, damping is inversely proportional to natural frequency, Eq. (6.16), and an optimum amplifier gain should be chosen.

The amplifier output is essentially a current which is proportional with acceleration. Variation in load resistance with temperature causes a corresponding error in the accelerometer output.

### 6.2.3 Usage Errors, Servo Accelerometers

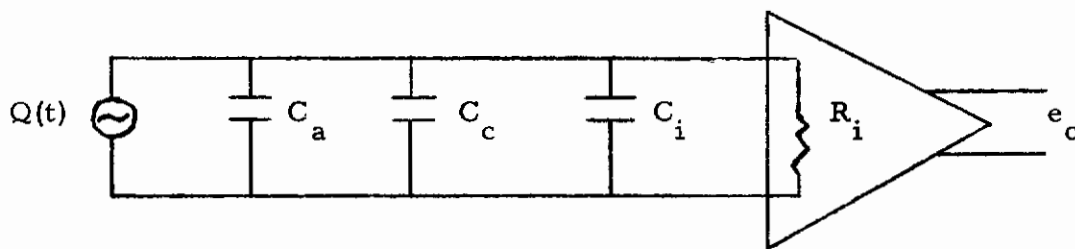
See Paragraph 6.1.3 for usage errors of all types of accelerometers.

## 6.3 PIEZOELECTRIC (QUARTZ) ACCELEROMETERS

Piezoelectric (quartz) accelerometers are listed as acceptable acceleration transducers for experimental test flight programs because of their small size and a flat frequency response approaching DC. Piezoelectric accelerometers of materials other than quartz exhibit a phenomenon called the pyroelectric effect. Temperature gradients cause extraneous signals to be generated in the frequency range from DC to 4 or 5 Hz. Quartz type crystals are much more stable and do not exhibit this effect. They may be used to as low as 0.5 Hz with an appropriate amplifier. However, even though quartz type piezoelectric accelerometers have a low frequency response which is superior to

piezoelectric accelerometers of different materials, the major errors are still the amplitude and phase variations at low frequencies. The piezoelectric accelerometer produces an electrical output charge proportional to the force on a crystal. The crystal is employed as a spring in a lightly damped spring mass system. A more complete review of piezoelectric accelerometers, including a discussion of the mechanism for charge generation, is presented in Reference 1, Section 4.6, Reference 2, Chapter 16; and Reference 3, page 257.

Two different types of amplifiers are commonly used with piezoelectric accelerometers. These are high input impedance voltage amplifiers and charge amplifiers. With voltage amplifiers the output voltage is a function of the external capacitance and the frequency response function of the RC circuit as well as the amplifier gain (see the equivalent circuit below and Eq. (6.19) ).



$$e_o = \ddot{x} K_a \frac{K_q}{C_a + C_c + C_i} \left[ \frac{1}{1 + \frac{1}{j2\pi f R_i C_t}} \right] \quad (6.19)$$

where

$K_q = K_e C_a$  — accelerometer charge sensitivity,  
picocoulombs/g

$K_e$  — accelerometer open circuit voltage  
sensitivity, volts/g

# Contrails

$Q(t) = \ddot{x}(t) K_q$  — accelerometer charge output

$C_a$  — accelerometer capacitance, picofarads

$C_c$  — cable capacitance, picofarads

$C_i$  — amplifier input capacitance, picofarads

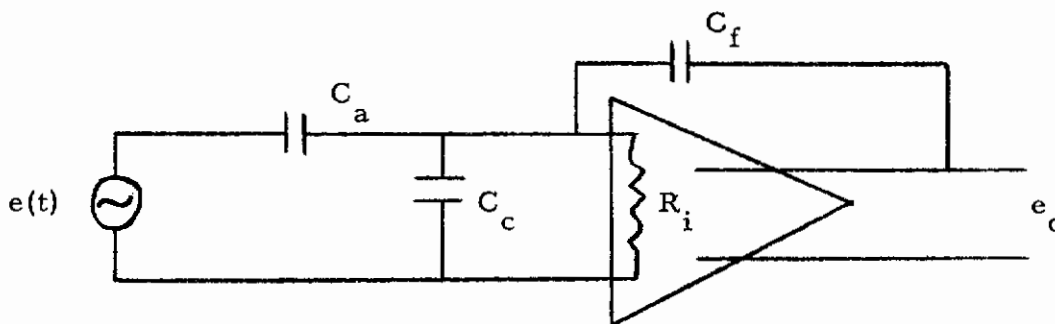
$R_i$  — amplifier input resistance, ohms

$C_t = C_a + C_c + C_i$

$K_a$  — amplifier gain, nondimensional

$\ddot{x}(t)$  — accelerometer acceleration, g

A charge amplifier is essentially an operational amplifier with capacity feedback. By summing current at the junction on the input of the amplifier, the output as a function of the acceleration is obtained.



$$e_o = -\ddot{x}K_q \frac{1}{C_f \left[ \left( 1 + \frac{1}{K_a} \right) + \frac{C_a + C_c}{K_a C_f} + \frac{1}{j2\pi R_i C_f K_a} \right]} \quad (6.20)$$

$$\approx \frac{-\ddot{x}K_q}{C_f \left[ 1 + \frac{1}{j2\pi R_i C_f K_a} \right]}$$

where

$$e(t) = \ddot{x}(t) K_e = \frac{\ddot{x}(t) K_q}{C_a} - \text{accelerometer voltage output}$$

$C_f$  - feedback capacitance, picofarads

With both types of amplifiers, the low frequency response is determined by an RC product. For a charge amplifier, large effective input capacity results from large amplifier gains. In actual practice, the charge would continue to accumulate on the feedback capacitor. Therefore, a resistor is usually installed in parallel with the feedback capacitor, and the RC product becomes  $R_f C_f$ . With typical values, the low frequency cutoff frequency ranges from 0.25 to 5 cps.



## 7. STRAIN GAGES

Variable resistance strain gage systems are widely used for the direct measurement of static and dynamic strains. In addition, they are used to measure many other physical quantities such as stress, load, and pressure when oriented, installed, and calibrated in an appropriate manner. The primary element in a strain gage system is the gage itself. The other elements of a strain gage system for flight loads measurement are an excitation source or power supply, circuitry for balancing out DC voltages and standardizing or calibrating the recording system, an amplifier, a lowpass filter, and a recorder, as indicated in Figure 2-4.

Variable resistance strain gages are available for mounting in either bonded or unbonded form. The resistance element is conventionally wire or foil. Two special types of strain gages, fatigue sensitive wire or foil and strain sensitive solid state or semiconductor gages have received considerable attention and/or use in recent years because of their unique properties. Fatigue sensitive gages are not covered in this report. For more information on this subject, see References 26 and 34. Semiconductor gages or transducers are treated separately in this section.

A strain gage functions as a transducer by changing resistance as its length is changed. The change in resistance of the strain gage is detected and measured by applying an electric current to the gage and measuring the change in voltage drop due to the change in resistance. This excitation may either be AC or DC. Since the full scale output of a conventional strain gage transducer will only be on the order of 10 millivolts per volt of excitation, the signal usually requires amplification before recording. AC excitation has the advantage that the amplifier may be an AC amplifier which does not have to possess the stability of



the DC type amplifier. With AC excitation the signal can be amplified to large voltage levels and only the output stage of the amplifier and the demodulator need possess good DC stability characteristics. The use of DC excitation requires signal conditioners with low drift characteristics. DC excitation and DC amplifiers eliminate the need for demodulation of the signal to obtain the analog data signal. Because of their high sensitivity, semiconductor strain gages may be used without amplifiers in many applications. For all the above cases, the output is proportional to the strain gage excitation voltage; and therefore, the excitation source must possess stability and noise characteristics commensurate with the desired quality of the measurement.

None of the system elements described limits the frequency response to the range of interest, 0-50 cps. In order to reject high frequency electrical noise, a lowpass filter is used.

Typical strain measuring systems employ from one to four gages depending on the parameter being measured. Figure 7-1 shows strain gage circuit arrangements for measuring simple strain, bending strain, torsion strain, and shear strain. A number of sources including References 27, 28, and 29 discuss the use of strain gage transducers for measuring quantities other than strain.

## 7.1 CONVENTIONAL STRAIN GAGES

Conventional strain gages function as transducers simply by changing resistance as their length is changed. When load is applied to the test specimen on which the bonded or unbonded strain gage is attached, the length of the specimen increases and the gage length changes from  $l_1$  to  $l_2$  as indicated in Figure 7-2.

# Contrails

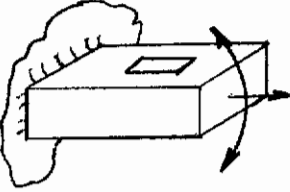
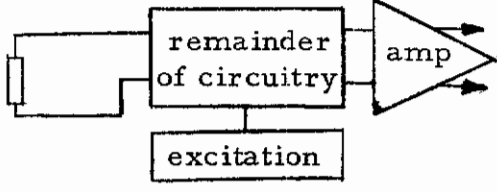
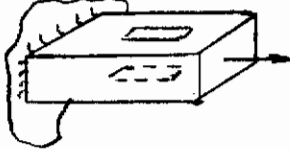
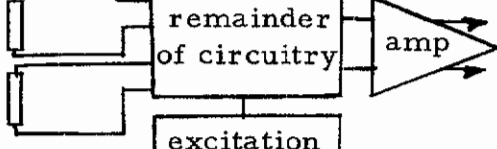
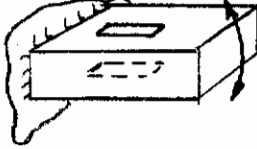
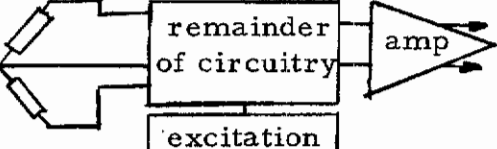
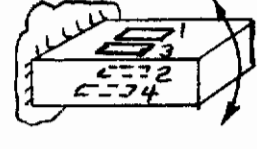
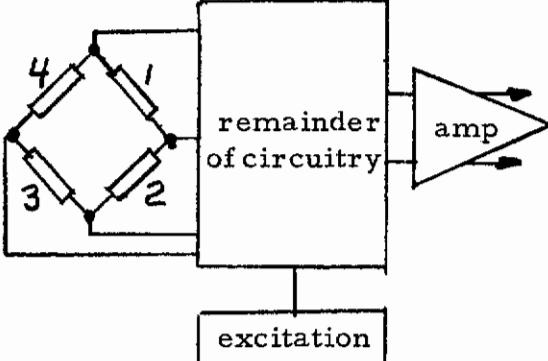
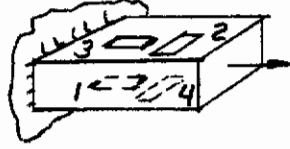
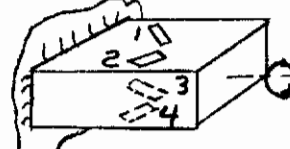
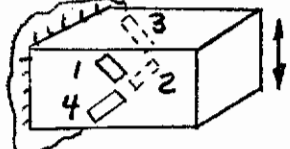
Case	Measured Parameter	Gage Orientation	Circuit Block Diagram
A	Simple Strain		
B	Tension Strain		
C	Bending Strain		
D-1	Bending Strain		
D-2	Tension Strain		
D-3	Torsion Strain		
D-4	Shear Strain		

Figure 7-1. Typical Strain Gage Orientations and Circuit Block Diagrams

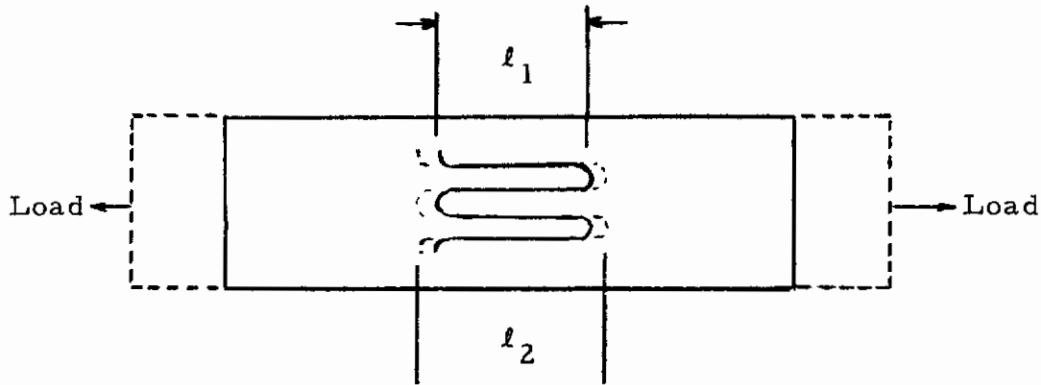


Figure 7-2. Strain Gage Elongation

The deformation or strain is given by

$$e = (l_2 - l_1) / l_1 = \frac{\Delta l}{l_1} \quad (7.1)$$

where

- $e$  = unit deformation, or strain, dimensionless
- $l_1$  = zero strain length in the gage, inches
- $l_2$  = length of the gage after the application of load, inches
- $\Delta l$  = change in length of the gage, inches

Strain sensitivity of the wire or foil gage is the ratio between the change in resistance and the strain and is given by Eq. (7.2)

$$K = \frac{\Delta R / R_0}{\Delta l / l_1} \quad (7.2)$$

# Contrails

where

- K = strain sensitivity or gage factor, nondimensional
- $\Delta_R$  = change in resistance due to applied strain, ohms
- $R_0$  = unstrained resistance of the gage, ohms

A number of sources, including References 27 and 29, point out that the dimensional change resulting from the strain cannot account entirely for the strain sensitivity or change in resistance for strain that most materials exhibit. This may be seen by considering the unstrained and strained resistances. The resistance of an element is given by Eq. (7.3)

$$R = \rho \frac{l}{A} \quad (7.3)$$

where

- $\rho$  = resistivity of the material, ohm-feet
- $l$  = length, feet
- $A$  = area, feet<sup>2</sup>

When the length is changed due to strain, the change in resistance is given by Eq. (7.4)

$$\Delta_R = R_2 - R_1 = \rho \frac{l_2}{A_2} - \rho \frac{l_1}{A_1} \quad (7.4)$$

# Contrails

The original and new areas are given by

$$A_1 = b_1 h_1 \quad (7.5)$$

$$A_2 = b_2 h_2 \quad (7.6)$$

where  $b_1, h_1, b_2, h_2$  = dimensions of wire, but

$$b_2 = b_1 \left( 1 - \mu \frac{\Delta \ell}{\ell} \right) \quad (7.7)$$

$$h_2 = h_1 \left( 1 - \mu \frac{\Delta \ell}{\ell} \right) \quad (7.8)$$

where  $\mu$  = Poisson's ratio — unit lateral deformation/unit longitudinal deformation, dimensionless. Therefore

$$A_2 = b_1 \left( 1 - \mu \frac{\Delta \ell}{\ell} \right) h_1 \left( 1 - \mu \frac{\Delta \ell}{\ell} \right) = A_1 \left( 1 - \mu \frac{\Delta \ell}{\ell} \right)^2 \quad (7.9)$$

Consider  $\rho$  a constant. Therefore combining Eq. (7.4) and Eq. (7.9)

$$\Delta_R = \rho \left[ \frac{\ell_2}{A_1 \left( 1 - \mu \frac{\Delta \ell}{\ell} \right)^2} - \frac{\ell_1}{A_1} \right] \quad (7.10)$$

Rearranging

$$\Delta_R = \frac{\rho l_1}{A_1} \frac{l_2 - l_1 (1 - \mu \Delta_l / l)^2}{l_1 (1 - \mu \Delta_l / l)^2} \quad (7.11)$$

Expanding, noting that  $\rho l_1 / A_1 = R_1$  and since  $\mu \leq 1$  for all conventional structural materials

$$\mu^2 \left( \frac{\Delta_l}{l} \right)^2 \quad (7.12)$$

may be neglected, and

$$\frac{\Delta_R}{R_1} \approx \frac{\frac{l_2 - l_1}{l_1} + 2\mu \left( \frac{l_2 - l_1}{l_1} \right)}{1 - 2\mu (\Delta_l / l)} \quad (7.13)$$

$$\frac{\Delta_R / R_1}{\Delta_l / l} \approx \frac{1 + 2\mu}{1 - 2\mu (\Delta_l / l)} \quad (7.14)$$

since  $\frac{\Delta_l}{l_1} \ll 1$

$$\frac{\Delta_R / R_1}{\Delta_l / l} \approx [1 + 2\mu] \equiv k \quad (7.15)$$

For most gage materials,  $\mu \approx 0.3$  and the expected gage factor would then be 1.6 which is less than actually experienced. Indeed, conventional strain gages have gage factors from 2.1 up to 5.1. The difference is attributable to a change in resistivity,  $\rho$ , with a dimensional change. High gage factor materials would be used for all applications except that these materials usually have undesirable characteristics such as a high sensitivity to temperature. The selection of the proper gage for the application is the subject of a number of investigations and writings, including References 30, 31, and 32.

Unbonded strain gages are constructed by wrapping the electrical wire elements around electrically insulated posts which are attached directly to the element whose length change is being measured or to some strain multiplying bar or lever. Typical strain multipliers are described in References 29 and 33.

Bonded strain gages are attached directly to the element whose change in length is to be sensed. Filaments of bonded filament strain gages normally have their resistant elements or filaments attached to a thin layer of insulation called the carrier. This carrier provides electrical insulation between the filament and test specimen and also facilitates the bonding of the strain gage to the test specimen. Unbacked gages are glued directly to the test specimen, the glue layer providing electrical insulation. Bonded filament strain gages are convenient to use and come in a very wide variety of configurations, resistance materials, carrier materials, and resistances designed for special applications.

7.1.1 Intrinsic Errors,  
Conventional Strain Gages

The intrinsic inaccuracies of conventional strain gages can be broken down into inaccuracies due to:

1. transverse or cross-axis sensitivity
2. hysteresis
3. fatigue
4. strain averaging
5. self-generating effects

Cross-axis sensitivity is the measure of how much the strain gage responds to strain perpendicular to its sensitive axis. Commercial strain gages presently are designed with part of the resistance element oriented nonparallel to the sensitive axis of the strain gage as illustrated in Figure 7-3. Foil gages are designed to minimize this effect by having a relatively low resistance tab connecting each of the parallel ribs also illustrated in Figure 7-3.

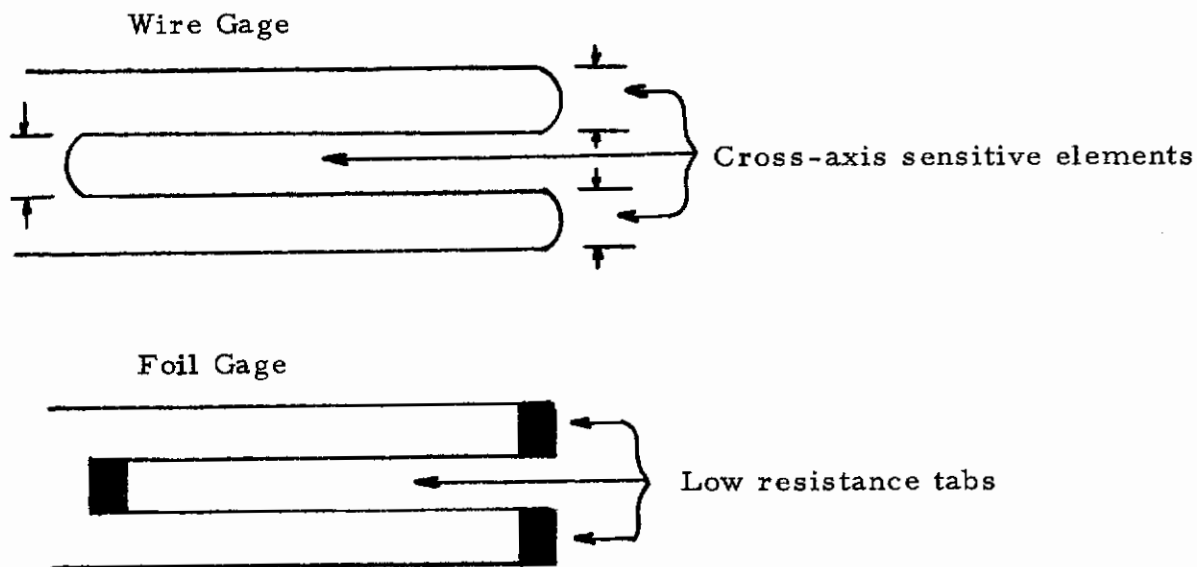


Figure 7-3. Strain Gage Configuration Showing Cross-Axis Sensitive Elements



References 35 and 36 present data showing typical cross-axis or transverse sensitivities for wire gages which are approximately 1-1/2% that of the sensitivity in the sensitive axis. For foil gages, transverse sensitivity is typically less than 0.5%. The indicated strain will be the sum of the strain in the sensitive direction and a percentage of the strain in the transverse direction as follows.

$$\hat{\epsilon}(t) = \epsilon(t) + \frac{\lambda_e}{100} \epsilon_T(t) \quad (7.16)$$

where

- $\hat{\epsilon}(t)$  = the total indicated instantaneous strain
- $\epsilon_T(t)$  = instantaneous strain transverse to the sensitive axis
- $\lambda_e$  = percent response of the strain gage to transverse strains

The percent error in the measurement of strain along the sensitive axis is given by

$$\% \text{ error} = \lambda_e \frac{\epsilon_T(t)}{\epsilon(t)} \quad (7.17)$$

The hysteresis of a strain gage may be described as its inability to return to zero resistance change with zero load and is usually measured after the gage has been subjected to three load cycles. For a single cycle, this error appears as an amplitude nonlinearity. Reference 18 presents an expression for the percent hysteresis. See Figure 7-4.

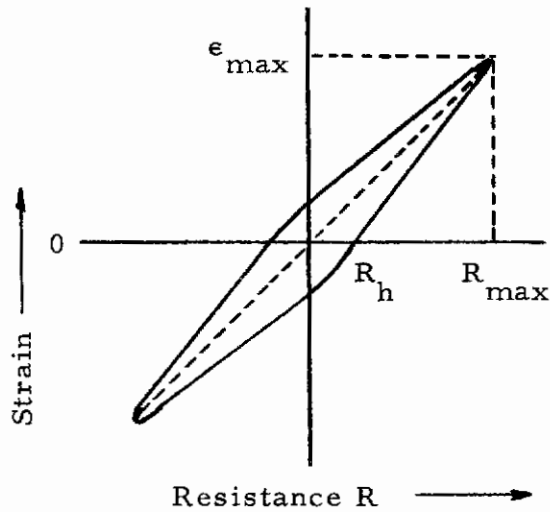


Figure 7-4. Illustration of Strain Gage Hysteresis

The percent hysteresis is

$$\% N = (100) \frac{R_h - R_0}{R_{\max} - R_0} \quad (7.18)$$

where

- $\% N$  = the hysteresis expressed in percentage of full scale
- $R_{\max}$  = the resistance of the strain gage corresponding to full scale strain, ohms
- $R_0$  = the resistance of the strain gage in ohms before force is applied
- $R_h$  = the resistance of the strain gage at no load after three complete cycles of plus and minus full scale strain, ohms
- $\epsilon_{\max}$  = the full scale strain

References 35, 36, and 37 summarize the results of tests measuring the hysteresis of strain gages. Reference 38 summarizes the results of tests to measure the contribution of bonding cement to hysteresis. All these references quote hysteresis errors of less than plus or minus one percent of full scale. The apparent hysteresis of a strain gage when installed on a complex redundant structure with riveted or fastened joints may easily be many times the hysteresis of the gage itself. This error is discussed in more detail in the section on usage errors.

Fatigue of strain gages may cause two types of errors. The gage may simply fail as a function of fatigue. Reference 39, a summary of present knowledge of the fatigue life of strain gages, concludes that insufficient information is presently available to determine whether gages will survive the structure to which they are attached. For experimental flight loads programs, the fatigue of the strain gage will be insignificant because the fatigue life of the aircraft will not be approached. The second type of error is an increase in the resistance as a function of the fatigue of the gage. This is the same type of effect which the SN gage utilizes in order to predict fatigue failure, References 26 and 34. Again, this error is negligible for low stress cycle applications. The indicated strain will not be equal to the strain at the midpoint of the gage if a non-linear strain gradient is present. For example, assume strain in a member is a function of the square of a dimension,  $x$ . Therefore

$$\epsilon = Cx^2 \quad (7.19)$$

where  $C$  is a constant. If the gage is centered at  $x$ , the strain at the midpoint of the gage is simply  $Cx^2$ .

The average strain is given by:

$$\epsilon_{\text{ave}} = \frac{1}{l} \int_{x - \frac{l}{2}}^{x + \frac{l}{2}} Cx^2 dx \quad (7.20)$$

$$= Cx^2 + \frac{Cl^2}{12} \quad (7.21)$$

where  $l$  - unstrained gage length, feet

The reading error expressed as a percent of the midpoint strain is given by:

$$\% \text{ error} = \frac{l^2}{12x^2} (100) \quad (7.22)$$

Equation (7.22) implies that the strain averaging error may be minimized if the gages are small compared with the parts being gaged. At the present time, gages are commercially available which are much smaller than characteristic dimensions of aircraft structural members. For the measurement of the high frequency strain associated with certain phenomena such as pyrotechnic shock, the strain averaging error is a function of the propagation velocity in the material. This error is not applicable to loads determination, but for further information, see Reference 40.

Another intrinsic strain gage error is the self-generating effect or magnetostriction. This effect is a function of the excitation current and the frequency and amplitude of the applied strain. Nickel and iso-elastic gages exhibit this effect but constantan does not. However,

magnetostriction is not a significant error because of the frequency range of interest. For further information, see Reference 2, Volume 1, Section 17, and Reference 41.

## 7.1.2 Environmental Errors, Conventional Strain Gages

Environmental errors of conventional strain gages are attributable to the temperature environment, the humidity environment, and the pressure or altitude environment. Errors associated with humidity and pressure may be avoided with proper installation and protection of the strain gages. In addition, these errors are extremely difficult to quantify. The most significant environmental errors of conventional strain gages are associated with temperature variations.

Relative humidity can cause inaccuracies in two manners. Reference 44 states "One of the principal causes of gage instability is moisture which is absorbed into the body of the gage. The effects of moisture are (a) dimensional changes of the bonding medium and cement which causes resistance changes due to the resulting strains set up in the gage filament, and (b) changes of resistances due to the conductivity and corrosion of the strain sensing materials caused by absorbed moisture."

There are three basic manners in which the inaccuracy to relative humidity can be reduced. In order of preference, these are

1. Control the relative humidity to which the strain gages are exposed.
2. Use the strain gages and the cements that are the least susceptible to the humidity.
3. Moistureproof the strain gage installation.

# Contrails

For experimental flight test programs, the first technique may not be feasible. Even if a gage is mounted on an internal member of the aircraft, pressure and temperature cycling coincident with the aircraft mission profile causes adverse humidity conditions.

Pressure variations due to changes in altitude may cause erroneous readings or gage failure if air bubbles are trapped between the gage and the test specimen. This may be avoided or at least detected with proper gaging techniques as discussed under usage errors.

Temperature effects may be broken down into the following items:

1. resistance changes of the gage due to temperature changes
2. strain due to differential thermal expansion between the gage and the specimen to which it is mounted.
3. catastrophic failure of the glue bond, the gage, or drastic changes in the gage characteristics beyond some upper temperature limit
4. the change of modulus of elasticity of the test specimen material with temperature
5. strain sensitivity changes due to temperature changes.

The first two effects are usually combined into a term called apparent strain which is defined in Eq. (7.23).

$$\text{Apparent Strain} = \left[ (\delta_s - \delta_g) + \frac{\text{TCR}}{K} \right] \Delta_T \quad (7.23)$$

where  $\delta_s$  = coefficient of thermal expansion of the test specimen, in/in °F  
 $\delta_g$  = coefficient of thermal expansion of the gage, in/in °F

# Contrails

$K$  = strain sensitivity or gage factor, nondimensional

$\Delta_T$  = temperature change,  $^{\circ}\text{F}$

$\text{TCR} = \Delta_R / R$   $^{\circ}\text{F}$  temperature coefficient of resistance,  $1/^{\circ}\text{F}$

Apparent strain should be considered an error if the steady state strain is being measured. The percent error may be expressed by

$$\% \text{ error} = \frac{\left[ \delta_s - \delta_g + \frac{\text{TCR}}{K} \right] \Delta_T}{\epsilon(t)} \quad (100) \quad (7.24)$$

Conventional wire and foil gages are available in selected melts or composition whereby the temperature coefficient of resistance effect is approximately equal and opposite to the differential coefficient of thermal expansion effect, and thus the apparent strain is minimized. References 30, 31, 32, and 42 indicate that if a compensated gage is installed on the proper specimen material, the apparent strain will be less than 1 micro-strain per degree Fahrenheit.

Another effect associated with an increase in resistance due to temperature occurs if constant current excitation is employed. Conventional strain gages are basically constant gage factor devices. That is, the unit change in resistance per unit strain remains constant for different or varying basic resistances. With a constant current excitation source, the change in resistance, not the unit change in resistance, is measured. With an increased basic resistance, the output with constant current excitation is in error by

$$\% \text{ error} = \frac{K (\text{apparent strain})}{R_g} \quad (100) \quad (7.25)$$

The modulus of elasticity of conventional structural materials decreases with an increase in temperature. For conventional aluminum alloys, data in Reference 43 indicates that the vibration in modulus of elasticity is approximately minus two percent per 100°F over the temperature range from 70° to 200°F and greater than -2 percent per 100°F beyond +70° to 200°F. Modulus of elasticity is defined by

$$E = S/\epsilon$$

or

$$\epsilon = S/E \quad (7.26)$$

where  $E$  = Young's modulus of elasticity, psi  
 $S$  = stress, psi

Since the strain gage senses the change in length, an error will occur if this strain is converted directly to stress or load without recognizing that the modulus of elasticity has changed. An expression for this error is

$$\% \text{ error} = -\% \text{ change } E \quad (7.27)$$

Refer to the section on Wheatstone bridge circuitry for methods of compensation.

### 7.1.3 Usage Errors, Conventional Strain Gages

Strain gages employed in experimental flight loads programs may be used to measure strain directly or may be oriented, installed, and



calibrated so as to give a signal which is related to a known load. When the strain gage is used in the latter fashion, as a calibrated transducer, a number of usage errors are minimized because the data signal is referred to the calibration load and knowledge of the circuit resistances and even the excitation voltage is not required. However, even if the strain gage is used as a calibrated transducer, usage errors are only minimized, not calibrated out of existence.

Strain gage usage errors may be listed by the phase of an experimental program in which they occur. Such a listing is presented in Table 7-1.

Table 7-1. Strain Gage Usage Errors versus Program Phase

Program Phase	Application	
	Direct Strain Measurement	Calibrated Transducer
1. Gage location selection	✓	✓
2. Gage orientation	✓	Error minimized
3. Gage installation	✓	Error minimized
4. Calibration		✓
5. Data measurement	✓	✓

The selection of strain gage locations may be the result of calculations, laboratory experiments, engineering judgment, or a requirement to obtain data to compare directly with previous tests. Two major criteria for the selection of a location for a gage are that the expected

strain is high, and that the strain be strongly correlated with the load to be measured. High strain locations are of greatest interest because structural failure will tend to occur there. In addition, high level strains produce large strain gage signals and thus high signal to noise ratios.

The second criterion, having a strong correlation with the load being measured, means the strain at the location chosen should be dependent upon only the type of load being measured. Computing a load from a number of measurements may easily produce a percentage error greater than the percentage error of individual measurements. Strains at locations other than the measurement location can be deduced from the geometry or static tests. However, an aircraft structure is usually a nonlinear spring-mass system and computing a strain from other measurements introduces significant errors.

A convenient method of experimentally determining the location of the points of maximum stress is by the use of a brittle lacquer coating. The test specimen is coated with this lacquer and then subjected to a test environment. The lacquer will develop cracks at points of high stress concentration. From these cracks one can also determine the strain orientation and concentration pattern and, to a limited extent, the strain magnitude. For more information on this technique, see Reference 27.

If a gage is oriented along an axis other than the axis to be measured, the output will be different from that which is anticipated. The resulting error is identical with the error for accelerometer misalignment, Eqs. (6.11) and (6.12).

The installation or mounting of strain gages is probably the largest source of usage inaccuracies. An inadequate glue bond will not transmit the strain of the test specimen to the gage faithfully and an inaccurate reading will result. This could occur only in compression and may not be apparent if calibration is performed in tension only. Improperly made solder joints may change resistance with time or even with load, thus generating false data. Fortunately, these types of errors can be minimized when the gages are installed under controlled conditions by trained and experienced technicians given sufficient time for all phases of the gaging operation. It is not the purpose of this report to serve as an instruction manual for the installation of strain gages. For this information, See References 2, Volume 1, Section 17; and References 27 and 44.

The most significant usage error associated with calibration is associated with not calibrating to full load. If the strain gage is used as a load calibrated transducer, the output may be nonlinear due to nonlinear stiffness and/or hysteresis caused by structural redundancy and fastened joint slippage, and an error will result if linearity is assumed. Another error is associated with the method of load application. If the calibration load does not simulate the load to be measured, say a bending load, in an exact distributed fashion, the response to extraneous strains due to torsion and shear may produce errors between calibration and test.

During data measurement, the gage is subject to self-heating due to the excitation current. The increase in temperature, and therefore resistance of the gage, is a function of the excitation voltage squared and heat transfer properties of the installation. The excitation voltage or current should be maintained at a value which will not cause unsatisfactory change in the circuit output.

## 7.2 SEMICONDUCTOR STRAIN GAGES

Semiconductor or solid state strain gages are fabricated from semiconductor materials such as silicon and germanium and are similar to wire and foil gages in that the resistance changes as a function of the change in length. However, solid state strain gages are different from wire and foil gages because the mechanism or physics of the change in resistance is a function of a change in the crystalline structure of the gage, not merely a dimensional change as with wire gages. As a result, positive and negative sensitivities, or gage factors, of between 40 and 200 are easily attainable with solid state strain gages. These gages are made of single crystals of doped materials. A description of the mechanism involved in the change in resistance with unit change in length, and an extensive bibliography, are presented in Reference 45.

The sensitivity or gage factor of semiconductor strain gages is usually expressed as

$$\frac{\Delta R}{R_0} = C_1 \epsilon + C_2 \epsilon^2 + C_3 \epsilon^3 + C_4 \epsilon^4 \quad (7.28)$$

where

$R_0$  = unstrained resistance at the measurement temperature, ohms

$C_1, C_2, C_3$  = constants for the particular gage material

In practice, the  $C_3 \epsilon^3$  and  $C_4 \epsilon^4$  terms are neglected. Reference 42 indicates that for negative gage factor materials, the  $C_2 \epsilon^2$  and  $C_3 \epsilon^3$  terms should be neglected, but the  $C_4 \epsilon^4$  term exists.

The constants  $C_1$  and  $C_2$  may be varied by adding foreign materials such as boron and phosphorus to the semiconductor material, silicon or germanium. This process is called doping. In general, the higher the basic gage factor,  $C_1$ , the higher the undesired effects such as temperature sensitivity. However, this rule does not hold for the temperature coefficient of resistance below a certain level. The selection of the proper gage for a specific application is discussed in many papers and bulletins, including References 46, 47, 48, and 49.

As was previously indicated, the high sensitivity of semiconductor gages may eliminate the requirement for amplification. As an example, with four gages as in case D, Figure 7-1, the output will be 1.0 volt, given 3 volts excitation, a strain of  $2780\mu$  in/in, and a gage factor of 120. However, these types of gages have not received wide acceptance for direct measurement of strain for field test programs because of problems in compensating for nonlinearity and temperature effects.

### 7.2.1 Intrinsic Errors, Semiconductor Strain Gages

Semiconductor strain gages exhibit only the strain averaging inaccuracy in common with conventional strain gages. Since these gages are usually single element devices, cross-axis sensitivity is negligible. References 46, 47 and 48 quote negligible hysteresis, pointing out that silicon is a perfectly elastic material below  $1000^{\circ}\text{F}$ . Fatigue is not a problem for the same reason. However, in addition to these errors, semiconductor strain gages exhibit a nonlinear response characteristic. Equation (7.29) repeated below indicates that the response of a semiconductor strain gage is not a straight line function, but is a parabola.

$$\frac{\Delta R}{R_0} = C_1 \epsilon + C_2 \epsilon^2 \quad (7.29)$$

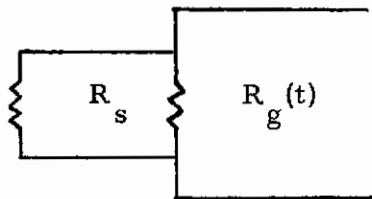
If the response is assumed to be linear, i. e., the  $C_2 \epsilon^2$  term is neglected, an error will result which may be expressed as follows:

$$\% \text{ error} = \frac{C_2}{C_1} \epsilon \quad (7.30)$$

An example using the parameters of a widely used P silicon gage material and a typical N gage material is presented below.

<u>Type</u>	<u>C<sub>1</sub></u>	<u>C<sub>2</sub></u>	<u>ε</u>	<u>% error</u>
P Silicon	118	4,000	2000	6.8
N Germanium	-110	+10,000	2000	17

It has been proposed in Reference 45 that linearity be improved by shunting the semiconductor gage with a resistor as indicated below:



where

$$R_s = \text{shunt resistor, ohms}$$

$$R_g(t) = R_0(1 + C_1 \epsilon + C_2 \epsilon^2) \quad (7.31)$$

For this arrangement, the unit change in resistance is given by

$$\frac{\Delta R}{R} = \frac{C_1 \epsilon + C_2 \epsilon^2}{1 + \frac{R_0}{R_s} (1 + C_1 \epsilon + C_2 \epsilon^2)} \quad (7.32)$$

The error from neglecting  $C_2 \epsilon^2$  can be shown to be

$$\% \text{ error} = \frac{C_2}{C_1} \epsilon \frac{1 + \frac{R_0}{R_s}}{1 + \frac{R_0}{R_s} (1 + C_1 \epsilon + C_2 \epsilon^2)} \quad (7.33)$$

This error does diminish as  $R_s$  becomes small, but the decreased sensitivity of the parallel combination may be more undesirable than the nonlinearity error.

### 7.2.2 Environmental Errors, Semiconductor Strain Gages

The most significant variations from the desired or ideal response of semiconductor strain gages are due to temperature fluctuations. These temperature effects may be broken down into the following items:

1. Resistance changes of the gage due to temperature changes
2. Strain due to differential thermal expansion between the gage and the specimen to which it is mounted
3. Strain sensitivity changes due to temperature changes

As with conventional strain gages, the first two effects are usually combined into a term called apparent strain which is defined in Eq. (7.23).

A representative value for apparent strain for a P gage mounted on aluminum is 14 to 16 microstrains per degree Fahrenheit. Since the basic gage factor  $C_1$  for N type gages is negative, the percent error may be minimized for these types of gages. This and other temperature compensation techniques are described in References 31, 46, 47, and 49.

The change in gage factor with temperature may be expressed as the temperature coefficient of gage factor. No mathematical expression was found in the literature for this coefficient as a function of temperature. It is defined as a modification of Eq. (7.29) as

$$\frac{\Delta R}{R} = (\text{TCGF}) \Delta_T C_1 \epsilon + C_2 \epsilon^2 \quad (7.34)$$

But the unstrained resistance  $R$  is given by

$$R = R_0 \left[ 1 + C_1 (\text{apparent strain}) \right] = R_0 + R_0 \Delta_T \left[ C_1 (\alpha_s - \alpha_g) + \text{TCR} \right] \quad (7.35)$$

Therefore,

$$\frac{\Delta R}{\epsilon} = \left[ (\text{TCGF}) C_1 \Delta_T + C_2 \epsilon \right] R_0 = \left[ 1 + C_1 (\alpha_s - \alpha_g) \Delta_T + (\text{TCR}) \Delta_T \right] \quad (7.36)$$



This function may be made somewhat independent of temperature with proper values of TCR and TCGF. The method of describing the gage sensitivity as  $\Delta_R/\epsilon$  has been proposed as a substitute for the other methods (see Reference 45).

### 7.2.3 Usage Errors, Semiconductor Strain Gages

The usage errors described for conventional strain gages (Section 7.1.3) apply to semiconductor strain gages.

## 8. PRESSURE TRANSDUCERS

In experimental flight loads determination, pressure transducers are used for three types of measurement. These are as follows:

1. differential pressure angle of attack sensors
2. pressure distributions
3. pitot pressures

The different measurements impose slightly different requirements on the pressure transducer characteristics. The frequency range for the first two types of measurement is from zero to approximately 20 Hz. Pitot pressures are used to determine the average aircraft velocity and Mach number, and the frequency range of interest is very low, from zero to less than one Hz. The environmental criteria for a particular pressure transducer depends on the particular installation. For the frequency ranges of interest, and within certain limitations, all the pressure transducers mentioned may be installed within the aircraft with connecting lines to the pressure point being measured (see paragraph 8.3).

Different types of pressure transducers are suitable for flight loads determination. Seven types which are considered are as follows:

1. variable reluctance
2. potentiometer
3. strain gage
4. piezoresistive
5. capacitive

6. servo or force balance
7. piezoelectric (quartz)

As with accelerometers, piezoelectric pressure transducers are unsuitable because of their lack of DC or zero-frequency response. Likewise, capacitive pressure transducers with a DC excitation are unsuitable. The servo or force balance type functions in a manner similar to servo accelerometers, with similar advantages and errors. However, they are not commonly used. The strain gage type functions in two different ways. In one instance, strain gages are installed directly on the diaphragm or deflecting member and measure the strain due to pressure. Other types of strain gage pressure transducers use unbounded strain gages to measure the deflection of the diaphragm. The other pressure transducers listed are all passive and are essentially identical in principle, merely employing different relative displacement pickoff devices. The frequency response of pressure transducers depends on both the transducer mechanical characteristics of the diaphragm-pickoff and the inertia and viscous effects of the fluid or gas whose pressure is being measured. Reference 3, page 391, presents the frequency response relationship for different classes of applications. In general, if a highly viscous, large mass fluid is used with a large volume pressure transducer, the overall system behaves as a first order system and is characterized by a time constant (Appendix A, Figures A-11 and A-12). For the measurement of gas pressures with transducers of small internal volume, the overall system behaves as a second order system whose response is determined primarily by the natural frequency and damping of the diaphragm-pickoff system, (Figures A-2 and A-3).

# Contrails

The intermediate transducing element for most pressure transducers is a diaphragm. For a diaphragm which is clamped, the deflection at the center and applied pressure are related by:

$$P = \frac{16Eh^4}{3r^4(1-\mu^2)} \left[ \frac{\Delta}{h} + 0.488 \left( \frac{\Delta}{h} \right)^3 \right] \quad (8.1)$$

where

- P - applied pressure, pounds/inch<sup>2</sup>
- E - Young's modulus of elasticity, pounds/inch<sup>2</sup>
- h - diaphragm thickness, inch
- r - diaphragm radius, inch
- $\mu$  - Poisson's ratio
- $\Delta$  - diaphragm deflection at center, inch

For small deflections  $\Delta < h$  and

$$P \approx \frac{16Eh^3}{3r^4(1-\mu^2)} \Delta \quad (8.2)$$

The lowest natural frequency of such a diaphragm is given in Reference 3, page 390, as follows:

$$f_n = \frac{10.21}{2\pi r^2} \sqrt{\frac{g E h^2}{12\gamma(1-\mu^2)}} \quad (8.3)$$

where  $\gamma$  = diaphragm material specific weight, pound/inch<sup>3</sup>. By substituting the natural frequency expression, Eq. (8.3), into the sensitivity expression, Eq. (8.2), it may be seen that the sensitivity  $\Delta/P$ , and natural frequency are related by

$$\frac{\Delta}{P} = \frac{3}{f_n^3} \left[ \frac{E}{1-\mu^2} \right]^{1/2} \left[ \frac{g}{12\gamma} \right]^{3/2} \left[ \frac{10.21}{2\pi} \right]^3 \left[ \frac{1}{r} \right] \quad (8.4)$$

Therefore, for a given diaphragm radius and material

$$\frac{\Delta}{P} = \frac{C}{f_n^3} \quad (8.5)$$

where  $C$  = constant for constant diaphragm radius. Expressed another way, the full scale pressure range for a family of pressure transducers is related to the natural frequency by

$$f_n = C_{FR} P_{FS}^{1/3} \quad (8.6)$$

The constant  $C_{FR}$  may be considered a figure of merit analogous to the accelerometer figure of merit, Table 6-2. For commercially available units,  $1500 < C_{FR} < 5500$ . However, other factors such as the mass of the fluid and the pickoff modify the natural frequency and Eq. (8.4) is not as valid as the relationship for accelerometers. Nevertheless, it is a convenient measure of the transducer design.

The advantages and disadvantages of the different types of pressure transducers for flight loads measurement are listed in Table 8-1. A number of references, including 1, 3, 50, and 51, present introductory and descriptive material on pressure transducers.

## 8.1 INTRINSIC ERRORS, PRESSURE TRANSDUCERS

The types of intrinsic errors common to pressure transducers are as follows:

1. amplitude and phase frequency response errors
2. resolution errors in the pickoff device
3. amplitude nonlinearity
4. hysteresis

The deviation of the sensitivity from a constant value as a function of frequency and damping depends on the type of transducer. As

Table 8-1. Comparison of Types of Pressure Transducers for Flight Loads Measurement

<u>Type</u>	<u>Major Advantage</u>	<u>Major Disadvantage</u>
Variable reluctance	High resolution	Precision AC source required Demodulation required
Potentiometer	Large DC output (no amplifier required) Simplicity	Large internal volume Large size Low natural frequency Wiper drag Wiper vibration sensitive Precision AC or DC source required
Strain gage	High natural frequency Small size	Precision DC or AC source required DC amplifier required
Piezoresistive (semiconductor strain gage)	High natural frequency Small size No amplification required	Precision DC or AC source required
Variable capacitance	High natural frequency	Precision AC source required Demodulation required
Servo or force balance	High accuracy High output	Complex
Piezoelectric	Small	No DC response Low sensitivity

previously indicated, if the transducer has a small internal volume, it will behave as a typical second order system with the errors identical in form to those of accelerometers and rate gyroscopes. The error curves, Figures A-4 and A-5, apply.

The diaphragm type pressure transducer has a basic amplitude nonlinearity. Equation (8.1) presents the relationship between deflection and applied pressure. The cubic term makes the relationship nonlinear. The nonlinearity error is as follows:

$$\% \text{ error} = .488 \left( \frac{\Delta}{h} \right)^2 (100) \quad (8.7)$$

The diaphragm type transducer is therefore linear for only small deflections where the ratio of deflection to diaphragm thickness is small. The error indicated in Eq. (8.7) is the worst case error. Calibration of the transducer with least squares linear curve fitting would reduce the magnitude of this error for large pressure measurements, but would correspondingly create large percentage errors around zero pressure measurement. In actual practice, the linearity of pressure transducers is on the order of  $\pm 0.5\%$ . On high quality units, the linearity and hysteresis are combined into one specification number. The value for combined linearity and hysteresis for commercially available units is approximately  $\pm 1\%$  maximum.

The resolution errors of pickoff devices, especially potentiometers, are covered in Section 3. It should be noted that the variable capacity type pickoff can be used to its full potential in pressure transducers. This is because the pickoff is basically non-contacting and may use the pressure transducer diaphragm as one of the elements of the variable capacitor. Combined resolution amplitude nonlinearity and hysteresis errors for these type devices may be significantly lower than for other types.

## 8.2 ENVIRONMENTAL ERRORS, PRESSURE TRANSDUCERS

The types of environmental errors common to pressure transducers are as follows:

1. zero shift due to temperature
2. sensitivity change due to temperature
3. variation of the damping constant with temperature
4. vibration effects

One of the major design criteria for a pressure transducer is to minimize the response of the bellows diaphragm or Bourdon tube to acceleration and temperature change. Indeed, the components of a pressure transducer are similar to those of an accelerometer or temperature sensor, and only careful choice of design parameters will minimize the side effects. Even with careful design, the largest errors of commercially available pressure transducers are attributable to the above-mentioned factors. Typical zero-shift specifications are 0.1% full scale per degree Fahrenheit, and for sensitivity  $\pm 0.02\%$  per degree Fahrenheit.

The variation in the frequency response characteristics due to changes in viscosity of the damping fluid are covered extensively in the section on accelerometers, 6.1.2. These errors apply in like manner to pressure transducers.

Vibration effects on the diaphragm or pressure sensing device are intuitively apparent. The diaphragm must have mass and therefore behaves as an accelerometer. Increasing the pressure sensitivity/vibration sensitivity ratio requires reduction of the diaphragm thickness, which also reduces the natural frequency. Some pressure transducers are compensated for vibration. The pressure transducer should be qualified for the vibration environment anticipated.



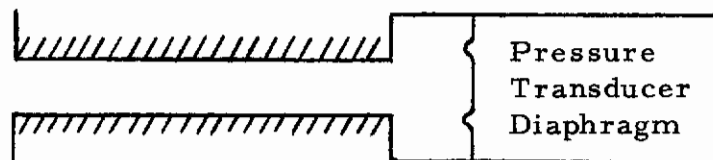
## 8.3 USAGE ERRORS, PRESSURE TRANSDUCERS

The major usage errors associated with pressure transducers are as follows:

1. Calibration
2. Tubing

Static calibration of pressure transducers using dead weight testers or other standards can be done with extremely high accuracies, especially when compared with other error sources considered. However, dynamic calibration is more difficult and less accurate. In the frequency range of interest for flight loads measurement, either a step function test or a frequency response test may be performed. Reference 52 presents a comprehensive review of the various methods. The error of calibration may be as small as  $\pm 1\%$ .

The pressure transducer is frequently installed within the aircraft with a tube to the pressure field,



The gas in the tube and transducer chamber may be considered a second order system. The expressions for the natural frequency and damping of this system are given by Reference 53 and Reference 3, page 391. Reference 54 also discusses the tubing problem. For the case where the tube volume is comparable to the chamber volume, the following equations for  $f_n$  and  $\zeta$  apply:

# Contrails

$$f_n = \frac{V_s}{2\pi l} \sqrt{\frac{1}{\frac{1}{2} + \frac{v}{v_t}}} \quad (8.8)$$

$$\zeta = \frac{16\mu l}{d_t^2 \rho V_s} \sqrt{\frac{1}{\frac{1}{2} + \frac{v}{v_t}}} \quad (8.9)$$

where

$V_s$  - velocity of sound, feet/second

$\mu$  - viscosity of the gas, slugs/foot-second

$l$  - tube length, feet

$d_t$  - diameter of the tube, feet

$v$  - internal volume, pressure transducer, inch<sup>3</sup>

$v_t$  - tubing volume, inch<sup>3</sup>

$\rho$  - density of the gas, slugs/foot<sup>3</sup>

## 9. SIGNAL CONDITIONING EQUIPMENT

The signal conditioning equipments which are common to the different types of measurement systems have been grouped together in this section. The types of equipment which are considered and their primary sources of errors are indicated in Table 9-1. The designation or applicability of the errors indicated is arbitrary. The errors indicated are those which are usually associated directly with the primary function of the particular equipment.

### 9.1 EXCITATION SUPPLIES

Precision AC and DC power supplies are used for the excitation of the pickoffs of all the open-ended type transducers discussed in this report. The outputs of all these devices are directly proportional to the excitation voltage. However, commercially available excitation supplies have errors which are small compared to the transducer errors. Drift and noise are the primary error sources. Typical noise and drift specifications are well below 1%. The sensitivity to line voltage variation is usually included in the noise and drift specifications. The vibration sensitivity or output voltage variation due to vibration is negligible for commercially available solid state airborne power supplies. However, each individual unit should be tested in the anticipated vibration environment to uncover possible workmanship errors. The effect of temperature is usually included in the drift specification which, as previously indicated, is typically less than  $\pm 1\%$ . However, some units are particularly sensitive to temperature and units with errors of  $\pm 5\%$  over the temperature range from  $-65^{\circ}\text{F}$  to  $250^{\circ}\text{F}$  are not uncommon.

Table 9-1. Analog Signal Conditioning Equipment and Applicability of Common Errors

Type of Equipment	Frequency Response	Amplitude Nonlinearity	Drift	Noise	Calibration	Sensitivity to Power Supply Variation	Vibration Effects	Temperature Effects
Excitation supplies			✓	✓		✓	✓	✓
Cabling	✓			✓			✓	
Demodulators	✓	✓		✓	✓			
Low pass filters	✓				✓			
Wheatstone bridges		✓			✓	✓		✓
AC bridges	✓	✓			✓	✓		✓
DC amplifiers	✓	✓	✓	✓	✓	✓	✓	✓
AC amplifiers	✓	✓		✓	✓	✓	✓	✓

## 9.2 CABLING

The cabling between the various components of the system should ideally introduce no errors into the system. However, the finite resistance of the wire and the capacity of the wire to ground and to other voltage sources introduce spurious signals into the system. The subject of proper grounding and capacity effects is covered in References 62 and 63. For the frequency range of interest, 0 to 50 Hz, capacitive pickup of the cabling should not introduce significant errors. However, errors due to ground loops are troublesome and typically large when compared with other system errors. Various portions of typical aircraft are not at the same ground potential. This is due primarily to the assembly procedure in which various parts of the aircraft are painted before assembly. As a result, perfect bonding or electrical grounding is not established. If the negative or ground side of both the transducer and the following amplifier are electrically connected to different parts of the aircraft, a ground loop is established (see Figure 9-1).

The effect of the ground loop depends on the frequency of the ground signal and the amplifier input characteristics. For AC amplifiers and direct coupled DC amplifiers, the error voltage depends on the current division between the ground and negative signal lead. The error is

$$\% \text{ error} = \frac{e_{cm}(t) R_o}{e_o(t) [R_o + R_{gl}]} \quad (9.1)$$

where

$e_{cm}(t)$  - ground loop or common mode potential, volts

$e_o(t)$  - signal potential, volts

$R_{gl}$  - ground resistance, ohms

$R_o$  - wire resistance, ohms

Note that the above error is frequency dependent; an AC amplifier will not be sensitive to DC ground voltages. For a differential input amplifier, the parameter which describes the ability to reject spurious voltages is common mode rejection. This is the effective attenuation of the spurious signals; commercially available units have common mode rejection specifications of  $10^4$  to  $10^6$ . These values depend on the frequency.

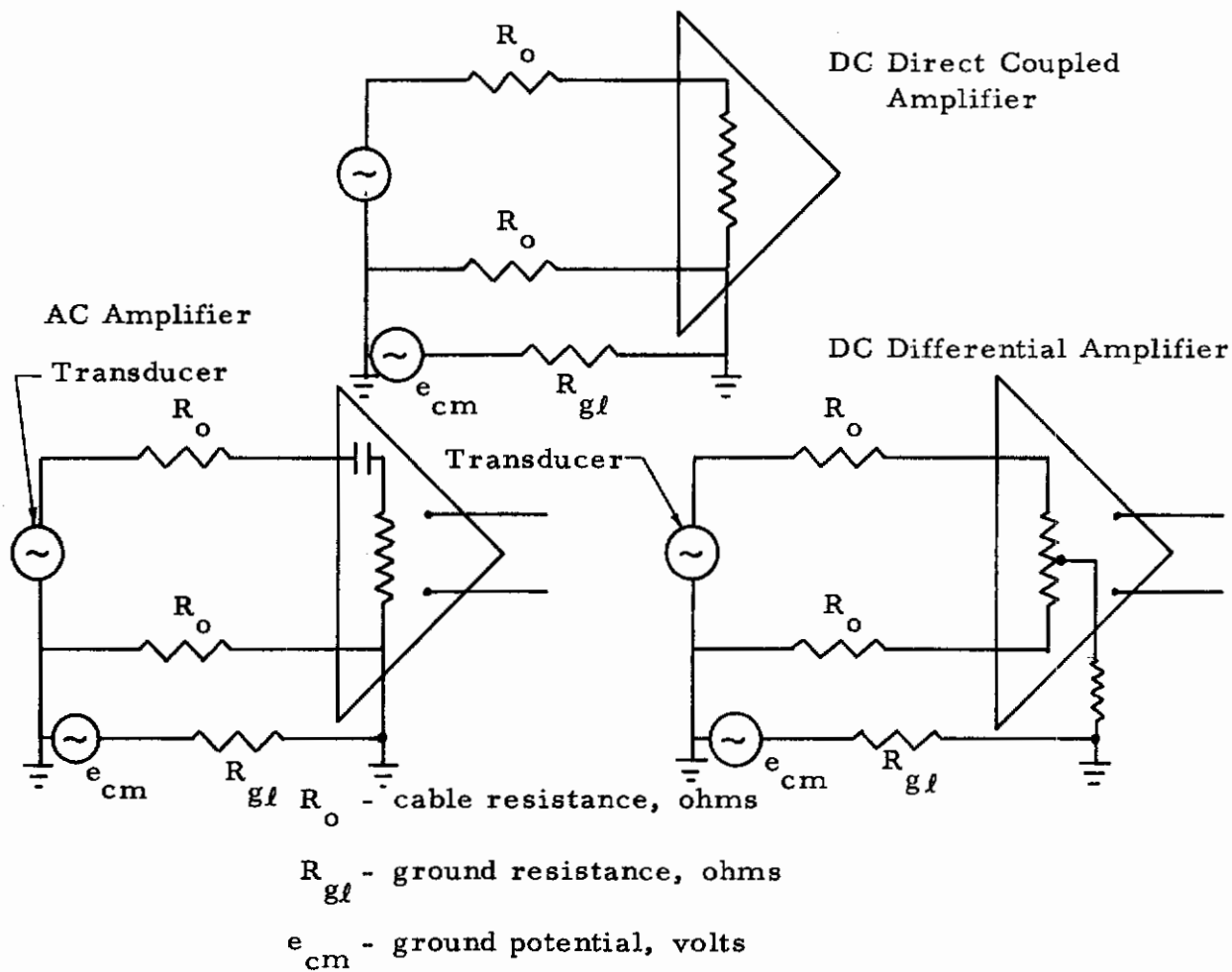
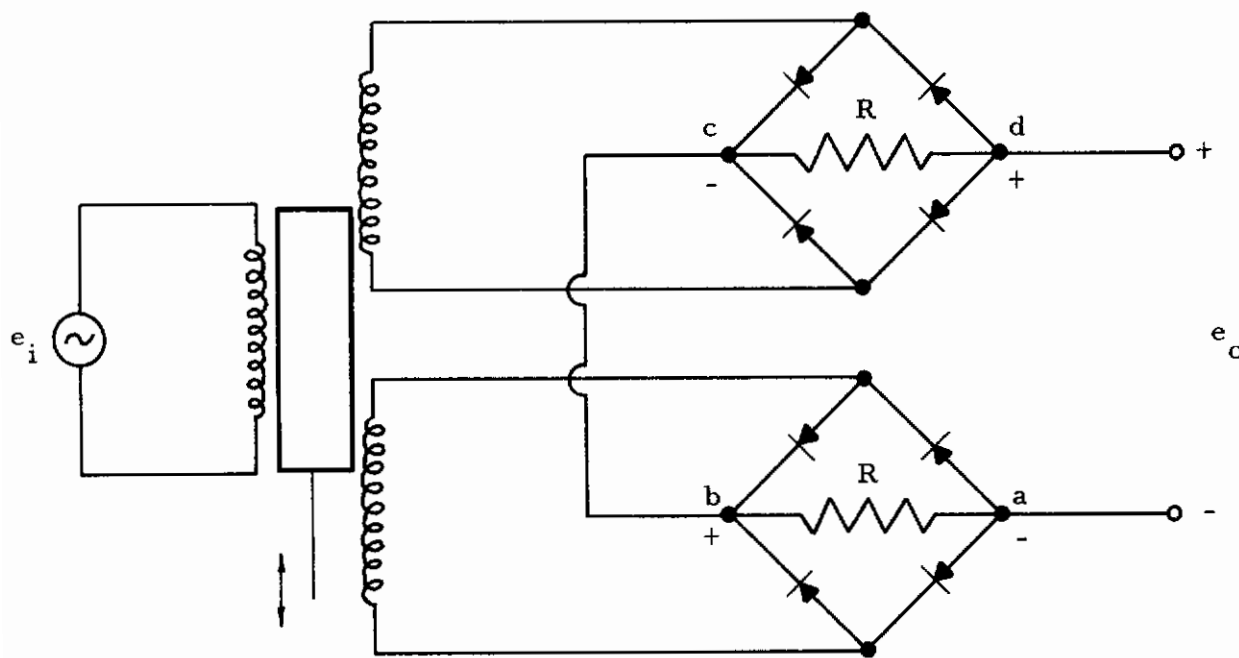


Figure 9-1. Ground Loops and Subsequent Stages

### 9.3 DEMODULATORS

The demodulation of the amplitude modulated signals induces errors into the system. The major errors associated with demodulators are nonlinearity due to the nonlinear characteristics of diodes and carrier noise or ripple. The latter is a function of the data frequency-carrier frequency ratio discussed in the section on variable inductance pickoffs, and the low pass filter characteristics. A simple phase sensitive demodulator is indicated in Figure 9-2. Demodulation circuits are discussed in References 1 and 3.



$$e_o = e_{ab} + e_{cd}$$

$$R \approx 1,000 \text{ to } 10,000 \text{ ohms}$$

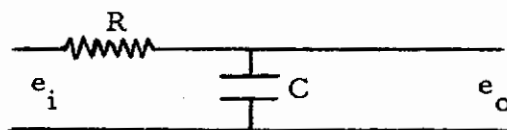
Figure 9-2. Simple Phase Sensitive Demodulator

## 9.4 LOW PASS FILTERS

Low pass filters are required for two main purposes as follows:

1. To remove the carrier from the amplitude modulated signal from variable inductive transducers
2. To limit the input frequency range for tape recorders.

The technology of filter design and application is a field by itself. A number of references, including 64, 65 and 66 among others, present design information for various types of filters. The design may be passive and use combinations of resistors, capacitors, and inductors, or may be active and use operational amplifiers in various applications. The particular frequency response function must be obtained by analysis of the particular network. However, a simple RC low pass filter is a convenient reference or base line for consideration of more complex filters.



The frequency response function is

$$H(f) = \frac{1}{1 + j 2\pi f RC} = \frac{1}{\sqrt{1 + (2\pi f RC)^2}} e^{-j\phi(f)} \quad (9.2)$$

$$\phi = \tan^{-1} 2\pi f RC \quad (9.3)$$

Above a nominal frequency, the denominator doubles for every doubling of the frequency, or octave, and the frequency response function is



attenuated at the rate of 6db per octave. For properly designed filters, the rolloff slope is a multiple of 6db per octave but the phase factor is not necessarily either zero or a linear function of frequency (constant time delay). The requirement for constant time delay is important for any cross spectra or cross correlation analysis and for peak statistic analysis.

#### 9.4.1 Intrinsic Errors, Low Pass Filters

The most significant errors of low pass filters are as follows:

1. Insertion loss
2. Impedance matching
3. Frequency response gain factor and phase factor

The insertion loss of a filter is the basic design parameter relating nominal input to nominal output. When inserting a filter into a circuit, loading effects must be considered and minimized by impedance matching.

The frequency response function gain factor design requirements are relatively easy to satisfy; a series of cascaded simple filters would suffice. However, the phase factor requirement is not easily satisfied. Butterworth filters have reasonably good phase characteristics. Reference 67 describes a seven-pole Butterworth filter designed for this very application.

#### 9.5 WHEATSTONE BRIDGE CIRCUIT

The Wheatstone bridge circuit is used extensively with strain gages because the quiescent excitation voltage can be balanced out. This is important when using conventional strain gages because the excitation voltage is much greater (by approximately 100:1) than the data signal voltage.

9.5.1 Intrinsic Errors, Wheatstone Bridge Circuit

9.5.1.1 Constant Voltage Source

An ideal Wheatstone bridge circuit with constant voltage excitation is shown in Figure 9-3.

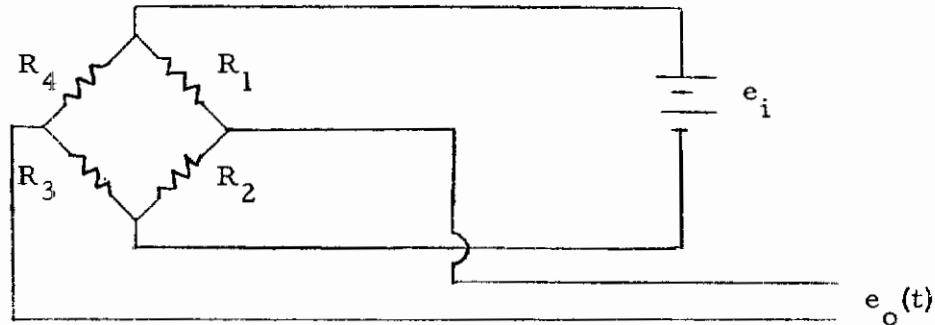


Figure 9-3. Ideal Wheatstone Bridge Circuit - Constant Voltage Excitation

$e_i$  = excitation potential, volts

$e_o(t)$  = instantaneous output potential, volts

$R_1, R_2, R_3, R_4$  = legs of Wheatstone bridge circuit, ohms

Figure 9-3. Ideal Wheatstone Bridge Circuit - Constant Voltage Excitation

The output from this circuit is given by Eq. (9.4).

$$e_o(t) = e_i \left[ \frac{R_3}{R_3 + R_4} - \frac{R_2}{R_1 + R_2} \right] = e_i \left[ \frac{R_1 R_3 - R_2 R_4}{(R_3 + R_4)(R_1 + R_2)} \right] \quad (9.4)$$

For the special case where one leg of the bridge is an active gage (Case A, Figure 7-1) and all legs have the same nominal resistance, References 18 and 49 among others point out that the circuit is nonlinear with amplitude. That is,

$$\begin{aligned} \text{when } R_1 &= R_2 = R_4 = R \\ R_3 &= R[1 + K\epsilon(t)] \end{aligned} \quad (9.5)$$

then

$$e_o(t) = e_i \frac{K\epsilon(t)}{4 + 2K\epsilon(t)} \quad (9.6)$$

Frequently, the  $2K\epsilon(t)$  term is omitted and the bridge output is taken as a linear function of the strain,  $\epsilon(t)$ . The percentage error in this assumption is given by:

$$\% \text{ error} = \frac{\text{Actual} - \text{Ideal}}{\text{Ideal}} (100)$$

$$\% \text{ error} = - \frac{K\epsilon(t)}{2 + K\epsilon(t)} 100 \approx - \frac{K\epsilon(t)}{2} 100 \quad (9.7)$$

This error along with nonlinearity errors for the two and four gage cases are summarized in Table 9-2. For all these cases, the strain is understood to be the average strain due to the load indicated, other strains being cancelled out. For the case of tension, the gages perpendicular to the applied load sense the Poisson strain,  $-(0.3)$  (tension strain).

Table 9-2. Wheatstone Bridge Nonlinearity Errors Summary Balanced Bridge

Case (See Fig. 7-1)	Active Gages	Excitation		Bridge Output, Volts		Nonlinearity Error %
		Constant Voltage	Constant Current	Constant Voltage Excitation	Constant Current Excitation	
A	1	x		$e_i K \epsilon(t) / [4 + 2K \epsilon(t)]$		$-(100)K \epsilon(t) / 2$
A	1		x	_____	$i_i RK \epsilon(t) / [4 + K \epsilon(t)]$	$-(100)K \epsilon(t) / 4$
C	2	x	x	$e_i K \epsilon(t) / 2$	$i_i RK \epsilon(t) / 2$	0
B	2	x		$e_i K \epsilon(t) / [2 + K \epsilon(t)]$	_____	$-(100)K \epsilon(t) / 2$
B	2		x	_____	$i_i RK \epsilon(t) / 2$	0
D-1	4	x	x	$e_i K \epsilon(t)$	$i_i RK \epsilon(t)$	0
D-2	4(2, 6)	x		$e_i 1.3K \epsilon(t) / [2 + 0.7K \epsilon(t)]$	_____	$-(100)0.7K \epsilon(t) / 2$
D-2	4(2, 6)		x	_____	$i_i 1.3RK \epsilon(t) / 2$	0
D-3	4	x	x	$e_i K \epsilon(t)$	$i_i RK \epsilon(t)$	0
D-4	4	x	x	$e_i K \epsilon(t)$	$i_i RK \epsilon(t)$	0

## 9.5.1.2 Constant Current Source

If the constant voltage source of Figure 9-3 is replaced by a constant current source, the current becomes:

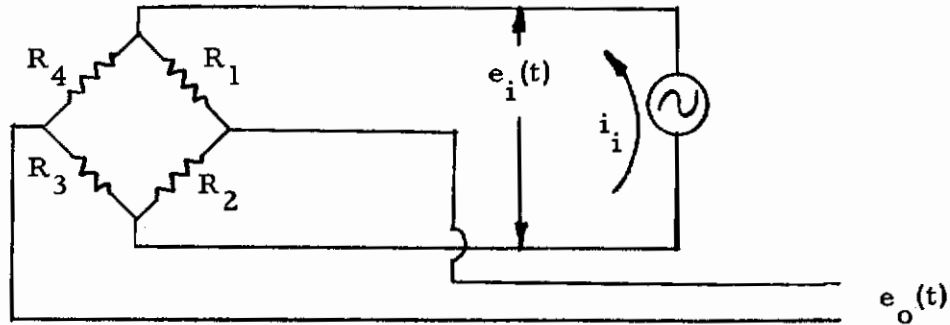


Figure 9-4. Ideal Wheatstone Bridge Circuit - Constant Current Excitation

where  $i_i$  = excitation current, amperes

$e_i(t)$  = instantaneous excitation voltage, volts

$$e_i(t) = i_i \frac{(R_1 + R_2)(R_3 + R_4)}{R_1 + R_2 + R_3 + R_4} \quad (9.8)$$

$$e_o(t) = e_i(t) \left[ \frac{R_3}{R_3 + R_4} - \frac{R_2}{R_1 + R_2} \right] \quad (9.9)$$

Substituting for  $e_i(t)$  and collecting terms gives the general expression for circuit output, Eq. (9.10).

$$e_o(t) = i_i \frac{R_1 R_3 - R_2 R_4}{R_1 + R_2 + R_3 + R_4} \quad (9.10)$$

For the special case where one leg of the bridge is an active gage (Case A, Figure 7-1) and all legs have the same nominal resistance

$$R_1 = R_2 = R_4 = R$$

$$R_3 = R [1 + K \epsilon(t)]$$

then

$$e_o(t) = i_i R \frac{K \epsilon(t)}{4 + K \epsilon(t)} \quad (9.11)$$

The error for neglecting the  $K \epsilon(t)$  term is given by

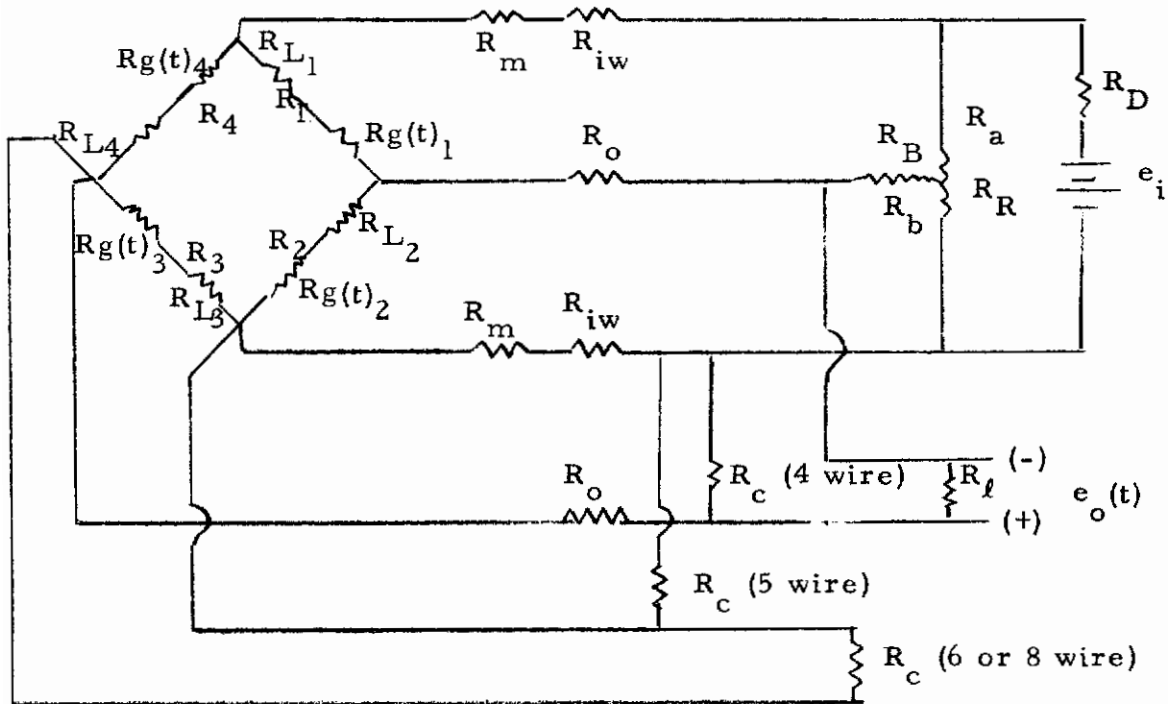
$$\% \text{ error} = - \frac{K \epsilon(t)}{4 + K \epsilon(t)} 100 \cong \left[ \frac{-K \epsilon(t)}{4} \right] 100 \quad (9.12)$$

This error and the nonlinearity error for two and four gage cases are summarized in Table 9-2.

### 9.5.2 Usage Errors, Wheatstone Bridge Circuits

In actual practice, a Wheatstone bridge circuit has nonzero lead wire resistances, a balancing network, finite load resistance, and shunt standardization or calibration resistors. In addition, modulus of elasticity compensating resistors and dropping resistors to simulate constant current excitation may be included. A complete Wheatstone bridge circuit is shown in Figure 9-5.

# Contrails



- $e_i$  = excitation potential, volts  
 $e_o(t)$  = instantaneous output potential, volts  
 $R_g(t)$  = instantaneous strain gage resistance, ohms  
 $R_1, R_2, R_3, R_4$  = legs of Wheatstone bridge circuit, ohms  
 $R_c$  = standardization or calibration resistor, ohms  
 $R_\ell$  = load resistor, ohms  
 $R_m$  = modulus compensation resistor resistance, ohms  
 $R_{iw}, R_o$  = wire resistance, input and output, ohms  
 $R_D$  = voltage dropping resistor, ohms  
 $R_B$  = bridge balance series resistor resistance, ohms  
 $R_R$  = bridge balance potentiometer resistance, ohms  
 $R_a, R_b$  = partial potentiometer resistances, ohms  
 $R_L$  = lead wire resistance in series with gage, ohms  
 Note:  $R_1 = R_{L1} + R_{g1}$

Figure 9-5. Complete Wheatstone Bridge Circuit

# Contrails

The exact output of this circuit may be calculated from the resistances or, inversely, the average strain may be calculated from output. One method would entail writing nine simultaneous equations and arranging the coefficients in a determinate which could easily be solved for a variety of cases by a digital computer. However, with a linear system, the individual error sources may be evaluated separately.

One case of particular interest is the comparison of outputs from a standardization or calibration resistor and from a strain induced output. Equating the outputs then gives a relationship for the standardization (calibration) resistor in terms of the strain it represents. The output due to a standardization or calibration resistor across leg 3 of an ideal bridge with constant voltage excitation is given by Eq. (9.13).

$$e_o = -e_i \frac{R_g}{2R_g + 4R_c} \quad (9.13)$$

where  $R_c$  = calibration resistor, ohms.

When this output is equated to the outputs listed in Table 9-2, the relationship between  $R_c$  and strain may be determined. For example, equating the outputs of Eqs. (9.6) and (9.13), remembering the calibration resistor is simulating a negative strain

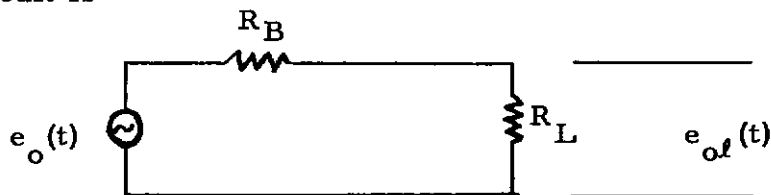
$$e_i \frac{(-)K\epsilon}{4 - 2K\epsilon} = -e_i \frac{R_g}{2R_g + 4R_c}$$
$$R_c = \frac{R_g}{K\epsilon} - R_g \quad (9.14)$$



# Contrails

This relationship along with calibration resistor equivalents and the errors associated with neglecting lead wire resistances for the four, five and six wire configurations are presented in Table 9-3. Note that a calibration resistor always simulates a negative strain. In these expressions, the terms  $R_i/R_c$  and  $R_0/R_c$  are considered negligible and are not included. Note that for the case of a single active gage, the calibration resistor calculation is slightly different from the general case. This is due to the amplitude nonlinearity of a single gage bridge; the expression given for calibration resistor is exact for one given strain.

The errors due to the balancing network and the load resistance are negligible when calculating standardization or calibration resistor values, especially if the strain gages are used as a load calibrated transducer. However, if standardization is not employed, the bridge voltage with a load resistance must be determined. The loaded output is usually determined from the the open circuit output by use of Thevenin's theorem. The equivalent circuit is



where

$$R_B = \frac{R_1 R_4}{R_1 + R_4} + \frac{R_2 R_3}{R_2 + R_3}$$

$e_{ol}$  - loaded output voltage

$R_l$  - load resistor, ohms

The open circuit and loaded outputs are related by

$$\frac{e_{ol}}{e_o} = \frac{1}{1 + \frac{1}{R_l} \left[ \frac{R_2 R_3}{R_2 + R_3} + \frac{R_1 R_4}{R_1 + R_4} \right]} \quad (9.15)$$

Table 9-3. Calibration Resistor Equivalents and Errors Due to Lead Wire Resistances

Type System	Usage		% Error for Neglecting $R_i$ and $R_0$ or Load Calibration Without $R_i$ and $R_0$
	Direct Strain Measurement	Load Calibrated Transducer	
Ideal, no $R_i, R_0$ Single gage, includes nonlinearity	$R_c = \frac{R_g}{nK \epsilon } - R_g$	$R_c = \frac{T}{\text{load}}$	0
Ideal, no $R_i, R_0$ General	$R_c = \frac{R_g}{nK \epsilon } - .5 R_g$	$R_c = \frac{T}{\text{load}}$	0
4 Wire	$R_c = \frac{R_g}{nK \epsilon } \left[ 1 + \frac{2R_{iw}}{R_g} \right] \left[ 1 + \frac{2R_0}{R_g} \right] - .5 R_g$	$R_c = \frac{T}{\text{load}}$	$\approx \frac{2(R_{iw} + R_0)}{R_g} (100)$
5 Wire	$R_c = \frac{R_g}{nK \epsilon } \left( 1 + \frac{2R_{iw}}{R_g} \right) - .5 R_g$	$R_c = \frac{T}{\text{load}}$	$\approx \frac{2R_{iw}}{R_g} (100)$
6 Wire	$R_c = \frac{R_g}{nK \epsilon } - .5 R_g$	$R_c = \frac{T}{\text{load}}$	$\approx 0$

n = Number of active gages  
T = A constant determined during calibration

# Contrails

If  $R_1 = R_2 = R_3 = R_4 = R$ , and the changes in resistances are small, then

$$\frac{e_{ol}}{e_o} = \frac{1}{1 + \frac{R}{R_\ell}} \quad (9.16)$$

The error if the load resistance is neglected is

$$\% \text{ error} = \frac{R}{R_\ell + R} 100 \quad (9.17)$$

Reference 68 presents expressions and typical values for errors when the balancing network resistances are neglected. Typically, these errors are less than  $\pm 1\%$  if  $R_R$  and  $R_B$  are large compared with  $R_g$ .

Modulus compensation resistors are used in series with the excitation source to compensate for the modulus of elasticity of the test specimen material decreasing with temperature. These resistors increase in resistance as the temperature increases, less voltage appears across the strain gage bridge, and a proportionately smaller output results. In practice, equal modulus compensating resistors should be used in the positive and negative excitation circuit to minimize errors during shunt calibration or standardization. If modulus resistors are used, the input lead resistance values in Table 9-3 should be increased by the value of  $R_m$ .

When the usage is as a load calibrated transducer and all the circuitry is unchanged between calibration and test, these lead wire errors are avoided. This procedure is generally considered "good practice"; the expressions in Table 9-3 indicate why.

### 9.5.3 Environmental Errors, Wheatstone Bridge Circuit

This section is included after usage errors because a description of the complete circuit is required for the presentation of this material.

The environmental errors considered are as follows:

1. Lead wire resistance variations due to temperature
2. Lead wire resistance variations due to strain
3. Vibration effects on potentiometers

The resistors and wires which complete the Wheatstone bridge circuit vary in resistance proportionally with temperature. In general, the resulting errors are minimized if symmetrical elements of the bridge are maintained at the same temperature. The errors associated with these changes in resistance are covered in the section on usage errors.

If the various lead wires are subject to strain, the output from the bridge is affected. Probably the most significant errors occur when the wires which are in series with the gage  $R_L$ , Figure 9-5, change resistance. The unit change in resistance of the leg of the bridge is given by

$$\frac{\Delta R}{R_g + R_L} = K \epsilon(t) + \frac{R_L}{R_g} K_L \epsilon_L(t) \quad (9.18)$$

where  $R_L$  = lead wire resistance in series with gage, ohms

$K_L$  = lead wire "gage factor"

$\epsilon_L(t)$  = instantaneous average unit deformation or strain of lead wire, dimensionless

If the strain of the lead wire is neglected, the resulting error is given by

$$\% \text{ error} = \left( \frac{R_L}{R_g} \right) \left( \frac{K_L \epsilon_L(t)}{K \epsilon(t)} \right) 100 \quad (9.19)$$

## 9.6 AC BRIDGES

AC bridges are used for variable inductance and capacitance pick-offs for the same reason that Wheatstone bridges are used for variable resistance strain gages, that is, to balance or null out the excitation voltage. The principles of operation and errors are similar to those of resistance bridges; however, the characteristics depend on the frequency of the carrier. Reference 1, page 225, presents an analysis of an AC bridge with balance potentiometers. Reference 69 presents basic principles of various types of bridges.

## 9.7 AMPLIFIERS

The types of amplifiers which are employed for flight loads measurement and the input characteristics are as follows:

	Input Characteristic		
	Capacitive Coupled	Direct Coupled	Differential
1. AC Amplifier	✓		
2. DC Amplifier - chopper		✓	✓
3. DC Amplifier - chopper stabilized		✓	✓
4. DC Amplifier - pure DC		✓	✓
5. Operational Amplifiers	✓	✓	✓

The primary application of amplifiers is to increase a low level transducer signal to a level suitable for recording. In other cases, an amplifier may be used for impedance matching with a voltage gain of approximately one. Operational amplifiers are used as building blocks to obtain various desired functions such as amplification, integration, and filtering (see Reference 70). Amplifiers are classified by their input characteristics and by the method of amplification. The various input configurations are shown in schematic in Figure 9-1. The differential input types have the advantage of rejecting common mode spurious signals.

Following the input circuitry, DC amplification is accomplished simply by direct coupling to an amplification stage as with AC amplifiers, or by modulating the signal and treating it as an AC signal. Two basic variations of modulation are employed: simple chopping and reconstruction of the signal, and chopper stabilization. In the latter, the low frequency portion of the signal is chopper amplified and then the recombined signal is amplified with a low gain DC amplifier using feedback (Reference 3, page 617). Improved components have permitted the manufacture of direct coupled DC amplifiers with performance characteristics comparable to chopper amplifiers. The main advantage of chopper stabilization is that the high frequency components are not modulated and the high frequency cutoff may be high while maintaining low drift characteristics. The major advantages and disadvantages of the types of DC amplifiers are given in Table 9-4. Variations of the simple chopper configurations have been designed with desirable features (Reference 71). Operational amplifiers are usually employed with feedback so that the effect of amplifier drift and amplitude linearity are minimized.

Table 9-4. Advantages and Disadvantages, DC Amplifiers

Type of Amplifier	Advantages	Disadvantages
Direct Coupled	Simplicity	Susceptible to drift
Chopper	Drift minimized	Frequency response limited
Chopper, stabilized	Drift minimized High frequency response	Complex

### 9.7.1 Amplifier Errors

The major amplifier errors are indicated in Table 9-1. These errors are not conveniently expressed as functions of the component parameters, but are conventionally specified as maximum values for a particular design. For flight loads measurement, particular emphasis should be placed on establishing the short term drift characteristics and susceptibility to temperature variations for the amplifier employed. Commercially available units have gains up to 1000 with combined frequency response, linearity, and temperature effect errors of approximately  $\pm 2\%$ .

### 9.8 OTHER STRAIN GAGE CIRCUITS

Because of the nonlinearities and cable effects associated with Wheatstone bridges, other circuits have been devised. The main feature of all these circuits is the elimination of the static voltage.

## 9.8.1 Dual Voltage Source

Conceptually, the simplest modification of the potentiometer circuit for the purpose of eliminating the bias voltage is the incorporation of a second, or bucking, voltage source (see Figure 9-6). The output of this circuit is as follows.

$$e_o = \frac{e_i [1 + K\epsilon(t)]}{(R/R_g) + 1 + K\epsilon(t)} - e_r \quad (9.20)$$

When  $R = R_g$  and  $e_r = e_i/2$

$$e_o = e_i \frac{K\epsilon(t)}{4 + 2K\epsilon(t)} \quad (9.21)$$

which is identical to the output of a Wheatstone bridge with equal arms (see Eq. 9.6). The disadvantage of this circuit is the requirement for the second voltage source.

## 9.8.2 Dual Current Source

Another strain gage circuit employs a second circuit source to obtain a reference voltage (Figure 9-6). In this case, the current through the gage is constant and the output is linear (see Eq. (9.22)).

$$e_o = i_r R [1 + K\epsilon(t)] - i_r R_3 \quad (9.22)$$

where  $i_r$  - reference current, amperes



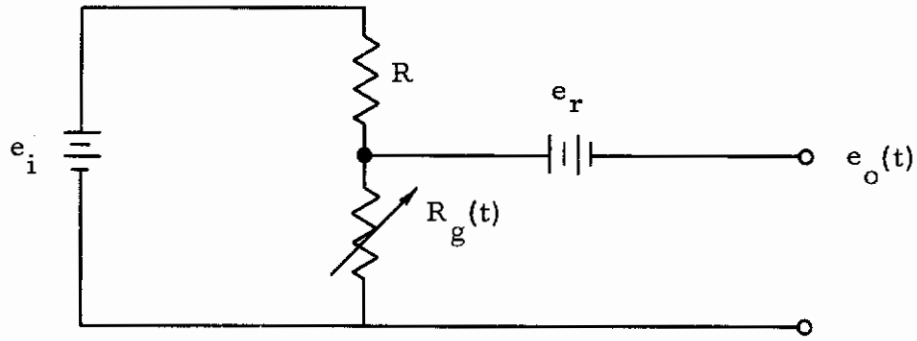


Figure 9.6. Dual Voltage Source

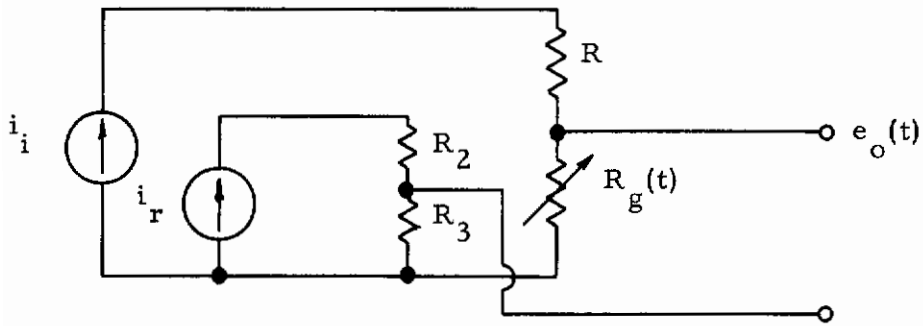


Figure 9.7. Dual Current Source

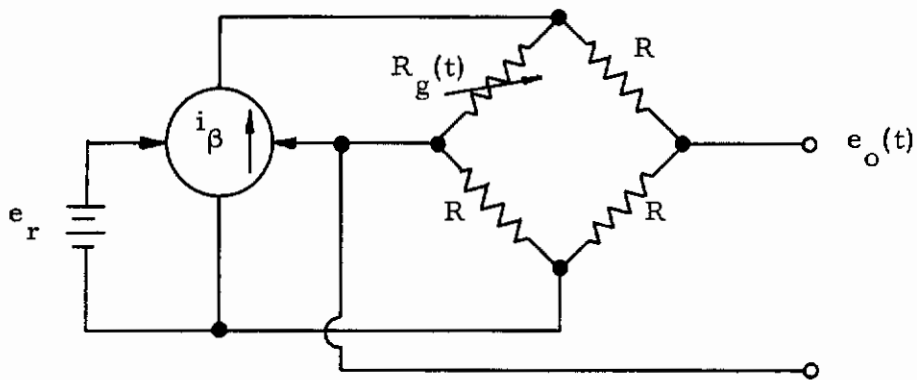


Figure 9.8. Wheatstone Bridge —  
Constant Gage Current

When  $R = R_3$ ,  $i_i = i_r$

$$e_o = i_r RK \epsilon(t) \quad (9.23)$$

which appears to be four times the output of the similar Wheatstone bridge, Eq. (9.11). However, for identical nominal gage currents,  $i_i$  must be reduced by two. The output is still twice that obtained with the single current source and Wheatstone bridge circuit.

### 9.8.3 Wheatstone Bridge - Constant Gage Current

If a current regulator is incorporated into a Wheatstone bridge circuit with constant voltage (see Figure 9-7), the output may be linearized and doubled (see Eq. (9.24)).

$$e_o = \frac{e_i K \epsilon(t)}{2} \quad (9.24)$$

This and other constant current circuits are discussed in Reference 59. The resistor in series with the gage senses current and produces a voltage different from  $e_r$  if the current changes. The current regulator then acts as a servo to maintain constant gage current. This and other constant current circuits are discussed in Reference 90.

### 9.8.4 Common Excitation

To minimize the number of components required for multiple strain gage installations, it is desirable to use a single excitation source for multiple Wheatstone bridges (see Figure 9-8). This is feasible only with

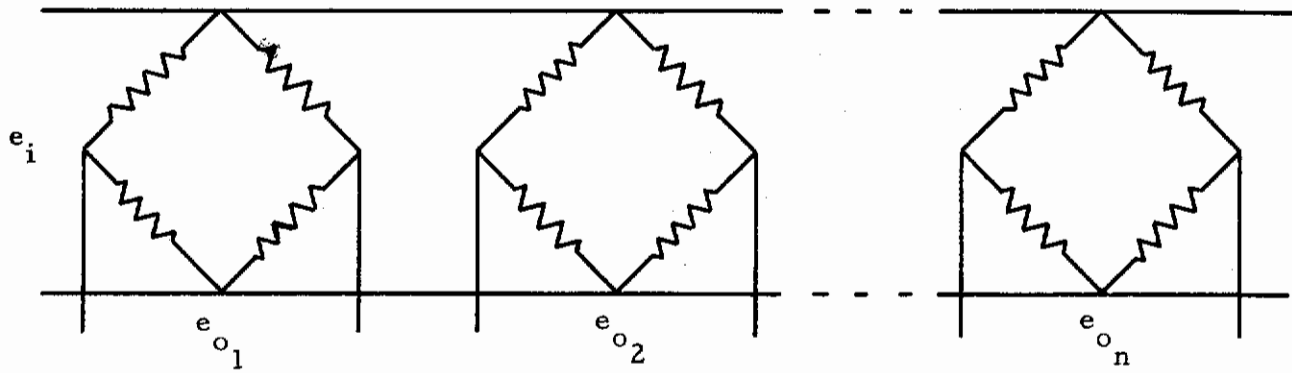


Figure 9-9. Common Excitation

constant voltage excitation. Individual constant current excitation may be approximated by using a large resistance in series with each of the individual bridges. A common usage error with multiple excitation occurs if the negative input to the next stage, usually an amplifier, is grounded. In this situation, three points of each bridge are common and any change in resistance on the ground side of any bridge appears as an output change on all channels.

## 10. MAGNETIC TAPE RECORDERS

### 10.1 CLASSIFICATION OF RECORDERS

Various types of recording devices for the storage of data from experimental flight test programs are commercially available. As indicated in Section 2, the classes of recorders covered in this study will be limited to analog and digital magnetic tape recorders. References 73, 74, and 91 all present introductory descriptive information on the various types of tape recorders. A classification of the various types of recorders and recording techniques is presented in block diagram form in Figure 10-1.

#### 10.1.1 Analog and Digital

The major division in magnetic tape recording as indicated in Figure 10-1, is between analog and digital machines. Analog recording is defined as the storage and reproducing of electrical signals which have some parameter such as amplitude or phase which is linearly related to the data signal. Note that pulse width modulation is classified under analog recording, not digital recording. Consider that during demodulation the original signal can be recovered by performing linear analog operations. This is not possible with pulse coded signals. Digital recording is the same as analog recording except the electrical signals are related to the data by a code, almost always binary.

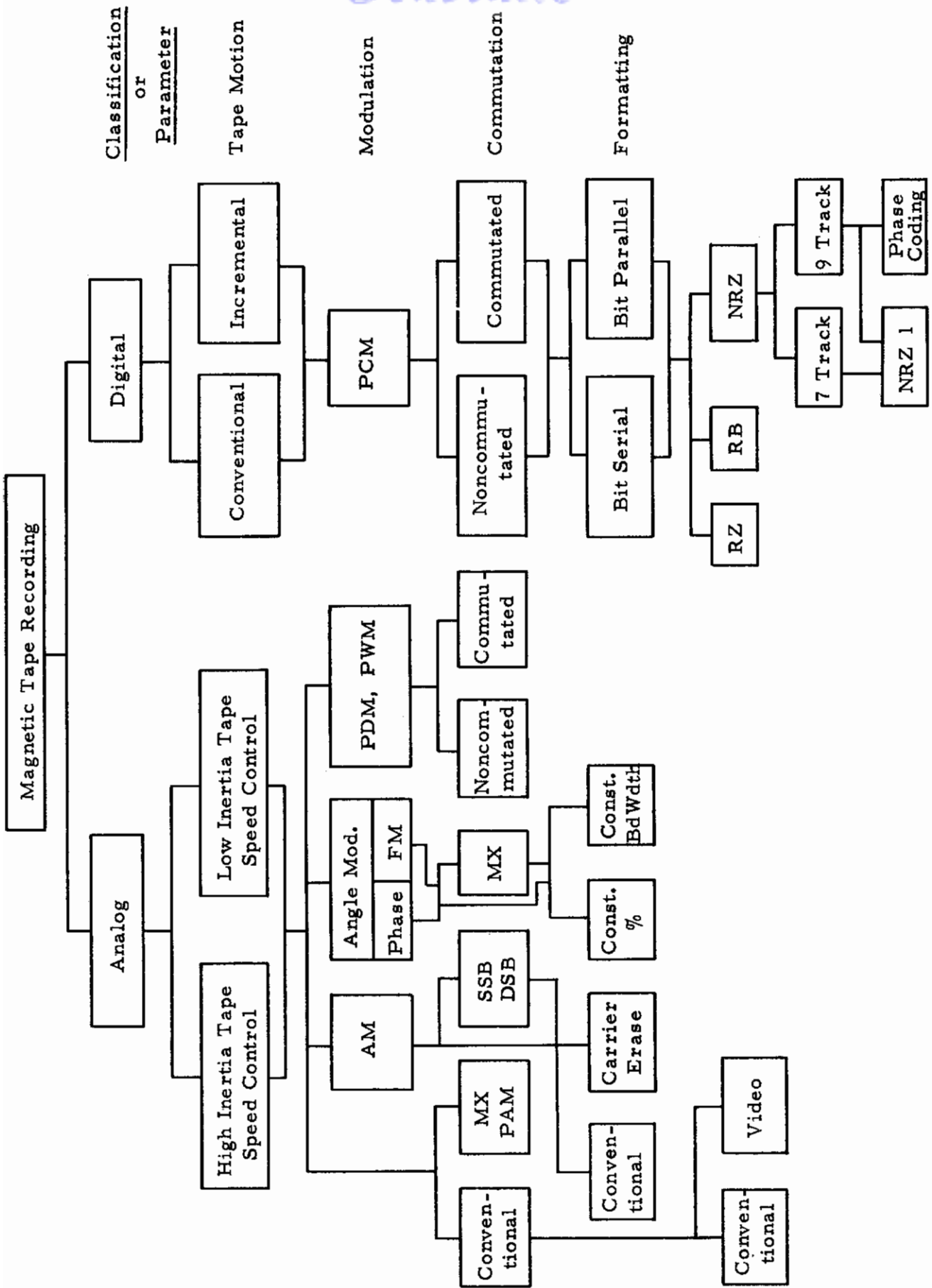


Figure 10-1. Classification of Magnetic Tape Recorders

## 10.1.2 Tape Motion

The next level of classification of tape recorders Figure 10-1 is the method of tape motion control. This is one of three basic functions of tape recorders. The detailed discussion of the types of tape motion mechanisms is presented in Section 10.3. Briefly, for analog recording, the tape is moved continuously. Two general types of speed control are employed. For digital recording, tape motion is either continuous, or incremental or stop and go for each character. The purpose of the latter is to permit tape motion only when a data point is to be recorded. During reproduction, the tape motion is always continuous.

## 10.1.3 Modulation

The type of modulation or coding of the data signal is usually the primary factor in classifying the recording method. Modulation or coding is required because the basic recording process has inadequate low frequency response and signal to noise ratio for instrumentation purposes see Section 10.4.

## 10.1.4 Commutation

Commutation or multiplexing is the sharing of a tape recorder channel by more than one data signal. Two types of sharing are used, time sharing and frequency or bandwidth sharing. When the data signal is sampled, pulse amplitude modulation (MX-PAM), commutated pulse duration or pulse width modulation (PDM, PWM), or commutated pulse code modulation (PCM), the tape channel is shared by sequentially

recording signals from each of the data **samples**. When phase or frequency modulation (FM) or amplitude modulation (AM) is used, the recorder frequency baseband is divided into sections which are used by the different channels.

## 10.1.5 Formatting

Various standards pertaining to number of tape tracks, tape track dimensions, recording frequencies, tape speeds etc., have been adopted. The best known and most widely used standard is that prepared by the Inter-Range Instrumentation Group (IRIG) Reference 76. For frequency modulation standard carrier and data frequencies are assigned for three categories, conventional, wideband, and extended wideband. In addition, constant bandwidth multiplexer standards are presented. However, for flight loads recording from 0-50 Hz, standard frequency assignments are inefficient. For digital recording, three parameters characterize the formatting

1. coding
2. track assignments
3. packing density

### 10.1.5.1 Coding

Present coding methods may be classified as one of the following:

1. Return-to-zero (Rz)
2. Return-to-bias (RB)
3. Nonreturn-to-zero (NRZ)

See Reference 76 for variations of these basic coding methods.

The RZ and RB methods are quite similar. In both cases, a logical "one" is generated by magnetizing the tape to saturation. Figure 10-2. The difference occurs in the recording of a logical "zero". With RZ recording, a "zero" is represented by a completely unmagnetized section of tape, while the RB method will record a low bias level.

In NRZ recording, two different techniques are presently in use. The first of these is known as NRZI or IBM standard. With this method, the tape is always magnetized to saturation, but the polarity of magnetization changes. A logical "one" will cause a polarity change from the existing to the opposite state. A logical "zero" is represented by a lack of polarity change. The NRZI method is the standard recording mode in the digital computer field, although some recent computers employ other methods.

The second NRZ technique is known as phase encoding. Again the tape is always magnetized to saturation. As with NRZI, a logical "one" is defined by a polarity change while a logical "zero" causes none. However, polarity changes also always occur at the boundaries between bits. Because of the additional polarity changes, higher reliability is possible. Also, higher bit packing densities may be used.

#### 10.1.5.2 Tape Track Assignments

Two standard digital tape track assignments are presently in use. The older utilizes seven tracks across the 1/2-inch width of the tape, Figure 10-3. Six of the tracks contain data bits while the seventh is reserved for parity information. The set of six bits recorded



at a given point on the tape is known as a character. This implies that the character set used may contain  $2^6$  or 64 different elements. The tracks are placed on the tape in their order of significance with the parity track at the top.

The newer track assignment standard spaces nine tracks across the 1/2-inch width of the tape, Figure 10-4. One track is still reserved for parity while the other eight tracks contain data bits. The character set in this system contains  $2^8$  or 256 different elements. In addition, the ordering of the tracks has been modified to place the more frequently used tracks near the center of the tape. This increases reliability because the edges of the tape are more likely to become damaged through crimping than the center.

It must be emphasized that the two formats described above are the only ones compatible with existing digital computers.

Both lateral and longitudinal parity bits are required for computer compatibility. Either odd or even parity is acceptable although even parity is usually used when recording data character by character. The value of the lateral parity bit is determined by calculating the logical sum of the six or eight data bits. The parity bit is then adjusted to make the total sum odd or even as required. The longitudinal parity is generated in the same way, excepting that the sum of all bits in a track for one record is used in the computation.

Since a digital computer reads a block of data at a time rather than individual characters, gaps must be placed on the tape to define data blocks of reasonable length. These gaps are also needed to allow the tape drive to accelerate to or decelerate from normal recording speed. If no gaps are inserted, the data may overflow the computer

# Contrails

memory when tape reading is attempted. In addition to inter-block or end-of-record gaps, beginning-of-tape, end-of-tape, and end-of-file gaps are also used. While not absolutely necessary, these additional gaps facilitate the use of the tape on computer tape drives.

It is emphasized that only the two track assignment standards described in Figures 10-3 and 10-4 with the NRZ or NRZI coding are compatible with existing digital computers. For flight loads recording where recorder weight is a premium, various other formats have been proposed and adopted. One such scheme puts sixty tracks on 1 3/8 inch wide tape, Reference 92. Data in this format must be converted to computer format with special equipment prior to computer entry.

## 10.1.5.3 Character Packing Densities

Four standard packing densities are presently in use. These are:

1. 200 characters/inch
2. 556 characters/inch
3. 800 characters/inch
4. 1600 characters/inch

Since both the amount of data which can be recorded and the recording speed are directly proportional to the packing density, an attempt should always be made to use the highest possible density. At present, computer tape drives may usually be adjusted to read at least two different densities although this is not always the case.

## 10.2 RELATIVE ADVANTAGES

As previously indicated, the primary factor in differentiating magnetic tape recording is the modulation method. The advantages and disadvantages of the various types of modulation methods when considered for experimental flight test programs are presented in Table 10-1. The differences on trade-offs are mostly due to the exchange of data bandwidth for accuracy and the complexity of the equipment required.

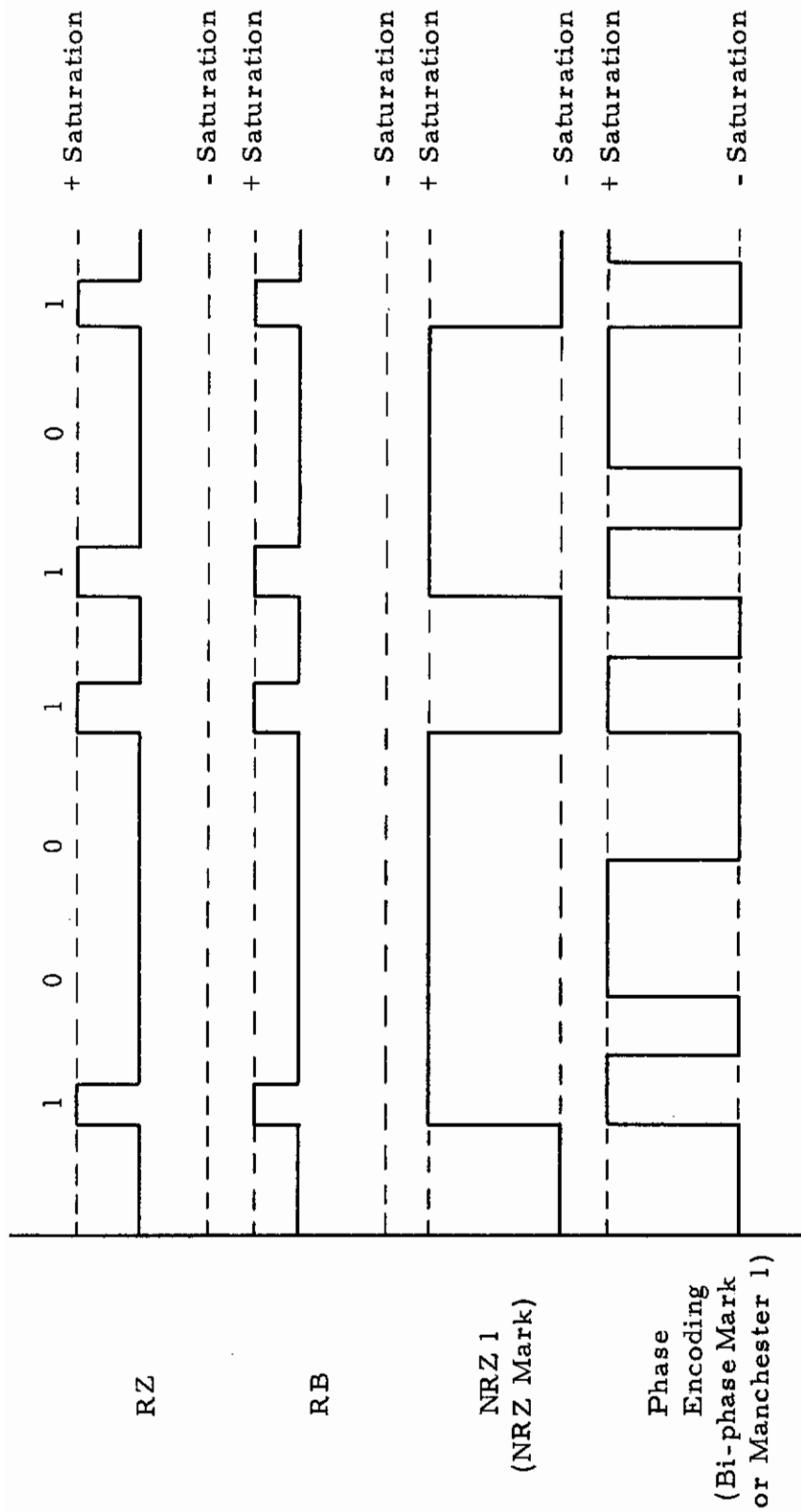


Figure 10-2. Digital Coding

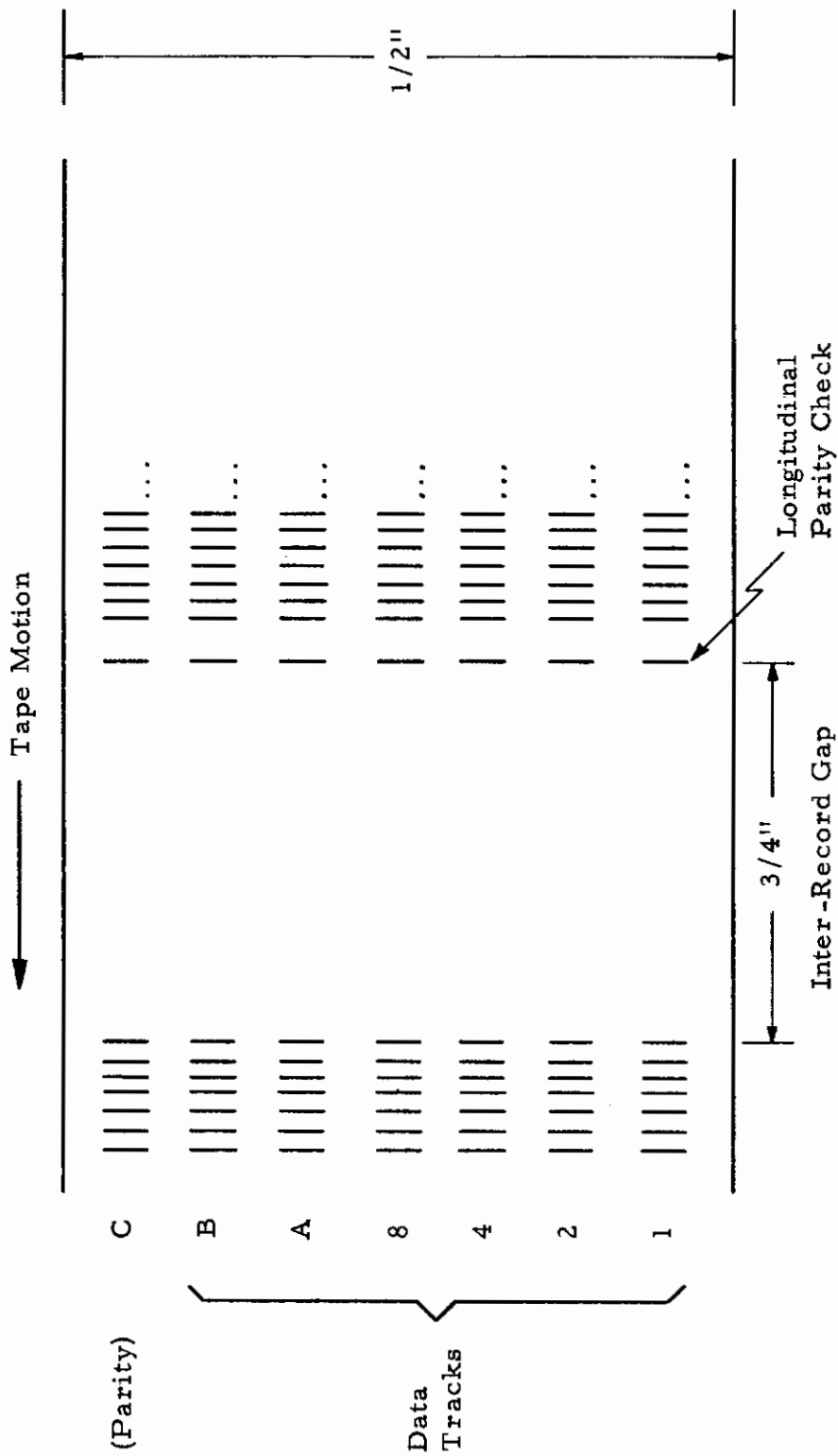


Figure 10-3. 7-Track Digital Format

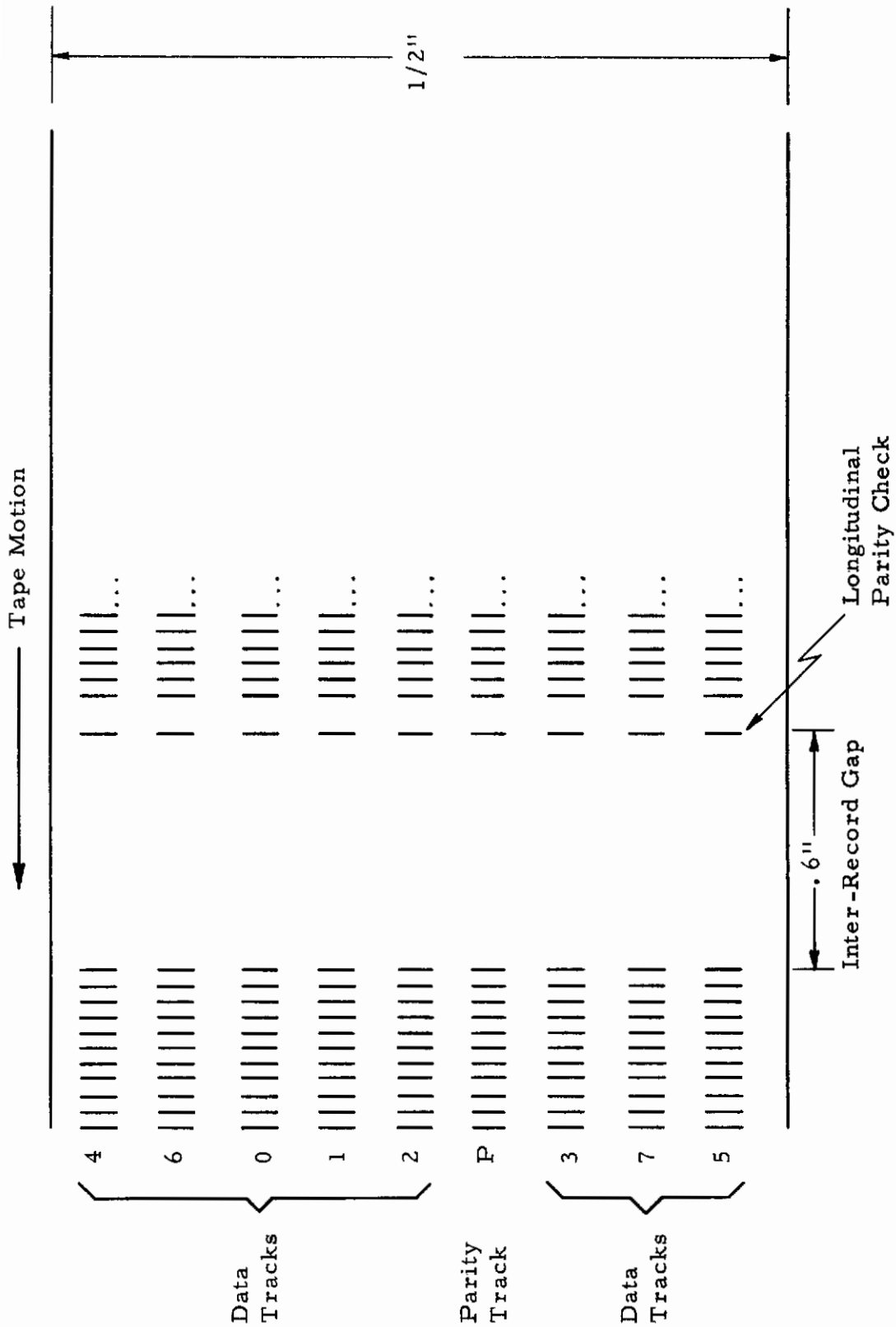


Figure 10-4. 9-Track Digital Format

Table 10-1. Comparison of Types of Magnetic Tape  
Recorders for Flight Loads Measurement

Recording Mode	Major Advantages	Major Disadvantages
Direct* (Conventional)	Wide data bandwidth	No DC response Low channel density Poor linearity
Pulse Amplitude Modulation (PAM)*	Good channel density Simplicity	Poor signal to noise Poor linearity
Carrier* Erase	Extreme simplicity	Poor linearity Poor channel density
Wideband Frequency Modulation	Excellent signal to noise Good linearity Good frequency response	Poor channel density
Constant Bandwidth Frequency Modulation Multiplex	Good channel density Good signal to noise Good linearity Good frequency response	Complexity
Constant Percentage Frequency Modulation Multiplex	Good channel density Good signal to noise Good linearity Good frequency response	Poor frequency response selection Complexity
Pulse Duration Modulation (PDM or PWM)	Good channel density	Low data bandwidth
Digital Conventional Computer Compatible	Good channel density Excellent linearity Excellent signal to noise possible Correct format	Fair data bandwidth

\* Unacceptable for Experimental  
Flight Test Applications

Recording Mode	Major Advantages	Major Disadvantages
Digital Conventional Computer Incompatible	Good channel density Excellent linearity Excellent signal to noise Good information density	Incorrect format
Digital Incremental	Records on command All other advantages same as conventional digital	Slower record rate than conventional digital

### 10.3 TAPE RECORDER COMPONENTS

For the purpose of describing the principles of operation and analyzing errors, magnetic tape recorders may be considered to be composed of three subsystems. These are indicated in Figure 10-1 and are as follows:

1. The record and read-out subsystem (including the heads and the magnetic tape)
2. The tape motion or tape transport subsystem
3. The modulation-demodulation or coding subsystem

### 10.4 RECORD AND READOUT SUBSYSTEM

The magnetic tape and the physics of magnetism are common to the different types of recording. An analog or coded signal is converted to a magnetic flux by passing a current through a record head. The resulting flux causes a change in state of an oxide-coated tape which is passed over the record heads. To recover this data signal, the tape is passed over a reproduce head. The change in flux with time, caused by the movement of the tape, causes an electrical signal to be generated in

the reproduce head (see Figure 10-5). With continuously moving tape, the signal impressed on the tape is proportional to the magnetic field that it saw as it was passing from the magnetic field of the record head. Thus, the trailing edge of the record head is essentially the point of recording. However, during playback or reproduction, the magnitude of the voltage generated by the magnetic tape passing across the reproduce

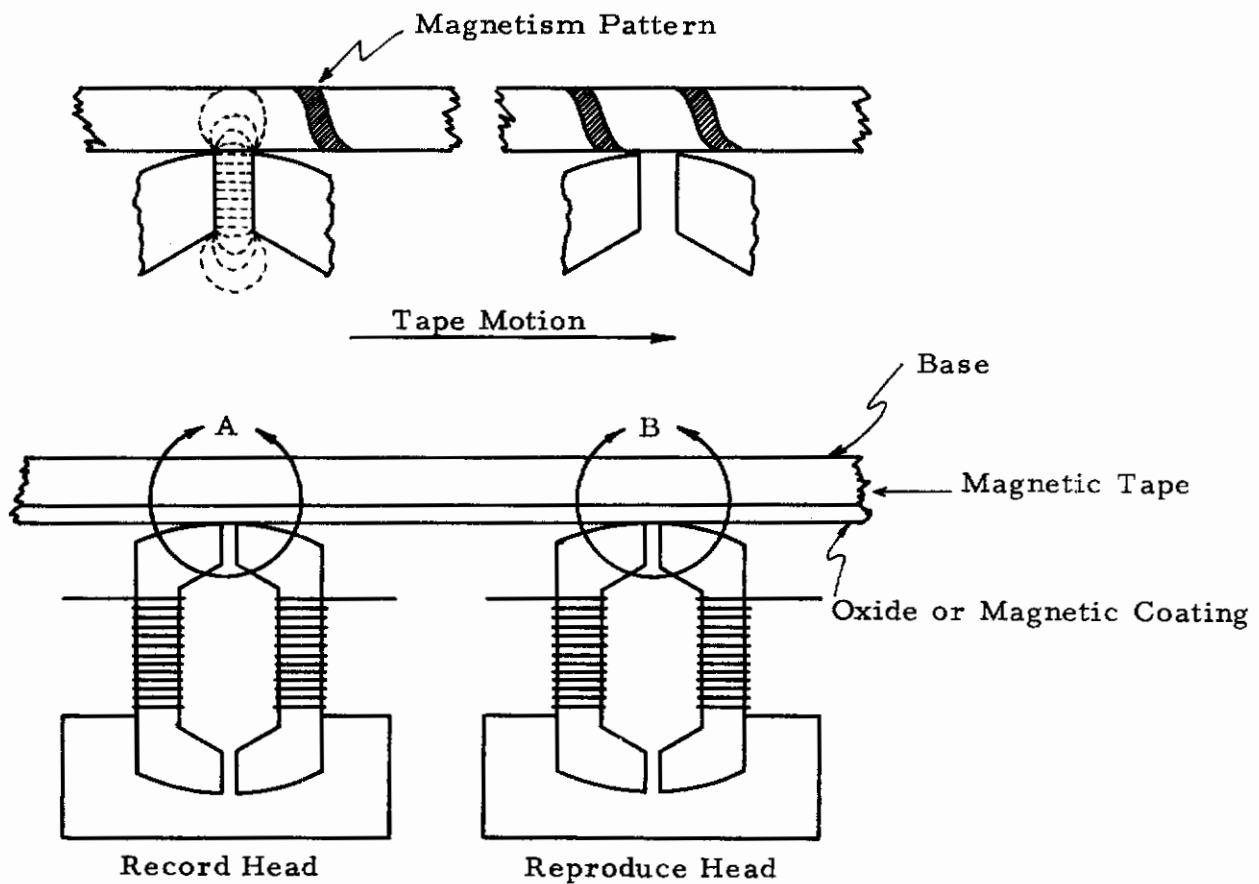


Figure 10-5. Schematic, Magnetic Tape Recording and Reproduction



head gap is proportional to the magnetism of the tape actually spanned by the gap at any particular instant. Therefore, the resolution which limits the density of information on the tape is basically a function of the reproduce head. The frequency response of the record-reproduce subsystem depends in the low frequency region upon the rate of change in flux per unit time across the reproduce head, and on the system noise level. Above a certain frequency, the wavelength of the data signal is shorter than the reproduce gap and a gap loss occurs. However, at multiples of the reproduce gap, the frequency response is finite and has the form  $\frac{\sin x}{x}$ . An idealized overall frequency response function of the record-reproduce subsystem is presented in Figure 10-6. Another type of reproduce heads is the flux sensitive; however, other problems limit their use.

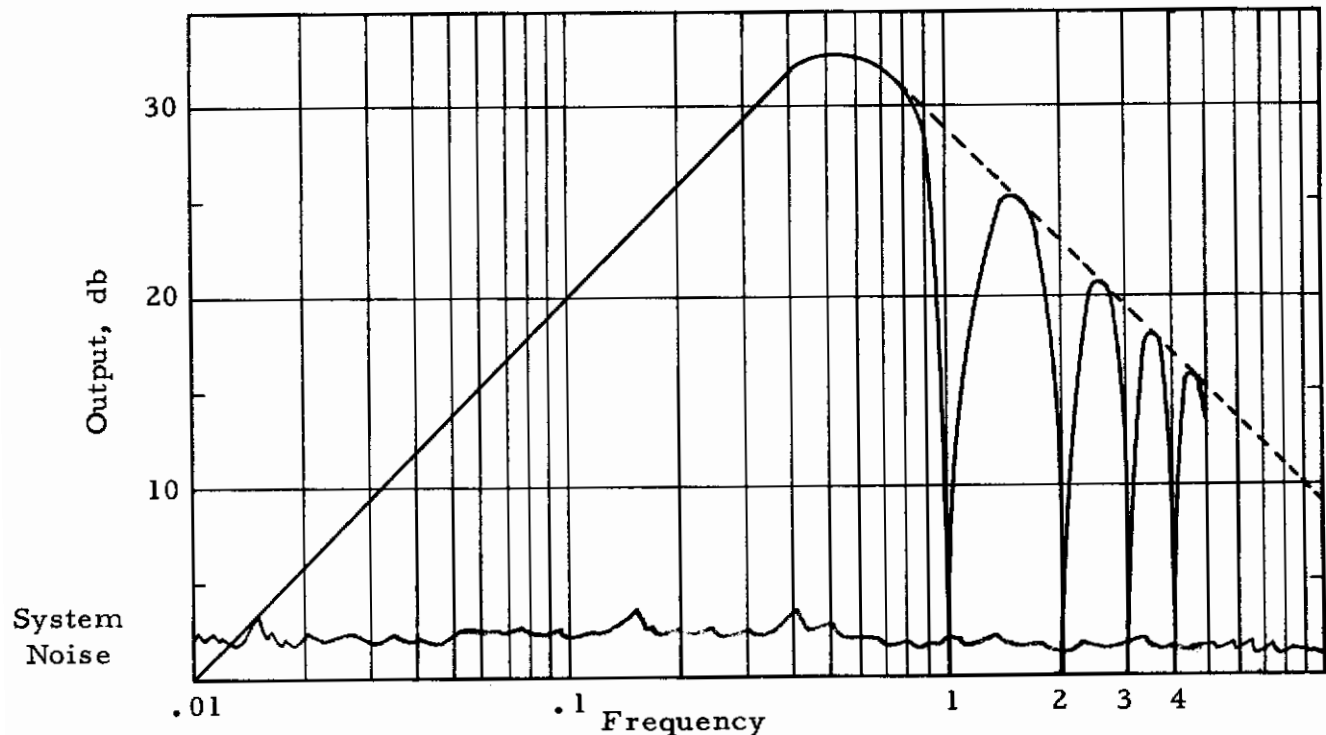


Figure 10-6. Reproduce Head Frequency Response

The other major design consideration besides gap dimensions is head material. The material used must have adequate magnetic susceptibility and must resist wear. Presently available materials combine both properties; however, head wear remains one of the major tape recorder problems, especially in an adverse environment.

The basic tape magnetizing process is nonlinear because the flux-magnetism (B-H) characteristic of ferrous oxide has the form of a hysteresis loop. Two techniques are used to overcome the resulting nonlinearity. A DC bias voltage will place the recording voltage on a linear portion of the flux-magnetism curve (see Figure 10-7). The second technique superimposes a high level, high frequency signal on the data signal. The effect of the AC bias is to collapse the hysteresis loop yielding a linear relationship between input and output. However, the underlying phenomena is not simple. Most references indicate that AC bias is difficult to understand, even mystical, but that it does linearize the process. Reference 75 discusses AC bias in terms of a model of the recording process which considers the depthwise variation of magnetization.

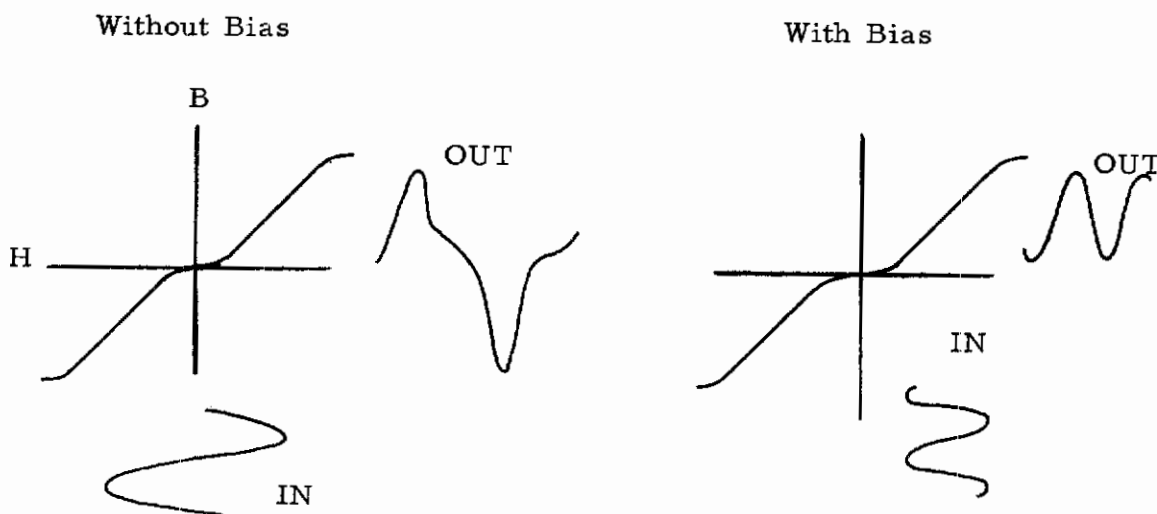


Figure 10-7. Record Amplitude Nonlinearity and DC Bias

The magnetic tape consists of a magnetic material, usually a ferrous oxide, deposited on a plastic base. The manufacture of consistent quality instrumentation tape is the subject of considerable study and effort (References 72, Chapter 9, and 75, Chapter 5). Three parameters which are of primary interest to tape users are as follows:

1. Magnetic frequency characteristics
2. Tape strength
3. Abrasiveness

Various oxides have different particle size or wavelength and therefore different high frequency characteristics. The tape strength is a function of the thickness, but storage requirements indicate reduced thickness. Commonly used tape thicknesses are 1.0 and 1.5 mm. The abrasiveness is a function of the oxide and binder and should be evaluated for the particular tape used.

#### 10.4.1 Errors, Record and Readout Subsystem

The errors associated with the record and readout subsystem are as follows:

1. Frequency response of reproduce gap
2. Amplitude nonlinearity
3. Self-demagnetization, record demagnetization, head losses and penetration losses
4. Misalignment of head gaps
5. Crosstalk - interleaved heads
6. Dropouts
7. Tape stretch
8. AC bias adjustment

# Contrails

The effect of the nonlinear frequency response function, Figure 10-6, is different for the different types of recording. For direct analog recording, a technique of equalization is used to produce a nominally flat frequency response. This is accomplished by integration of the low frequency end and filtering the high frequency end. For various modulation techniques, a reasonably flat portion of the frequency response characteristic is employed to minimize the effects of this nonlinearity. In addition, the modulation methods themselves are designed to be insensitive to frequency response. This frequency response error appears as noise in the resulting signals when modulation is employed. Equalization is not employed when recording modulated signals because the resulting phase shifts perturb the sidebands of the modulation signal and data errors result. For multiplexed FM signals, the amplitude of the low frequency carriers is located so that the signal power for each channel is comparable on reproduction. In addition, for flight loads measurement, the effect of the frequency response error is minimized because the data is reproduced on a laboratory machine on which high frequency reproduce heads may be employed. The amplitude nonlinearity error, Figure 10-7, is minimized with AC biasing. However, this error contributes to noise in direct recording and therefore defines the baseline for modulation methods. The other major contributor is irregular tape motion discussed in subsequent sections.

As the wavelength of the recorded signal decreases, positive and negative poles are placed closer together and they demagnetize each other. This effect, along with head losses, record demagnetization, and penetration losses, decreases the high frequency response.

Misalignment of the individual gaps in the head block causes the

magnetism pattern to be skewed. The attenuation of the signal is given by

$$\text{Loss, db} = 20 \log \frac{\sin (\pi y \tan \phi) / \lambda}{(\pi y \tan \phi) / \lambda} \quad (10.1)$$

where

- y - track width, inches
- $\phi$  - angle of misalignment, degrees
- $\lambda$  - wavelength, inches

Maximum allowable standards have been established for this misalignment (Reference 76).

Crosstalk between heads is an error which should be insignificant for properly designed heads. However, tests should be performed on occasion to verify that the characteristic has not degraded with wear.

Dropouts are associated more with digital recording than analog recording. The probability of miscoding is a specification parameter of digital tape.

Tape stretch is a function of the tape, the tape transport, and the environment. The effect of stretch on the time base is covered in the following section. The effect of temperature on the particular tape employed should be evaluated carefully. The AC bias current level determines the relative output level and distortion, Figure 10-8. The distortion is a minimum at a low current level but the region is narrow with large bias on either side. Therefore, bias current is usually set at a high level where output is somewhat lower. An error results if the bias current is adjusted incorrectly and unwarranted distortion occurs.

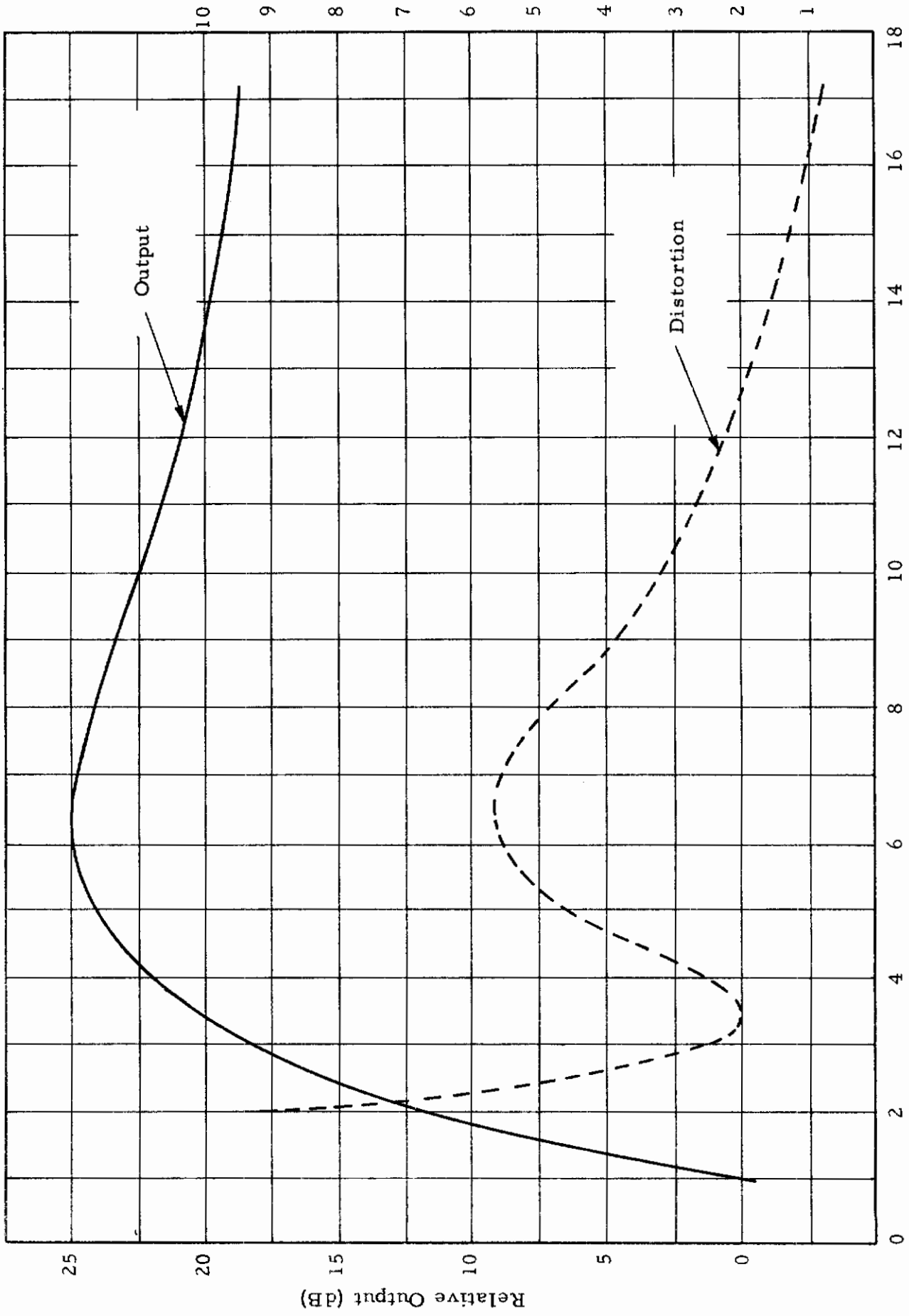


Figure 10-8. Output and Distortion Versus Bias Level



## 10.5 TAPE TRANSPORT SUBSYSTEM

Tape transport systems are logically divided between those that move the tape continuously and those that move the tape in steps or increments. The implementation of each method imposes different requirements and different errors. For continuously moving tape transports, two basically different approaches for the control of the speed are employed. In both, the tape is passed over a capstan that is rotating at essentially a constant speed. One method employs a capstan with high inertia to maintain the constant speed. The second type of system senses the tape speed, compares the speed with a reference frequency, and uses this error signal to servo a low inertia capstan to the proper speed (Reference 78). A number of variations of these two different schemes are employed in commercially available machines. For incremental recording, which is used for digital recorders only, the tape is moved or stepped one digital character at a time instead of continuously. Existing incremental recorders use one of three basic approaches to step the magnetic tape forward the required distance. These techniques may be classified as follows:

1. pulsed pinch roller
2. integral stepping motor
3. servo drive motor

The pulse pinch roller technique employs a constant speed capstan similar to the continuous motion machine. When stepping is required, a pinch roller presses the tape against the capstan for the required length of time. The integral stepping motor has a series of magnetic detents which are precisely spaced. The tape is kept in contact with the capstan and moves the required distance when the drive motor is pulsed. Servo drive motors are a recent development which employ a drive motor and a code wheel. Motion of the code wheel is sensed and is used to trigger a brake or clutch to stop the motion when the tape has moved the required distance. The advantages and disadvan-

tages of the various types of tape motion methods are listed in Table 10-2. The errors associated with the tape transport subsystem are all attributable to imperfect tape motion. Both static and dynamic variations of the tape speed from the ideal tape speed cause significant errors.

The other basic tape transport design consideration is the method of controlling tape tension. The tape must be held against the recording and reproduce heads with controlled stretching of the tape. Three tech-

Table 10-2. Comparison of Types of Tape Motion Transports for Flight Loads Measurement

Tape Motion	Mode of Tape Advance	Major Advantages	Major Disadvantages
Continuous	High mass capstan	Simplicity	Large weight Sensitive to environment Won't follow tape speed variations
	Low mass capstan	Light weight Follows tape speed variations	Complex
Incremental	Pulsed pinch roller	Simplicity	Causes tape damage Low bit density
	Integral stepping motor	Good stepping speeds Good bit density	
	Servo drive motor	High stepping speeds High bit density	Complexity



niques commonly employed are

1. One capstan with tape drag
2. Two capstans
3. Differential diameter capstan

The principles of operation and relative merits of the various techniques are covered extensively in the literature. The method of controlling tape tension does affect the flutter, tape damage, and even head wear.

### 10.5.1 Intrinsic Errors, Tape Transport Subsystem

The major errors attributable to the tape transport subsystem are as follows:

1. Tape speed variation, static
2. Flutter-dynamic deviation of the tape speed from the nominal
3. Dynamic skew-interchannel effect
4. Interchannel time displacement error

Constant or slowly varying tape speed errors are a result of manufacturing tolerances or adjustment and errors in the frequency or time reference. However, for commercially available recorders, these errors are on the order of  $\pm 0.25\%$ . If a tape speed difference occurs between recording and playback the zero shift and frequency error result with frequency modulation and a frequency error and gain factor result with pulse width modulation. However, these errors may be minimized by recording a frequency reference signal on one of the tape tracks and using it to correct the data signals during demodulation. This correction is for the amplitude error and not for the frequency error. Tape speed

variation will have no effect on pulse code modulation unless, if combined with dynamic errors, the total tape speed variation causes incorrect recording or readout of digital bits, or exchange of bits, between characters. Skew and inter-channel time displacement errors are time based errors between channels. Both dynamic and static skew occur when the tape goes across the record or reproduce head at some incorrect angle. Inter-channel time displacement errors are usually associated with both the gap scatter on the individual interleaved heads and the tolerances between heads. For standard recorders, both the record and reproduce head stacks are divided with odd and even numbered channels going to the main stack. The standard configuration for these stacks is 1-1/2 inches apart. A convenient way of expressing all these time displacement errors is in terms of displacement. Typical values for these error parameters are given in Reference 77 and are presented in condensed form in Table 10-3. The displacement attributable to tape stretch are included for comparison. The displacement error can be

Table 10-3. Typical Time Displacement Errors

Type of Time Base Error	Distance, $\mu$ inches		Time, milliseconds Tape speed, 1-7/8 ips	
	Adjacent heads, same stack	Outside Tape Tracks	Adjacent heads, same stack	Outside Tape Tracks
Dynamic skew	84	786	0.04	0.42
Static skew	110	692	0.06	0.37
Inter-channel time displacement	200	1200	0.11	0.64
Tape stretch	0	1312	0	0.70

converted to a time error by dividing by the particular tape speed. However, noting that the error may occur on both record and playback, the time is multiplied by two. The time base errors for a tape speed of 1-7/8 inches per second for each of the types of error are indicated in Table 10-3.

When considering skew and inter-channel time displacement, a number of things should be kept in mind. These are as follows:

1. The error depends on which channels are being compared. The error for outside tracks is much greater than for adjacent even or adjacent odd numbered tracks, that is, those on the same head stack.
2. The overall time displacement error depends on both the recording and reproduction processes. The numbers indicated in Table 10-3 are for one recording-reproduction process. Successive re-recording will increase the time base error.
3. Care should be exercised when combining the different types of errors indicated above into one error. Dynamic skew is definitely a random process and should be described by the RMS value. Reference 77 assumes the maximum value to be the  $2\sigma$  level. The static RMS value is assumed to be 1/3 the maximum value.
4. The magnitude of these time base errors may be compared to the transducers with constant time delays equal to  $1/4f_n$ .

Flutter is the single channel time varying tape speed error. This error is well defined for commercially available machines. Flutter is usually expressed as a percentage of the nominal tape speed. In addition,

the frequency spectra of the flutter must also be indicated. Flutter is generated by the passage of the tape over slightly irregular surfaces, by the tape itself being slightly irregular, by vibration of the tape, and by vibration of the tape transport members. The resulting flutter is characterized approximately by white noise. The noise increases, then, as the square root of the bandwidth. Commercially available airborne quality tape recorders have flutter specifications from 0.5 to 3% for peak to peak values. The effect of flutter on frequency modulation and pulse width modulation is to generate noise. For frequency modulation, Reference 73, page 111, points out that the noise value is obtained by dividing the peak flutter percentage by the peak carrier deviation and multiplying by 100. Thus, for channels with small percentage deviation, the effect of flutter can be serious. However, as previously indicated, this error appears as a noise error and should be indicated in the noise specifications. For pulse duration modulation, Reference 73 also presents the relationship between flutter and signal error. For nominal values of flutter, the accuracy of a pulse width modulation signal will not be significantly degraded.

In addition to the conventional errors described above, the tape transport subsystem may be responsible for side effects such as tape stretch and other forms of tape mishandling.

#### 10.5.2 Environmental Errors, Tape Transport Subsystem

Two significant environmental errors of the tape transport subsystem are as follows:

1. Vibration effects increasing flutter
2. Angular velocity effects on capstan speed

In general, the presence of a vibration environment increases the intrinsic flutter of a tape transport. This may be expected since flutter itself is a vibration phenomenon. The characteristics of this response depends on the individual characteristics of the recorder. Care should be exercised in qualifying the particular tape recorder for the vibration environment expected. This sensitivity to vibration is one of the major potential errors of the entire flight loads recording system, and should be examined carefully.

Another environmental error occurs if the aircraft has angular velocity about the center line of the capstan. This error in the tape speed is given by

$$\% \text{ error} = -\frac{\dot{\theta}}{\dot{v}} (100) = \frac{\dot{\theta}\pi d}{\dot{x}} (100) \quad (10.2)$$

where

- $\dot{\theta}$  - aircraft angular velocity about capstan center line, radians/second
- $\dot{v}$  - capstan angular velocity, radians/second
- $d$  - capstan diameter, inches
- $\dot{x}$  - tape speed, inches/second

For example, if  $\dot{x} = 1-7/8$  inches per second,  $d = 1$  inch, and the aircraft motion is  $\pm 2^\circ$  with a 1 cps sinusoidal period, the error in tape speed would vary sinusoidally  $\pm 37\%$ .

### 10.5.3 Usage Errors, Tape Transport Subsystem

The usage errors associated with the tape transport subsystem are mainly those due to abuse. Damage to the tape guides and reels

will increase the flutter significantly. Dirt will affect the magnetic tape and head directly, but will also promote wear of the tape transport.

## 10.6 MODULATION-DEMODULATION SUBSYSTEM

The modulation-demodulation scheme employed to encode the data signals is the major parameter which differentiates the various recording methods. The three basic methods discussed are as follows:

1. Pulse amplitude modulation
2. Frequency modulation
3. Pulse duration or pulse width modulation,  
pulse position modulation
4. Digital pulse code modulation

Only the latter three methods are considered suitable for flight loads recording. The main reasons for modulating a data signal is to obtain a better signal to noise ratio than would be possible with direct recording, and to obtain DC response. These goals are accomplished at the expense of data bandwidth. Reference 79, among others, develops the expressions for the idealized signal to noise improvements or superiority of the various modulation methods when compared to amplitude modulation. These relationships are presented in Table 10-4. These are ideal relationships with many constraints and should be used only as a guideline. Realizable factors were developed by analysis and test (Reference 67) and are also indicated in Table 10-4.

The theory of modulation has been developed extensively, especially with emphasis on the radio transmission of data signals. References 80, 81, and 82, among others, cover this technology in great detail. A gen-

Table 10-4. Idealized Improvement of Signal to Noise Ratio over Direct Recording and Required Bandwidths

Modulation Method	Signal to Noise Power Improvement (Reference 79)	Bandwidth Requirements - $\Delta_f$	Realizable S/N Improvement (Reference 67)
AM - Double Sideband	2	$2f_d$	
PAM	2	$2f_d$	
FM - Narrow Band (MX)	$3m_f^2$	$2f_d$ ( $m_f < 0.6$ )	} $3m_f^2$
FM - Wideband	$3m_f^3$	$2m_f f_d$ ( $m_f > 0.6$ )	
PWM, PDM	$\frac{2t_o^2 \Delta_f^3}{f_m} = \frac{2}{f_m t_r} \left( \frac{t_o}{t_r} \right)^2$	$1/t_r$	$\frac{1}{2} \left( \frac{t_o}{t_r} \right)^2$
PCM	$S/N = 2^{2n} - 1$	$mf_d$	$2^n - 1$

$m_f$  - modulation index,  $\frac{f\Delta}{f_d}$

$\Delta_f$  - deviation frequency

$f_d$  - maximum data or modulating frequency

$t_o$  - maximum pulse variation

$t_r$  - pulse rise time

$n$  - number of code symbols/data point.



erally accepted set of standards for both radio telemetry and tape recording is presented in Reference 76. The errors associated with modulation-demodulation of flight loads data signals are evaluated in Reference 67. In general, most of the theory developed for radio transmission may be applied directly to the tape recording process where the tape recorder replaces the telemetry link. However, the definitions of signal and noise for the two systems are somewhat different and this difference should be kept in mind at all times. When analyzing radio telemetry, noise is assumed to be introduced in the transmission process at some point, usually the input, but is always referred or converted back to equivalent noise occurring on the very first stage of the modulation process. In tape recording, the noise of the transmission link comes from the various errors associated with the magnetic tape recording process and the tape motion process as covered in the two previous sections, 10-4 and 10-5. It is therefore convenient to apply the development of modulation theory by thinking of the elimination or minimization of the inherent errors of the actual recording process. However, the errors of the magnetic recording process do not necessarily behave in the same manner as the assumed noise sources in radio telemetry work. A number of specific sources should be treated separately, and their effects on the output signal evaluated. Typical work of this kind is presented in References 83, 84, and 85.

#### 10.6.1 Pulse Amplitude Modulation

The pulse amplitude modulation method time multiplexes or samples a data signal or group of signals and records the resulting pulse



train in the direct record mode. This method suffers from all the problems of direct recording except the lack of DC response. The best signal to noise ratio improvement is only 2. However, if the intrinsic errors are acceptable, the PAM Method has the distinct advantage of simplicity (a commutator is the only equipment required).

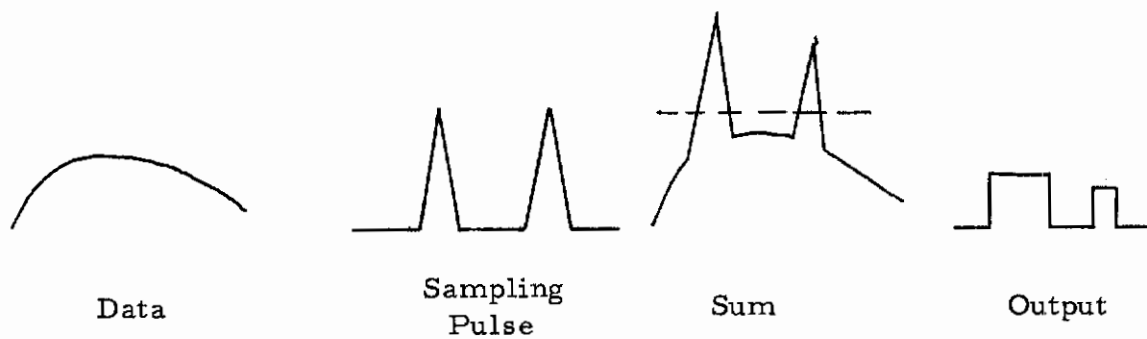
## 10.6.2 Frequency Modulation

Frequency modulation is a form of phase modulation. It may be considered a method of converting amplitude, which is not faithfully reproduced by the tape recording process, to frequency, which is much more faithfully reproduced. With a time varying data signal, the modulated signal, "instantaneous frequency," is proportional to the data signal amplitude and the frequency of change of the modulated signal is the data signal frequency. A number of references, including 73, 80 and 82, develop the expression for the expected content of the modulated signal. Actually, an infinite number of sidebands exist about the center frequency. The distortion or elimination of these sidebands effectively causes noise. This is evident in Table 10-4 where signal to noise is shown to be proportional to the bandwidth.

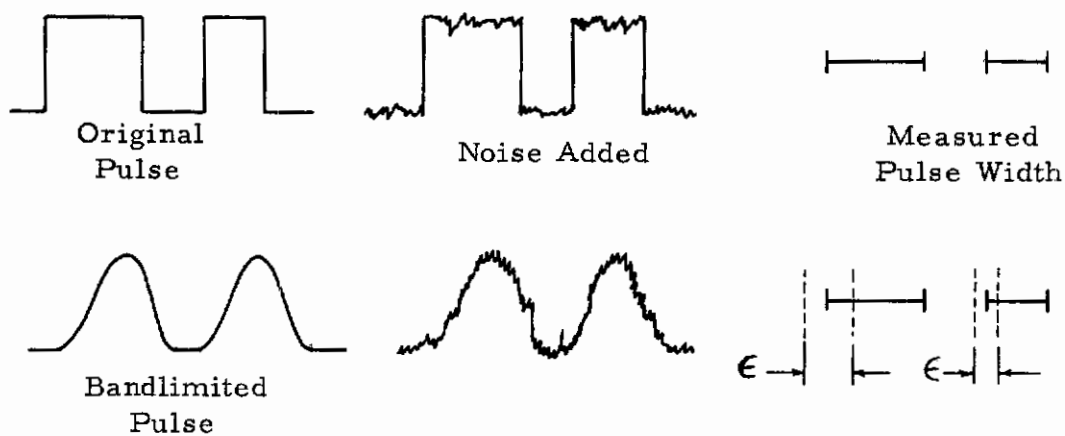
## 10.6.3 Pulse Duration Modulation

Pulse duration modulation is a process of converting amplitude to a pulse width. This is also referred to as pulse width modulation. Another variation, pulse position modulation, leads to the same result. In practice, a sampling pulse is added to the data signal, and the resulting signal is clipped and squared as indicated below:

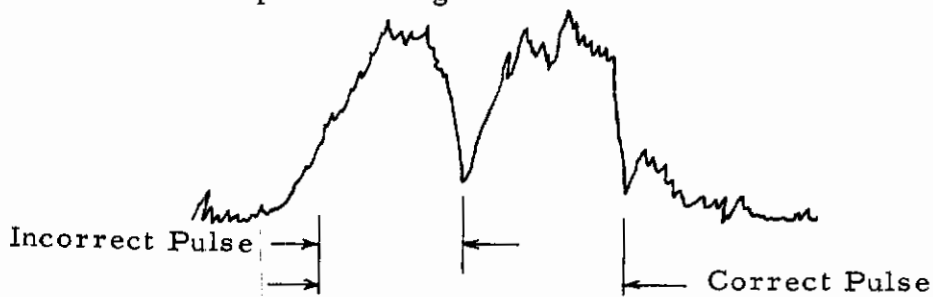
# Contrails



As with FM, the resulting signal has a frequency spectrum composed of a characteristic center frequency and sidebands. The greater the bandwidth, the more faithfully the edges of the pulse are reproduced and the greater the signal to noise ratio.



The threshold or minimum allowable signal to noise ratio is that level at which incorrect pulses are generated.



## 10.6.4 Pulse Code Modulation

Pulse code modulation consists of dividing the analog signal into various levels and converting to a train of coded pulses. The digital binary code is the most convenient to implement and the only one considered. Pulse coding has a significant advantage over other modulation methods. Above a threshold level, the signal to noise ratio is a function only of the number of quantizing levels.

## 10.6.5 Errors in Modulation

Noise, amplitude nonlinearity, and frequency response are characteristics of each particular modulation method. These errors are usually affected by the other two tape recorder subsystems. The one error which has not previously been covered is aliasing or frequency folding. If frequency components exist above the Nyquist sampling frequency, they appear as data. As pointed out in Reference 67, this type of error occurs in FM as well as pulse types modulation. The method for minimizing this effect is to incorporate a low pass filter before the modulator.

## 10.7 ANALOG-TO-DIGITAL CONVERTERS

The components of analog-to-digital converters are indicated in Figures 2-1 through 2-5. The main component is the A/D converter itself. The basic method of operation is to compare the data signal to a reference level and generate a pulse if the data signal is higher. Various techniques are employed to make subsequent comparisons to generate the total digital word. Reference 85 presents introductory material on the principles of operation and errors of A/D converters. The error models used to describe the performance of connectors are discussed in Reference 86. Two basically different approaches may be employed.

# Contrails

1. Evaluate each internal noise source (noise spikes, quantization error, drift, etc.) and combine
2. Evaluate the overall performance with an input which is representative of the intended operation.

The usual method for expressing the overall error is the probability of an error of magnitude  $\epsilon$  over a given time period.

An error associated with high frequency A/D conversion is the aperture error. The converter requires a finite time to sample. In that time period, the level is changing. However, for the frequency range of interest, this is not a problem.

## REFERENCES

1. Neubert, H. K. P., Instrument Transducers, Oxford University Press, London, 1963.
2. Harris, C. M. and Crede, C. E., Shock and Vibration Handbook, Vol. 1, McGraw-Hill Book Company, Inc., New York, 1961.
3. Doebelin, E. O., Measurement Systems: Application and Design, McGraw-Hill Book Company, Inc., New York, 1966.
4. Fisher, H. F., Jr., "Telemetry Transducer Handbook," Air Force Flight Dynamics Laboratory Report WADD-TR-61-67, Vol. 1, Revision 1, September 1963.
5. Houbolt, J. C., Steiner, R., and Pratt, K. G., "Dynamic Response of Airplanes to Atmospheric Turbulence Including Flight Data on Input and Response," NASA TR R-199, June 1964.
6. Loving, N. V., "Clear Air Turbulence (CAT) Measurement for Design Criteria," American Institute of Aeronautics and Astronautics Paper No. 65-510, July 1965.
7. Rhyne, R. H. and Steiner, R., "Power Spectral Measurement of Atmospheric Turbulence in Severe Storms and Cumulus Clouds," NASA Technical Note, NASA TN D-2469, October 1964.
8. Milne-Thomson, L. M., Theoretical Hydrodynamics, The MacMillan Co., New York, 1950.
9. Rogal, B., "Differential Pressure Measurements in Sensing Sideslip and Angle of Attack," Reprinted from Flight Test Instrumentation, Vol. 3, Proceedings of the Third International Symposium, Pergamon Press, London, 1964.
10. Giannini Controls Corp., "Gust Probe," New Product Technical Note, September 1960.
11. Kuethe, A. M. and Schetzer, J. D., Foundations of Aerodynamics, John Wiley & Sons, Inc., New York, 1955.

12. Crooks, W. M., "A Fixed Vane Sensor for Measuring Turbulent Air Flows," Proceedings of the ISA 10th National Aerospace Instrumentation Symposium, 1964.
13. Lichtenstein, P. E., "Gyros, Platforms, Accelerometers," Kearfott Division, General Precision Aerospace, June 1963.
14. Machover, C., Basics of Gyroscopes, John F. Rider, Inc., New York, 1960.
15. Savet, P. H., Gyroscopes: Theory and Design, McGraw-Hill Book Company, Inc., New York, 1961.
16. Ahrendt, W. R., Servomechanism Practice, McGraw-Hill Book Company, Inc., New York, 1954.
17. Stedman, C. K., "Some Characteristics of Gas Damped Accelerometers," Statham Instruments, Inc. Note No. 33, October 1958.
18. Kelly, R. D., "Transducers for Sonic Fatigue Measurements," Air Force Flight Dynamics Laboratory Report AFFDL-TR-64-171, February 1965.
19. White, G. E., "Secondary Effects in Seismic Instruments," Statham Instruments, Inc. Note No. 23, September 1952.
20. American Standards Association, Inc., "American Standard Methods for the Calibration of Shock and Vibration Pickups 52.2-1959," New York, 1959.
21. Scull, J. R., "Spacecraft Guidance and Control," Vol. IV, Space Technology, NASA SP-68, 1966.
22. Sorrenson, Arthur S., "Measurement of Gyro Error Coefficients," Air Force Ballistic Systems Division Report BSD-TR-66-227, June 1966.
23. Kearfott Systems Division, General Precision Technical Bulletin "High Accuracy Displacement Gyros C70 4101 Series," March 1966.
24. Stern, H., "Which Rate Gyro to Use," Control Engineering, February 1958, p. 79.

# Contrails

25. Friedman, G. L., "Frequency Response Analysis of the Vane-Type Angle of Attack Transducer," Aero/Space Engineering, March 1959.
26. Harting, D. R., "The S/N-Fatigue-Life Gage: A Direct Means of Measuring Cumulative Fatigue Damage," Experimental Mechanics, February 1966.
27. Perry, C. C. and Lissner, H. R., The Strain Gage Primer, McGraw-Hill Book Company, Inc., New York, 1955.
28. Dean, M., III, Semiconductor and Conventional Strain Gages, Academic Press, New York, 1962.
29. Murray, W. M., Sc.D. and Stein, P. K., S.M.P.E., "Strain Gage Techniques," Lectures and laboratory exercises presented at the Department of Engineering, University of California at Los Angeles, August 20-31, 1962.
30. Baldwin-Lima-Hamilton Corp., Wire Strain Gage Sales Catalog No. 100-2.
31. Baldwin-Lima-Hamilton Corp., Foil Strain Gage Sales Catalog No. 101-2.
32. Micro-Measurements, Inc., Foil Strain Gage Sales Catalog No. 10.
33. Statham Instruments, Inc., "Statham Transducer Element General Description," Statham Instruments, Inc. Note No. 1, December 1956.
34. Horne, R. S., "A Feasibility Study for the Development of a Fatigue Damage Indicator," Air Force Flight Dynamics Laboratory Report AFFDL-TR-66-113.
35. Baldwin-Lima-Hamilton Corp., "SR-4 Strain Gage Bonding Cement Evaluation Report," No. 4310-2, March 1958.
36. Baldwin-Lima-Hamilton Corp., "SR-4 Strain Gage Evaluation Report," No. 4310-3, March 1958.
37. Baldwin-Lima-Hamilton Corp., "SR-4 Strain Gage Evaluation (continued)", Technical Data No. 4310-7, May 1959.



38. Baldwin-Lima-Hamilton Corp., "SR-4 Strain Gage Bonding Cement Evaluation (continued)," Technical Data No. 4310-8, May 1959.
39. Wolf, N. D., "Summary of Strain Gage Fatigue Data," DSD-TR-63-202, Aeronautical Systems Division, AFSC, USAF, WPAFB, Ohio, April 1963.
40. Smith, P. W., Starr, E. A., Dietrich, C. W., and Noiseux, D. U., "Study of a Response Load Recorder," Air Force Flight Dynamics Laboratory Report ASD-TDR-62-165, Volume II, March 1963.
41. Vigness, I., "Magnetostrictive Effects in Wire Strain Gages," Proceedings of the Society of Experimental Stress Analysis, Vol. 14, No. 2, pp. 139-148, 1957.
42. Davis, Harry J. and Horn, Leon, "Notes on the Use of Semiconductor Strain Gages," U. S. Army Material Command Report TR-1285; DA-1 P010501 A008 AMCMS Code 5011.11.82600 HDL Project 30300.
43. MIL-Hdbk-5, "Metallic Materials and Elements for Flight Vehicle Structures," August 1962.
44. Baldwin-Lima-Hamilton Corp., "Strain Gage Handbook."
45. Smith, C. S., "Piezoresistive Effect in Silicon and Germanium," Physics Review, Vol. 94, p. 42, 1952.
46. Micro Systems Semiconductor Strain Gage Sales Bulletin, January 1962.
47. Kulite-Bytrex Corp., Semiconductor Strain Gage Sales Bulletin K-101.
48. Baldwin-Lima-Hamilton Corp., Semiconductor Strain Gage Sales Catalog No. 102, October 1964.
49. Dorsey, J., "Semiconductor Strain Gage Handbook," Baldwin-Lima-Hamilton Corp., Section I Theory, October 1964; Section II Data Reduction, August 1964; Section III N-Type Self Compensated Gages, January 1965; Section IV Gage Application; Section V Transducer, October 1964; Section VI Semiconductor Gage Selection for Transducer Application, April 1965; Section VII Strain Measurement, November 1965.



50. Minnar, E. J., ISA Transducer Compendium, Plenum Press, New York, 1963.
51. Considine, D. M., ed., Process Instruments and Controls Handbook, "Section 3, McGraw-Hill Book Company, Inc., New York, 1957.
52. Schweppe, J. L., et al., "Methods for the Dynamic Calibration of Pressure Transducers," National Bureau of Standards Monograph 67, 1963.
53. Hougen, J. O., Martin, O. R., and Walsh, R. A., "Dynamics of Pneumatic Transmission Lines," Control Engineering, September 1963, p. 114.
54. Barton, J. R., "A Note on the Evaluation of Designs of Transducers for the Measurement of Dynamic Pressures in Liquid Systems," Statham Laboratories Instrument Note No. 27, October 1958.
55. Davis, S. A., and Ledgerwood, B. K., Electromechanical Components for Servomechanisms, McGraw-Hill Book Company, Inc., 1961.
56. Bendat, J. S., and Piersol, A. G., Measurement and Analysis of Random Data, John Wiley & Sons, Inc., New York, 1966.
57. Miller, A., "Differential Transformers," The Right Angle, The Sanborn Co., August and November 1956.
58. Schaevitz Engineering Co. Bulletin AA-1A, Schaevitz Engineering Company, Camden, N. J.
59. Bowes, C. A., "Variable Resistance Sensors Work Better with Constant Current Excitation," Instrumentation Technology, Vol. 14, No. 3, March 1967.
60. Hammon, R. L., "An Application of Random Process Theory to Gyro Drift Analysis," IRE Transactions on Aeronautical and Navigational Electronics, pp. 84-91, September 1958.
61. Stewart, R. M., "Some Effects of Vibration and Rotation on the Drift of Gyroscopic Instruments," American Rocket Society Journal, pp. 22-28, January 1959.

# Contrails

62. Morrison, R., "Shielding and Grounding for Instrumentation Systems," Dynamics Instrumentation Co. TP/755-1.
63. Instrumentation Grounding and Noise Minimization Handbook, Consolidated Systems Corp., Pomona, California, AD612-027 Technical Report AFRPL TR 65-1, January, 1965.
64. International Telephone and Telegraph Corp., Reference Data for Radio Engineers, Stratford Press, Inc., New York, 1956.
65. Pezirtzoglou, E., "Design of Filters and Networks," Ampex Corp. TR-62-11, October 1963. Defense Documentation Center No. AD 4 30092.
66. Gibson, J. E., and Tuteur, F. B., Control System Components, McGraw-Hill Book Company, Inc., New York, 1958.
67. Foster, E. J., "Study of Effects and Degrees of Error of Modulation-Demodulation," Air Force Flight Dynamics Laboratory Report AFFDL-TR-65-6.
68. Dickson, Glenn E., "Shunt Calibration of Strain Gage Transducers," Instruments and Control Systems, April, 1966.
69. Hague, B., Alternating Circuit Bridge Methods, Sir Isaac Pitman & Sons, Ltd., London, 1946.
70. Jackson, A. S., Analog Computation, McGraw-Hill Book Company, Inc., New York, 1960.
71. Howden, P. F., "A Review of Chopper Amplifiers," Electro-Technology (New York), p. 64, June 1963.
72. Athey, S. W., Ph.D., "Magnetic Tape Recording," NASA Technology Survey, NASA SP-5038, January 1966.
73. Davies, G. L., Magnetic Tape Instrumentation, McGraw-Hill Book Company, Inc., New York, 1961.
74. Weber, P. J., "The Tape Recorder as an Instrumentation Device," The Ampex Corporation, 1963.

75. Mee, C. D., The Physics of Magnetic Recording, North-Holland Publishing Co., Amsterdam, 1964.
76. Telemetry Working Group, Inter-Range Instrumentation Group, Range Commanders Council, "IRIG Telemetry Standards," Revised March 1966, Document 106-66.
77. Kelly, R. D., Systems for the Collection and Analysis of Dynamic Data, "Air Force Flight Dynamics Laboratory Report AFFDL-TR-65-94, August 1965.
78. Schulze, G. H., "Applications of a Light Mass Capstan Tape Recorder," 1962 National Telemetry Conference Proceedings.
79. Hancock, J. C., An Introduction to the Principles of Communication Theory, Maple Press Co., York, Pa., Copyright McGraw-Hill Book Company, Inc., 1961.
80. Black, H. S., Modulation Theory, D. Van Nostrand Co, Inc., Princeton, N. J., 1953.
81. Painter, P. F., Modulation, Noise, and Spectral Analysis, McGraw-Hill Book Company, Inc., New York, 1965.
82. Nichols, M. H., and Rauch, L. L., Radio Telemetry, John Wiley & Sons, Inc., New York, 1956.
83. Bradford, R. S., and Jaffe, R. M., "An Analysis of the Effects of Flutter and the Associated Time Base Errors Upon the Performance Characteristics of a Tape Recorder," Revere-Mincom Company, Division of the 3M Company, Inc.
84. Ratz, A. G., "The Effect of Tape Transport Flutter on Spectrum and Correlation Analysis," IEEE Transactions on Space Electronics and Telemetry, pp. 129-134, Vol. SET-10, No. 4, December 1964.
85. Chao, S. C., "The Effect of Flutter on a Recorded Sinewave," Proceedings IEEE (Correspondence) pp. 726-727, July 1965.
86. Stephenson, Barbera W., "Analog-Digital Conversion Handbook," Digital Equipment Corporation, Maynard, Massachusetts.
87. Otnes, R. K., "Analog to Digital Converter Tests," MAC 510-02, November 1965.

88. Peloubet, R. P., and Haller, R. L., "Application of a Power Spectral Gust Design Procedure to Bomber Aircraft," Air Force Flight Dynamics Laboratory Report AFFDL-TR-66-35, June 1966.
89. Bouche, R. R., and Ensor, L. C., "Use of Reciprocity Calibrated Accelerometer Standards for Performing Routine Laboratory Comparison Calibrations," The Vibration and Shock Bulletin No. 34, Part 4, 1965, pp. 21-29.
90. Ackerman, J. T., Berens, A. P., Braun, J. F., Peckham, G. G., "Continued Evaluation of Giannini Model 580 T3 Data Acquisition and Statistical Recorder," Technical Report SEG-TR-66-35, Systems Engineering Group, Research and Technology Division, Air Force Systems Command, Wright-Patterson AFB, Ohio, October 1966.
91. Howard, J. A., and Ferguson, L. N., "Recording Handbook," U. S. Army Electronics Command, Fort Monmouth, N. J., Technical Report ECOM-01829-M1096, AD649812.
92. Dominic, R. J., "Flight Test Evaluation of the A/A24U-6 Structural Loads Data Recording System," Air Force Flight Dynamics Laboratory AFFDL-TR-65-178, September 1965.

## APPENDIX

FREQUENCY RESPONSE OF SINGLE DEGREE-  
OF-FREEDOM TRANSDUCERS

For constant parameter linear systems, the input-output relationship may be defined by the frequency response function,  $H(f)$ . This complex valued quantity may be thought of in terms of a magnitude and an associated phase angle which are the gain factor and phase factor relating the input and output. The frequency response function can be considered a special case of the transfer function where the Laplace operator  $p = A + jB$  is set equal to  $j2\pi f$ . For stable systems which are physically realizable, that is a response due only to past inputs, this conversion loses no useful information. However, the Laplace transformation notation is familiar and widely used, especially in the literature for gyroscopes and servo accelerometers. Therefore, the method for deriving frequency response functions will be to solve the Laplace transform ratio of output over input and to convert to the Fourier transform transfer function by setting  $p = j2\pi f$ . For a more comprehensive discussion of frequency response functions, see Reference 56, Chapter 2.

The frequency response function for the transducers discussed relate the physical properties being transduced to an intermediate physical property which can be measured with an electric pickoff. Typically intermediate properties are relative displacement and force. The frequency response functions of rate gyros, vertical gyros, pressure transducers and accelerometers are similar in form. The developments all assume an idealized, single degree-of-freedom system which can be described by second order differential equations. Rate

integrating gyroscopes are characterized by a first-order differential equation. The frequency response functions for the type of transducers discussed are summarized in Table A-1.

**A-1. OPEN LOOP TYPE ACCELEROMETERS**

The typical open loop type accelerometer is represented in schematic and functional block diagram in Figure A-1.

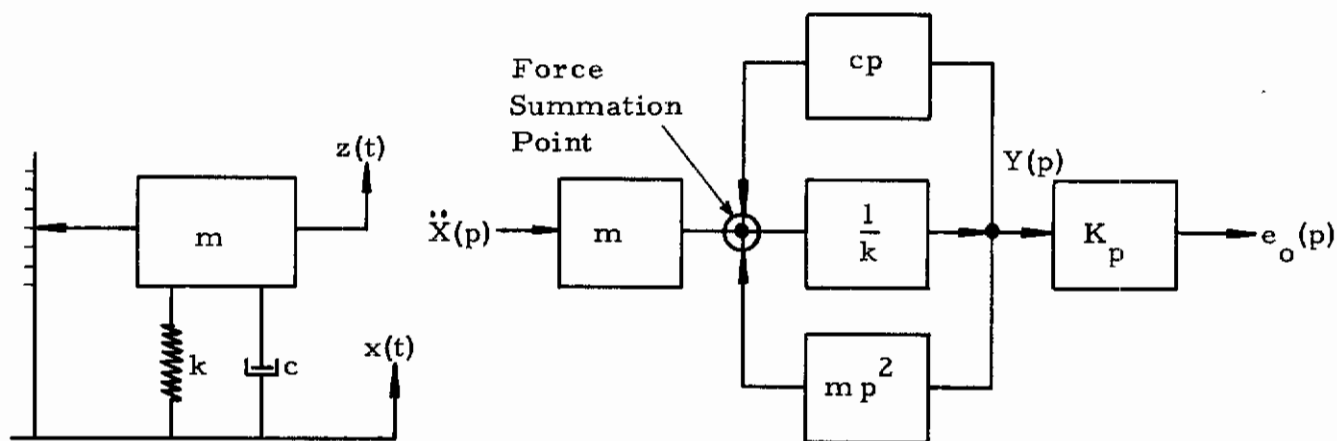


Figure A-1. Schematic and Functional Block Diagram, Open Loop Type Accelerometer

- where
- $x(t)$  = displacement of base, feet
  - $\ddot{X}(p)$  = Laplace transform, base acceleration
  - $z(t)$  = displacement of inertial mass, feet
  - $y(t) = z(t) - x(t)$  - relative displacement, feet
  - $Y(p)$  = Laplace transform, relative displacement
  - $m$  = mass, slugs
  - $k$  = spring constant, lbs/feet
  - $c$  = coefficient of viscous damping, lb-sec/feet

Table A.1  
Frequency Response Functions

Type Transducer	Input Parameter	Output Parameter	Gain Factor	Phase Factor (lag)
Rate Gyro	Base Angular Velocity	Voltage	$ H(f)  = \frac{I \Omega K_p}{I_o (2\pi f_n)^2} \frac{1}{\sqrt{\left(1 - \frac{f^2}{f_n^2}\right)^2 + \left(2\zeta \frac{f}{f_n}\right)^2}}$	$\phi(f) = \tan^{-1} \frac{2\zeta \frac{f}{f_n}}{1 - \frac{f^2}{f_n^2}}$
Rate Integrating Gyro	Base Angular Displacement	Voltage	$ H(f)  = \frac{K_H}{c} \frac{1}{\sqrt{1 + \left(\frac{2\pi f J}{c}\right)^2}}$	$\phi(f) = \tan^{-1} \frac{2\pi f J}{c}$
Open Loop Accelerometer	Base Linear Acceleration	Voltage	$ H(f)  = \frac{K_p}{(2\pi f_n)^2} \frac{1}{\sqrt{\left(1 - \frac{f^2}{f_n^2}\right)^2 + \left(2\zeta \frac{f}{f_n}\right)^2}}$	$\phi(f) = \tan^{-1} \frac{2\zeta \frac{f}{f_n}}{1 - \frac{f^2}{f_n^2}}$
Servo Accelerometer	Base Linear Acceleration	Voltage	$ H(f)  = K_p K_a \frac{1}{(2\pi f_n)^2} \frac{\sqrt{1 + 4\zeta^2 \left(\frac{f}{f_n}\right)^2}}{\sqrt{\left(1 - \frac{f^2}{f_n^2}\right)^2 + 4\left(\zeta_1 + \zeta_2 \left(\frac{f}{f_n}\right)^2\right)^2}}$	$\phi(f) = \tan^{-1} \frac{2\left(\frac{f}{f_n}\right) \zeta_1 + 2\left(\frac{f}{f_n}\right)^3 \zeta_2}{1 - \left(\frac{f}{f_n}\right)^2 + 4\left(\frac{f}{f_n}\right)^2 \zeta_2 (\zeta_1 + \zeta_2)}$
Movable Vane	Base Angular Displacement	Voltage	$ H(f)  = K_p \frac{1 - \left(\frac{f}{f_n}\right)^2}{\sqrt{\left(1 - \frac{f^2}{f_n^2}\right)^2 + \left(2\zeta \frac{f}{f_n}\right)^2}}$	$\phi(f) = \tan^{-1} \frac{2\zeta \frac{f}{f_n}}{1 - \left(\frac{f}{f_n}\right)^2}$



# Contrails

$K_p$  = pickoff transfer function, volts/feet  
 $p$  = Laplace operator  
 $e_o$  = output, volts

The sum of the forces on the mass must equal zero. That is:

$$\text{spring force} + \text{damping force} + \text{inertial force} = 0$$

where            spring force =  $-k [z(t) - x(t)] = -ky(t)$   
                  damping force =  $-c [\dot{z}(t) - \dot{x}(t)] = -c\dot{y}(t)$   
                  inertia force =  $m\ddot{z}(t) = -m[\ddot{y}(t) + \ddot{x}(t)]$

The equation of motion is therefore given by

$$m[\ddot{y}(t) + \ddot{x}(t)] + c\dot{y}(t) + ky = 0 \quad (\text{A1})$$

or

$$m\ddot{y}(t) + c\dot{y}(t) + ky(t) = -m\ddot{x}(t) \quad (\text{A2})$$

The base acceleration term on the right assumes the function of an input to the system and relative displacement the output. The Laplace transform of this equation is given by the equation

$$m\ddot{X}(p) + mY(p)p^2 + cY(p)p + kY(p) = 0 \quad (\text{A3})$$

The functional block diagram, Figure A-1, can be seen to be a representation of this equation. It is desirable to put Eq. (A3) in a general form by dividing by (m) and making the following substitutions:



$$\zeta = \frac{c}{2\sqrt{km}} = \text{damping ratio}$$

$$f_n = \frac{1}{2\pi} \sqrt{k/m} = \text{undamped natural frequency, Hz}$$

By making the above substitutions, solving for the transfer function  $Y(p)/\ddot{X}(p)$ , multiplying by the pickoff transfer function  $K_p$ , substituting  $p = j2\pi f$ , and converting to polar coordinates, the base acceleration to output voltage frequency response function is obtained.

$$H(f)_{a-e_o} = \frac{K_p}{(2\pi f_n)^2} \frac{1}{\sqrt{\left[1 - \frac{f^2}{f_n^2}\right]^2 + \left[2\zeta \left(\frac{f}{f_n}\right)\right]^2}} e^{-j\phi(f)} \quad (A4)$$

$$\phi(f) = \tan^{-1} \frac{2\zeta \left(\frac{f}{f_n}\right)}{1 - \left(\frac{f}{f_n}\right)^2} \quad (A5)$$

where  $H(f)_{a-e_o}$  = frequency response function, acceleration to output voltage

$\phi(f)$  = phase angle lag between response and input, radians

The magnitude and phase angle of this frequency response function are plotted on Figures A-2 and A-3 respectively.

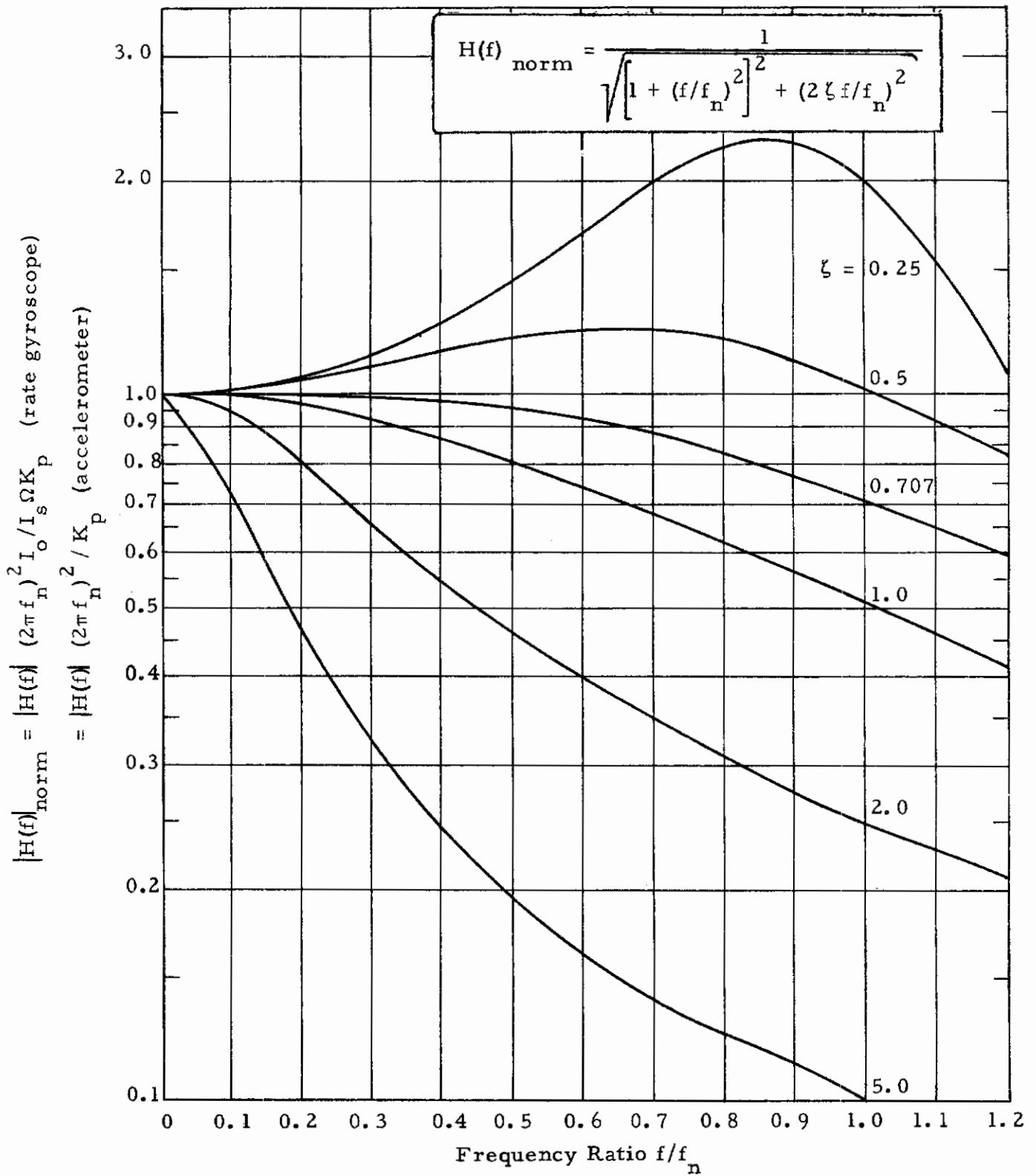


Figure A-2. Normalized Frequency Response Gain Factor, Second Order, Single Degree-of-Freedom Transducers

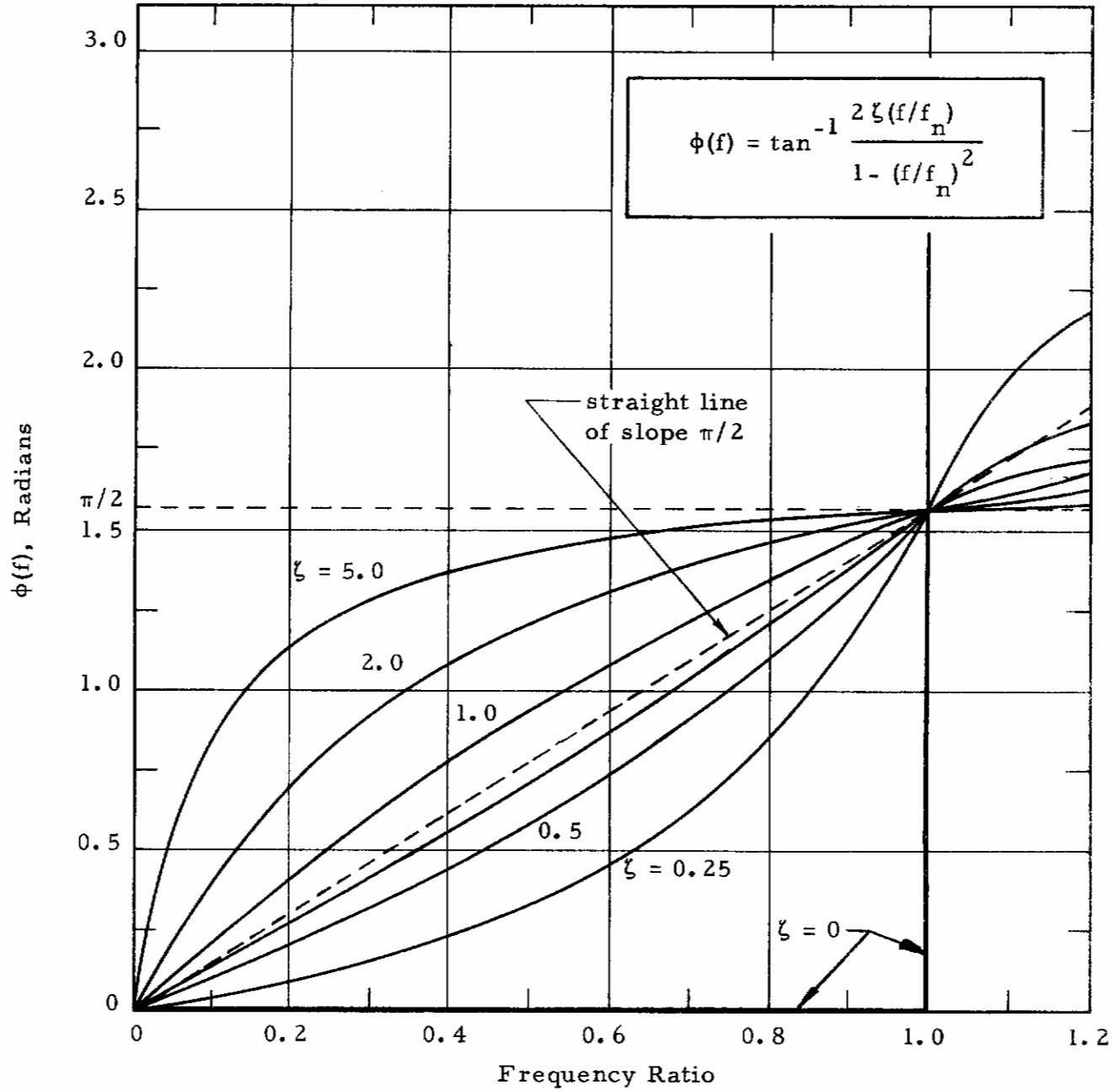


Figure A-3. Frequency Response Phase Lag

## A-1.1 Frequency Response Error

The frequency response curves, Figures A-2 and A-3, show the basic physical characteristics of open loop accelerometers. However, the areas of greatest interest, around unity gain and constant time delay, have poor resolution on this type of curve. In addition, when selecting and using a transducer, the percentage error may be of greater interest than the gain factor and phase factor themselves.

The percentage error from a constant gain factor is

$$\% \text{ error} = \left[ \left| H(f) \right| - 1 \right] 100 \quad (\text{A6})$$

Substituting the frequency response expression Eq. (A4) into Eq. (A6) and rearranging, the damping for a given gain factor error and frequency is obtained.

$$\zeta = \frac{1}{2} \sqrt{\left[ \frac{1}{1 + \frac{\% \text{ error}}{100}} - 1 \right] \frac{f_n^2}{f^2} - \frac{f^2}{f_n^2} + 2} \quad (\text{A7})$$

This expression is presented in Figure A-4. This figure is essentially a difference plot and has much greater resolution around zero error than Figure A-2. An advantage of having damping as the ordinate is that a temperature scale for a particular damping fluid may be easily superimposed. For zero error, Eq. (A7) reduces to

$$\zeta = \sqrt{\frac{1}{2} - \frac{1}{4} \left( \frac{f}{f_n} \right)^2} \quad (\text{A8})$$

Then for zero frequency, the damping factor is

$$\zeta = \sqrt{1/2} = 0.707$$

## A-1.2 Time Delay Error

The phase lag plot, Figure A-3, suffers from the same lack of resolution around the constant time delay as does the magnification plot around zero error. In addition, the time delay between input and output is of great interest when combining instantaneous signals or when performing cross spectra or cross correlation analyses. The error which results if a constant time delay,  $\tau = \frac{1}{4f_n}$ , is assumed to be:

$$\% \text{ error}_{\tau} = \left[ -1 + \frac{2}{\pi} \left( \frac{f}{f_n} \right) \tan^{-1} \frac{2\zeta \frac{f}{f_n}}{1 - \left( \frac{f}{f_n} \right)^2} \right] 100 \quad (\text{A9})$$

This error is plotted in Figure A-5.

## A-2 SERVO OR FORCE BALANCE ACCELEROMETER

The servo or force balance accelerometer is represented in schematic and functional block diagram in Figure A-6.

As with the open loop accelerometer, the equation of motion is obtained by summing forces on the mass.

$$-m[\ddot{y}(t) + \ddot{x}(t)] - c\dot{y}(t) + F_c(t) = 0 \quad (\text{A10})$$

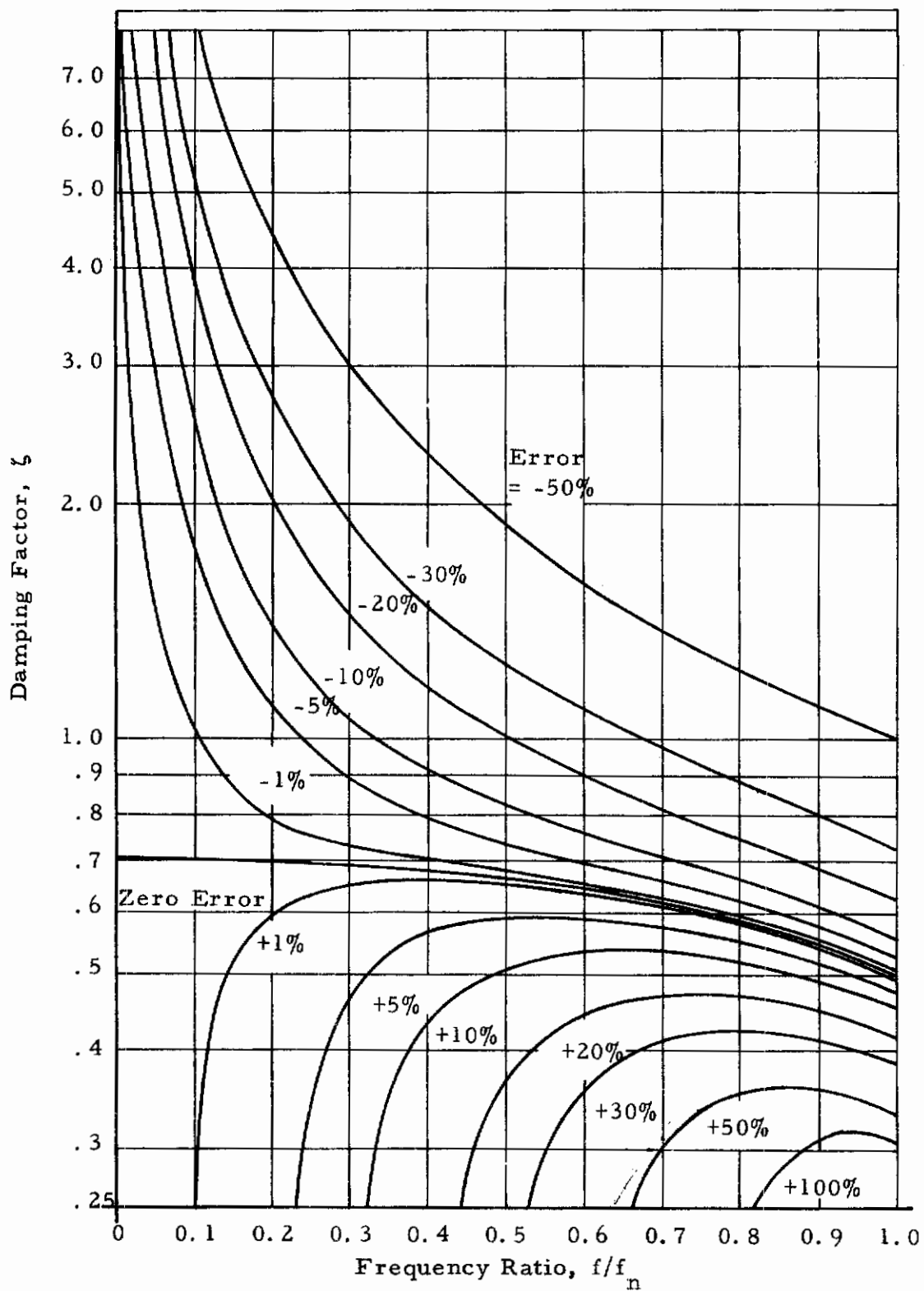


Figure A-4. Frequency Response Gain Factor Error versus Frequency Ratio and Damping Factor, Open Loop Accelerometers and Rate Gyroscopes

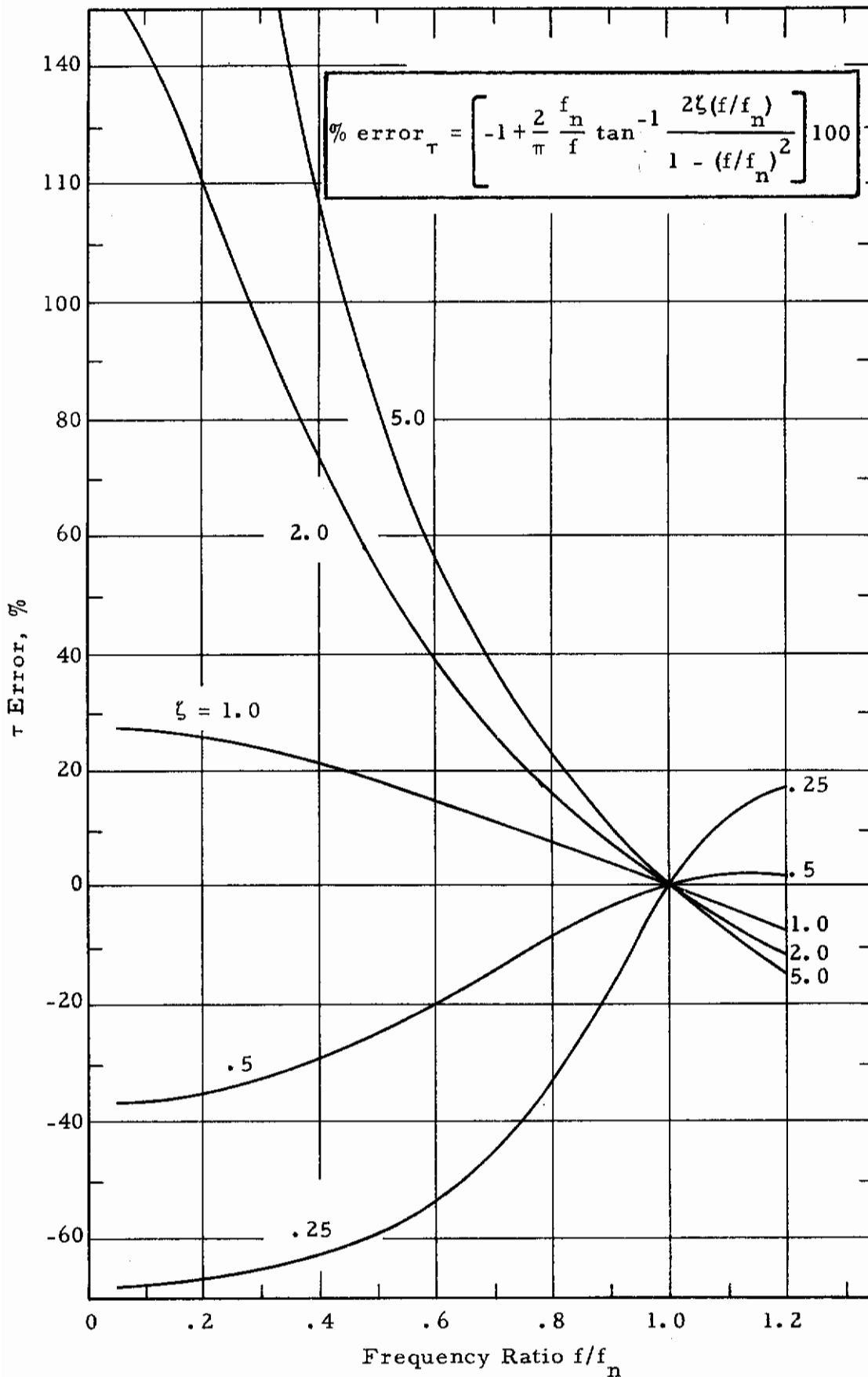


Figure A-5. Frequency Response Time Delay Error, Reference Constant  $\tau$

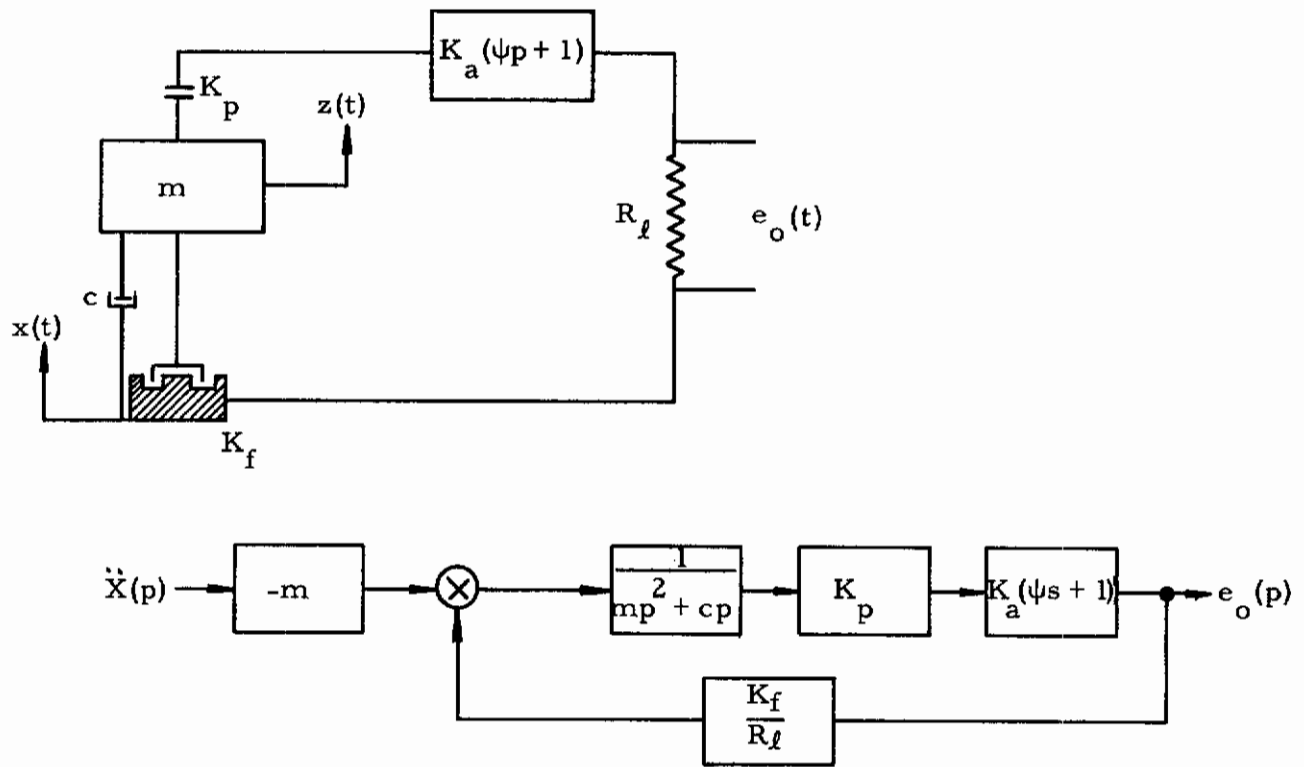


Figure A-6. Schematic and Functional Block Diagram, Servo Accelerometer

$K_p$  = Pickoff transfer function, volts/feet

$K_a(\psi p + 1)$  = Feedback amplifier transfer function

$K_f$  = Restoring coil transfer function, lbs/ampere

$R_l$  = Load resistor,

$c$  = coefficient of viscous damping, lb-sec/ft

$m$  = mass - slugs



# Contrails

where  $F_c(t)$  = restoring coil force. But the coil force is expressible in terms of the output voltage

$$F_c(t) = \frac{e_o(t)}{R_\ell} K_f \quad (A11)$$

where  $K_f$  = force coil transfer function, lbs/ampere. In turn the output voltage is a function of the relative displacement in Laplace transform notation.

$$e_o(p) = -y(p)K_p K_a (\psi p + 1)$$

or 
$$y(p) = -e_o(p)/K_p K_a (\psi p + 1) \quad (A12)$$

Taking the Laplace transform of Eqs. (A10), (A11), and combining with Eq. (A12),

$$-m \left( x(p) - \frac{e_o(p)}{K_p K_a (\psi p + 1)} p^2 \right) + c \frac{e_o(p)}{K_p K_a (\psi p + 1)} p + \frac{e_o(p)}{R_\ell} K_f = 0 \quad (A13)$$

rearranging,

$$-m\ddot{x}(p) + e_o(p) \frac{K_f}{R_\ell} + \frac{mp^2 + cp}{K_p K_a (\psi + 1)} e_o(p) = 0 \quad (A14)$$

The functional block diagram, Figure A-6, can be seen to be a representation of this equation. Solving for the overall transfer function,

$$\frac{e_o(p)}{\ddot{x}(p)} = \frac{mR_\ell K_p K_a (\psi p + 1)}{mp^2 R_\ell + cpR_\ell + K_p K_a (\psi p + 1)}$$

$$\frac{e_o(p)}{\ddot{x}(p)} = \frac{K_p K_a (\psi p + 1)}{p^2 + p\left(\frac{c}{m} + \frac{\psi K_f K_p K_a}{mR_\ell}\right) + \frac{K_f K_p K_a}{mR_\ell}} \quad (A15)$$

This equation may be put in a more general form by making the following substitutions:

$$f_n = \frac{1}{2\pi} \sqrt{\frac{K_f K_p K_a}{R_\ell m}} \quad \text{undamped natural frequency}$$

$$\zeta_1 = \frac{c}{4\pi f_n m} \quad \text{mechanical damping factor}$$

$$\zeta_2 = \pi f_n \psi \quad \text{electrical damping factor}$$

Making the above substitutions, substituting  $p = j2\pi f$ , and converting to polar coordinates, the frequency response function is obtained.

$$H(f) = \frac{e_o}{\ddot{x}} = \frac{R_\ell m}{K_f} \frac{\sqrt{1 + 4\zeta_2^2 \left(\frac{f}{f_n}\right)^2}}{\sqrt{\left[1 - \left(\frac{f}{f_n}\right)^2\right]^2 + 4(\zeta_1 + \zeta_2)^2 \left(\frac{f}{f_n}\right)^2}} e^{-j\phi(f)} \quad (A16)$$

$$\phi = \tan^{-1} \frac{2\left(\frac{f}{f_n}\right) \zeta_1 + 2\left(\frac{f}{f_n}\right)^3 \zeta_2}{1 - \left(\frac{f}{f_n}\right)^2 + \left(4\frac{f}{f_n}\right)^2 \zeta_2 (\zeta_1 + \zeta_2)} \quad (\text{A17})$$

Note that if  $\zeta_2 = 0$ , the frequency response function is identical in form to the open loop accelerometer frequency response function. If all the damping is electrical,  $\zeta_1 = 0$ , the frequency response function assumes the form of the function for the base excited open loop system with identical parameters, that is, velocity to velocity (Reference 56). The frequency response and phase angle of this system are plotted in Figures A-7 and A-8.

### A-3. RATE GYROSCOPE

The analysis of gyroscopes is a complex field in itself. However, the study of the idealized frequency response function gives an understanding which is adequate for most applications. The typical rate gyroscope is represented in schematic and functional block diagram in Figure A-9.

The equation of motion is derived by summing torques on the gyro wheel. These forces are

$$\begin{aligned} \text{spring torque} &= -k\eta(t) \\ \text{damping torque} &= -c\dot{\eta}(t) \\ \text{inertia torque} &= -I_o \ddot{\eta}(t) \\ \text{precession torque} &= -H\dot{\theta}(t) \end{aligned}$$

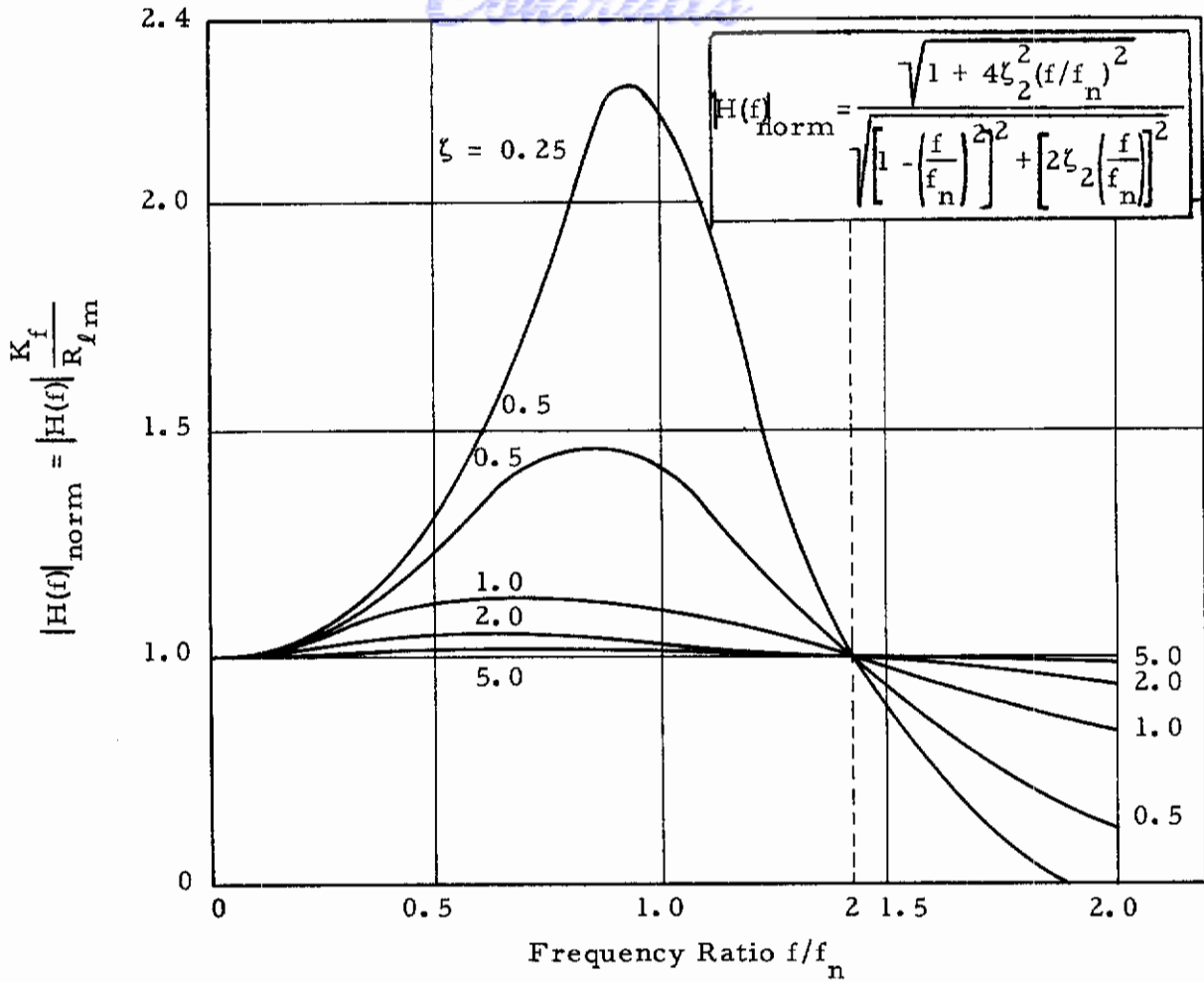


Figure A-7. Frequency Response Gain Factor, Displacement Damped Servo Accelerometer

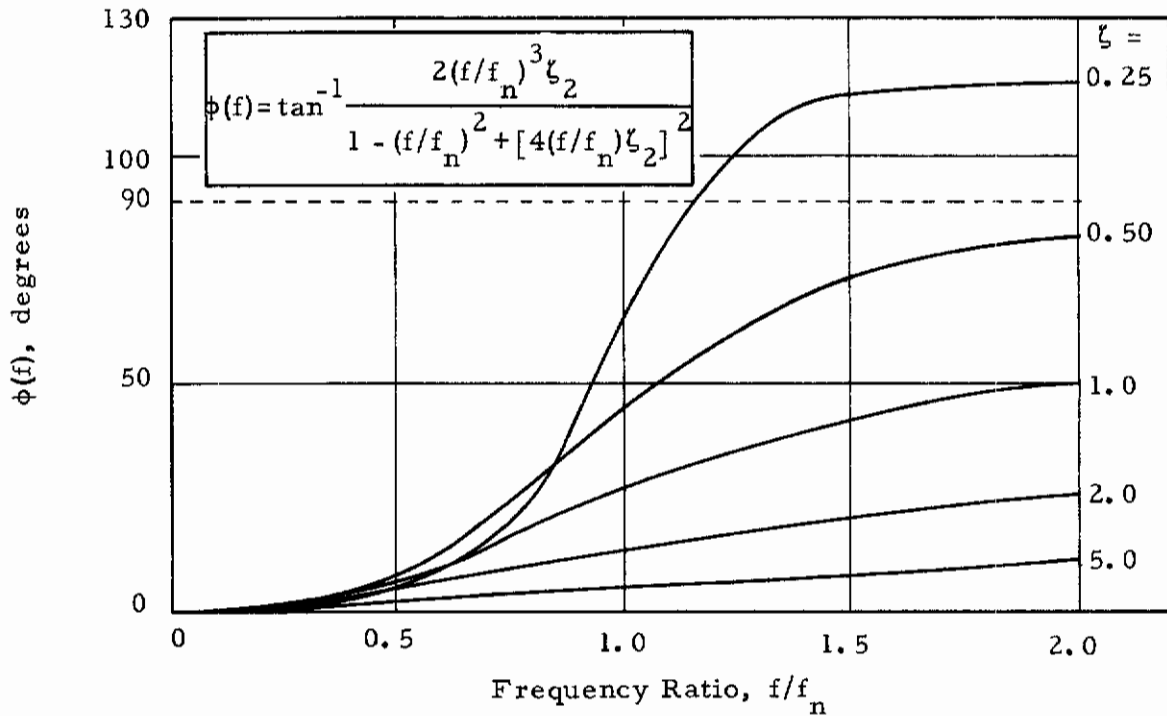


Figure A-8. Frequency Response Phase Lag, Displacement Damped Servo Accelerometer

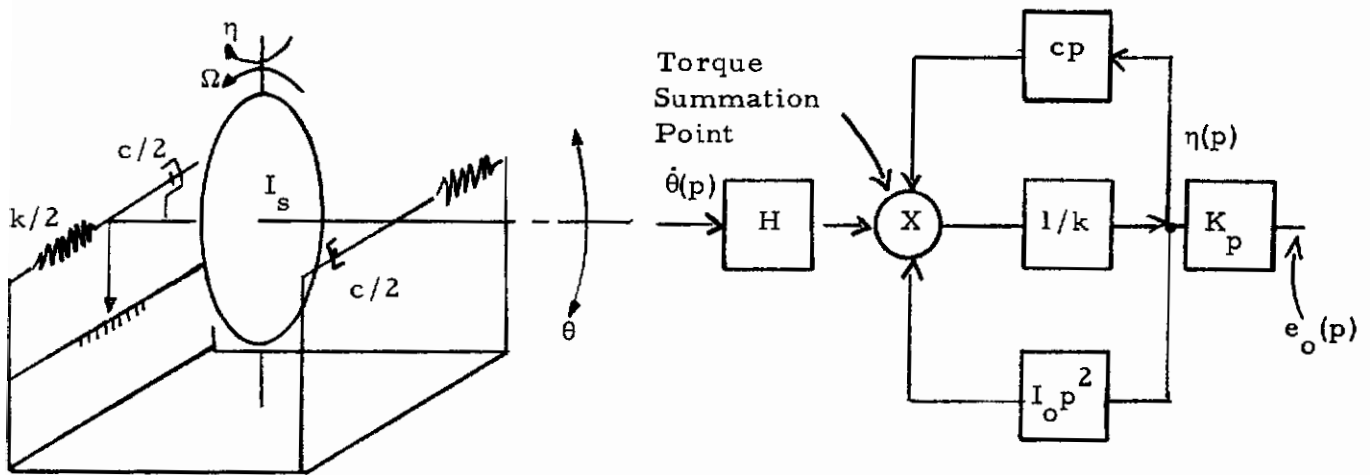


Figure A-9. Schematic and Functional Block Diagram, Rate Gyroscope

$\dot{\theta}(t)$  - input angular rate

$\eta(t)$  - angular displacement, spin axis

$H = I_s \Omega$  - momentum of gyro wheel

$\Omega$  - angular velocity, gyro wheel

$I_o$  - moment of inertia, output axis

$k$  - spring constant

$c$  - coefficient of viscous damping

$K_p$  - pickoff transfer function

$e_o(t)$  - output

The rotor absolute displacement,  $\lambda$ , and relative displacement,  $\eta$ , are essentially identical. The rotor and case have the same velocity if the case rotates about the output axis.

The angular displacement of the gyro spin axis about the output axis is equivalent to the relative displacement.

The equation of motion is therefore given by

$$I_o \ddot{\eta}(t) + c \dot{\eta}(t) + k\eta(t) = -H\dot{\theta}(t) \quad (A18)$$

The Laplacé transform of this equation is

$$H\dot{\theta}(p) + I_o \eta(p) p^2 + c\eta(p) p + k\eta(p) = 0 \quad (A19)$$

The functional block diagram, Figure A-9, is a representation of this equation.

Noting that this expression is identical in form to that for the open loop accelerometer (Eq. A3), the frequency response function relating input angular rate and output voltage may be written directly.

$$H_{\dot{\theta}-e_o}(f) = \frac{I_s \Omega K_p}{I_o (2\pi f_n)^2} \frac{1}{\sqrt{\left[1 - \frac{f^2}{f_n^2}\right]^2 + \left[2\zeta \frac{f}{f_n}\right]^2}} e^{-j\phi(f)} \quad (A20)$$

$$\phi(f) = \tan^{-1} \frac{2\zeta \frac{f}{f_n}}{1 - \left(\frac{f}{f_n}\right)^2} \quad (A21)$$

where

$$f_n = \frac{1}{2\pi} \sqrt{\frac{k}{I_o}}$$

$$\zeta = \frac{c}{2\sqrt{kI_o}}$$

$H(f)_{r-d}$  = frequency response function angular rate  
to relative output voltage

The frequency response gain factor response, Figure A-2, applies to the rate gyroscope when the ordinate becomes  $|H(f)| (2\pi f_n)^2 I_o / K_p I_s \Omega$ . Note that  $I_o$  is referred to an axis in space and will vary with angular displacement. However, for small angles and the purposes of this development, the analysis is sufficiently accurate.

#### A-4 RATE INTEGRATING GYROSCOPE

The typical rate integrating gyroscope is represented in schematic and functional block diagram in Figure A-10.

The equation of motion for a rate integrating gyroscope is essentially identical with that of the rate gyroscope, Eq. (A18), except that the spring restraint is reduced to approximately zero. Therefore, Eq. (A18) becomes

$$I_o \ddot{\eta}(t) + c \dot{\eta}(t) = -H(\dot{\theta}) \tag{A22}$$

The Laplace transform

$$I_o \eta(p)p^2 + c\eta(p)p = -H\dot{\theta}(p) = -H\theta(p)p$$

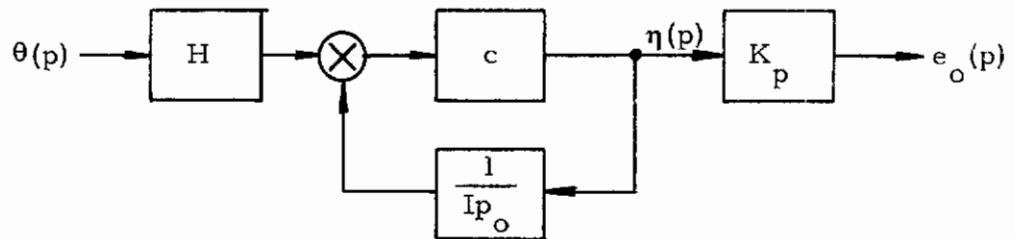
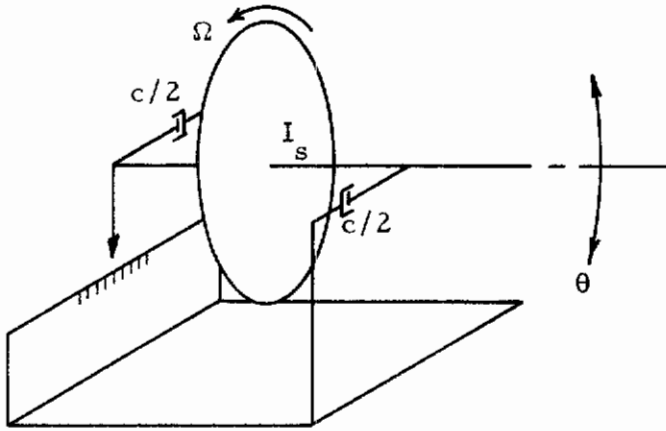


Figure A-10. Schematic and Functional Block Diagram, Rate Integrating Gyroscope

$\theta(t)$  = input angular displacement, radians

$\gamma(t)$  = angular displacement of gyro spin axis, radians

$\eta(t)$  =  $\gamma(t) - \theta(t)$  - relative angular displacement, gyro spin axis and case, radians

$H$  = momentum of gyro wheel, foot-pound-second/radian

$c$  = coefficient of viscous damping, inch-pound-second/radian



or

$$I_o \eta(p)p + c \eta(p) = -H\theta(p) \quad (A23)$$

The functional block diagram, Figure A-10, is a representation of this equation. The Laplace transform of the transfer function

$$\frac{\eta(p)}{\theta(p)} = \frac{H}{I_o p + c} \quad (A24)$$

Substituting  $p = j2\pi f$  and putting in polar coordinates,

$$H_{\theta-e_o} = \frac{K_p H}{c} \frac{1}{\sqrt{1 + \left(\frac{2\pi f I_o}{c}\right)^2}} e^{-j\phi(f)} \quad (A25)$$

$$\phi = \tan^{-1} 2\pi f I_o / c \quad (A26)$$

This is the frequency response of a first-order single degree-of-freedom system. The frequency response of output voltage to input angular displacement may be obtained by multiplying by the pickoff transfer function,  $K_p$ . These frequency response functions are presented in Figures A-11 and A-12.

## A-5. MOVEABLE VANE SENSORS

The moveable vane sensor, at first impression, appears identical in form to an open loop accelerometer or rate gyroscope. However, closer examination (Reference 25) shows that the spring is between the forcing function (angle of attack) and the vane instead of between the vane and the aircraft (see Figure A-13).

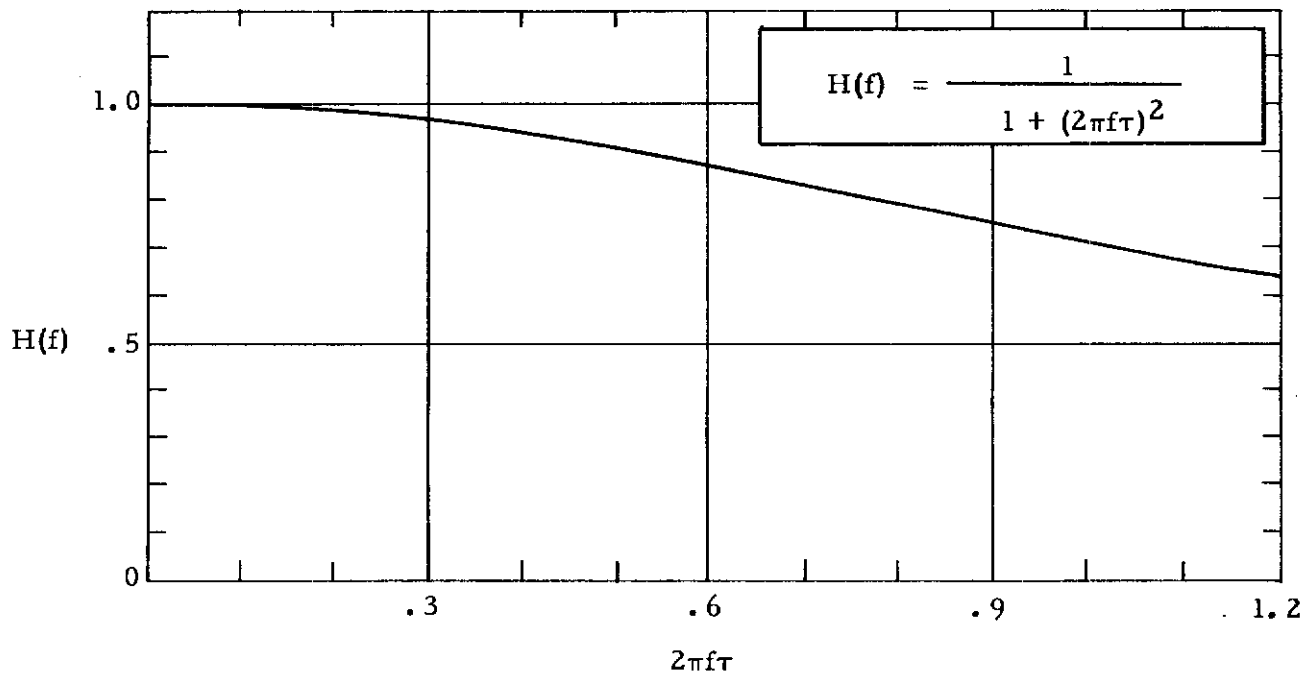


Figure A-11. Frequency Response Gain Factor, Rate Integrating Gyroscopes

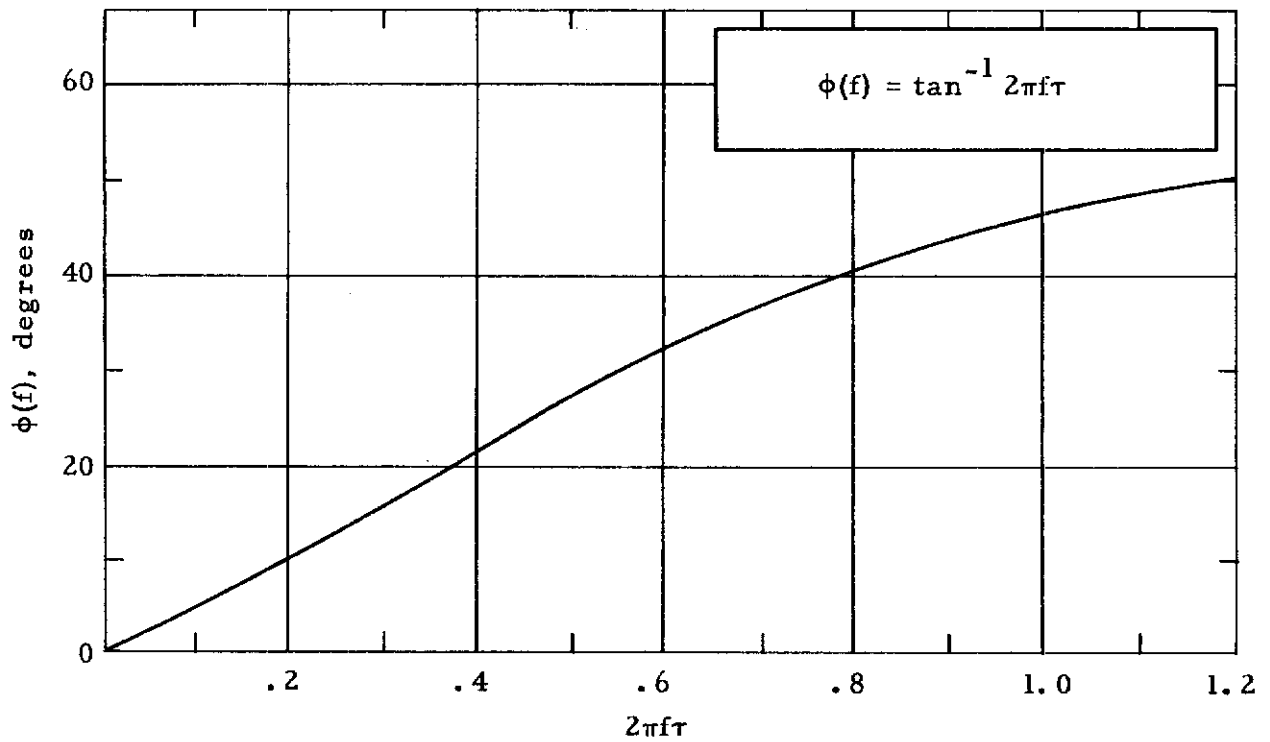


Figure A-12. Frequency Response Phase Lag Rate Integrating Gyroscopes

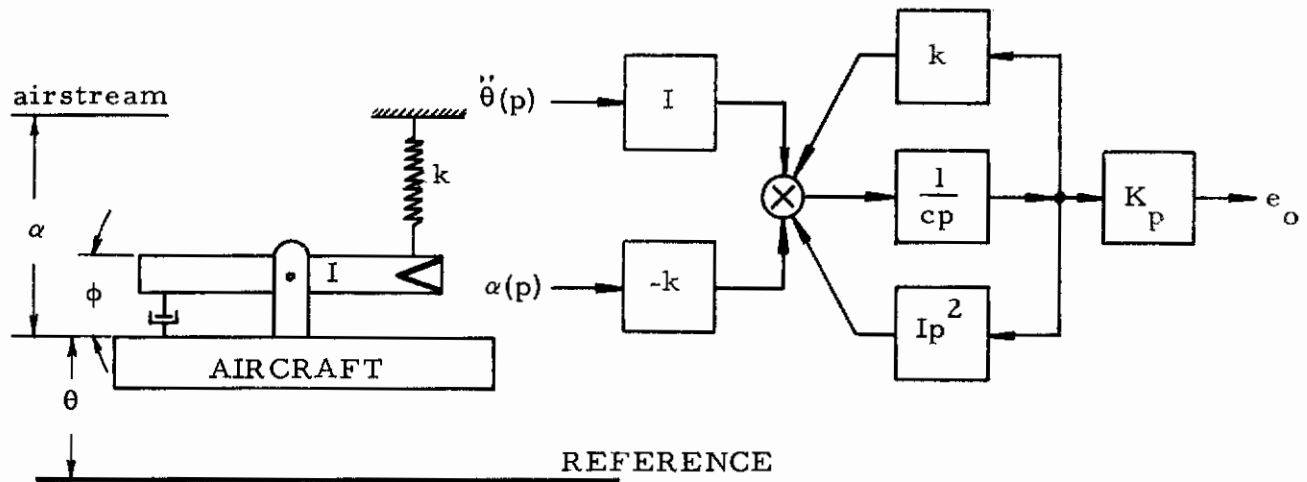


Figure A-13. Schematic and Functional Block Diagram, Moveable Vane Sensor

- where
- $\alpha$  - angle of attack, radians
  - $\phi$  - relative displacement of vane, radians
  - $c$  - damping coefficient inches-pounds-seconds/radians
  - $I$  - moment of inertia, slug feet<sup>2</sup>
  - $k$  - effective spring constant, airstream to vane, inches-pounds/radian

The torques are as follows:

$$\begin{aligned} \text{Inertia torque} &= -I[\ddot{\phi}(t) + \ddot{\theta}(t)] \\ \text{Damping torque} &= -c\dot{\phi}(t) \\ \text{Input torque} &= k[\alpha(t) - \phi(t)] \end{aligned}$$

The equation of motion is

$$\begin{aligned} -I[\ddot{\phi}(t) + \ddot{\theta}(t)] + k[\alpha(t) - \phi(t)] - c\dot{\phi} &= 0 \\ I\ddot{\phi}(t) + c\dot{\phi}(t) + k\phi(t) &= -I\ddot{\theta}(t) + k\alpha(t) \end{aligned}$$

If the aircraft attitude is zero, the angle of attack is produced entirely by vertical air velocity, and the frequency response function is

$$H(f)_{\alpha-e_o} = K_p \frac{1}{\sqrt{\left[1 - \left(\frac{f}{f_n}\right)^2\right]^2 + \left[2\zeta \frac{f}{f_n}\right]^2}} e^{-j\phi(f)} \quad (A27)$$

where  $K_p$  - pickoff transfer function, volts/radian

$$f_n = \frac{1}{2\pi} \sqrt{k/I}$$

$$\zeta = c/2 \sqrt{km}$$

When normalized, this is identical to the frequency response function for open loop accelerometers and rate gyroscopes (see Figures A-2, A-3, and A-4). Note that the sensitivity is not a linear function of the natural frequency as with accelerometers. However, if the angle of attack is generated by aircraft attitude variation,  $\theta(t) = \alpha(t)$  and the result of Reference 25 is obtained.

$$H(f)_{\alpha-e_o} = K_p \frac{1 - \left(\frac{f}{f_n}\right)^2}{\sqrt{\left[1 - \left(\frac{f}{f_n}\right)^2\right]^2 + \left[2\zeta \frac{f}{f_n}\right]^2}} e^{-j\phi(f)} \quad (A28)$$

$$\phi(f) = \tan^{-1} \frac{2\zeta \frac{f}{f_n}}{1 - \left(\frac{f}{f_n}\right)^2}$$

The gain factor is presented in Figure A-14.

$$H(f)_{\text{norm}} = \frac{1}{K_p} \frac{H(f)}{p} = \frac{1 - (f/f_n)^2}{\sqrt{[1 - (f/f_n)^2]^2 + [2\zeta(f/f_n)]^2}}$$

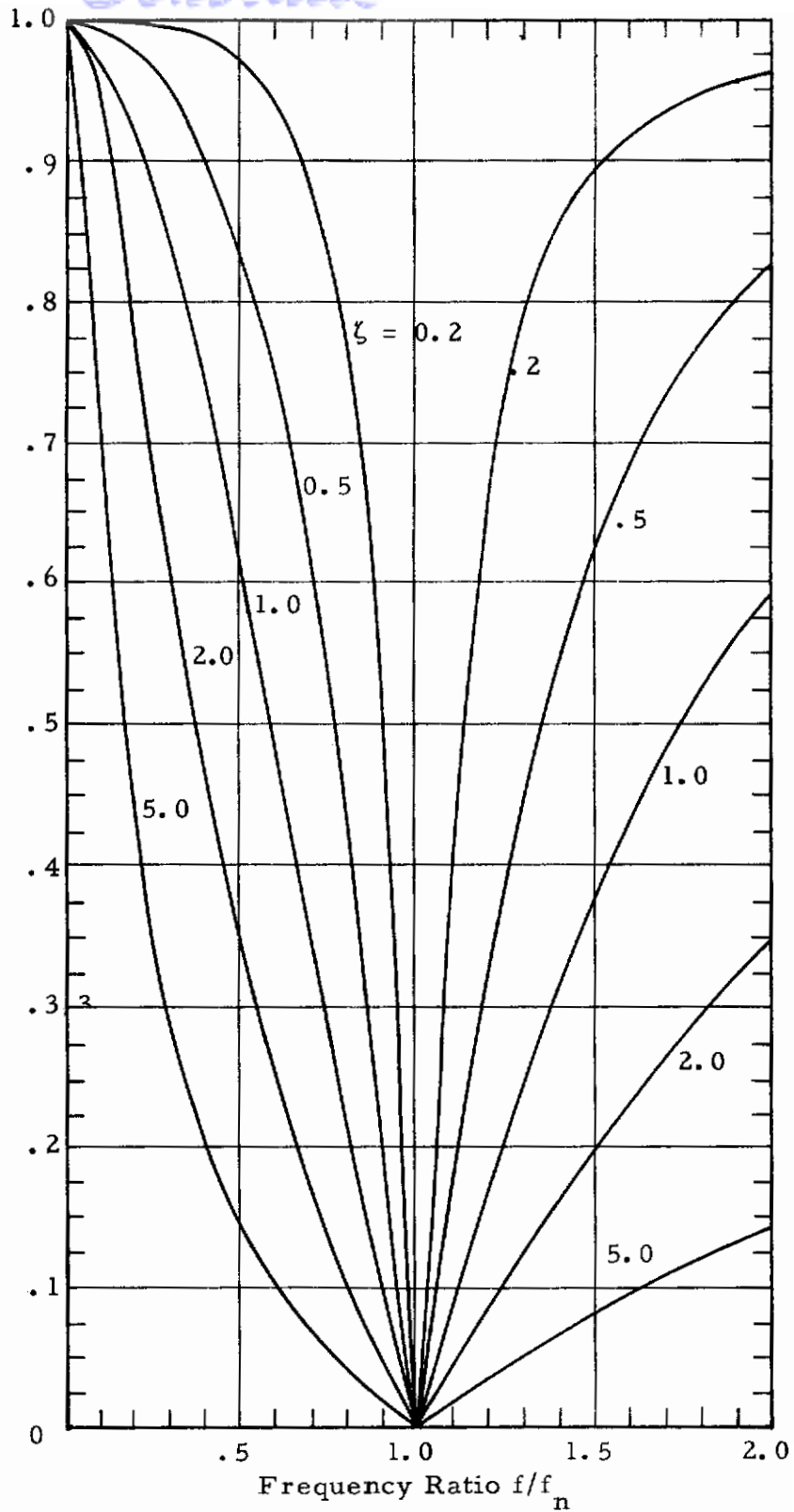


Figure A-14. Frequency Response Gain Factor, Moveable Vane, Excitation from Aircraft Motion Only

# *Contrails*

Unclassified

Security Classification

DOCUMENT CONTROL DATA - R&D		
(Security classification of title, body of abstract and indexing annotation must be entered when the overall report is classified)		
<b>1. ORIGINATING ACTIVITY (Corporate author)</b> Measurement Analysis Corporation 10960 Santa Monica Boulevard Los Angeles, California 90025	<b>2a. REPORT SECURITY CLASSIFICATION</b> Unclassified	
	<b>2b. GROUP</b> N/A	
<b>3. REPORT TITLE</b> EVALUATION AND UTILIZATION OF AIRPLANE FLIGHT LOADS DATA PART II. DATA ACQUISITION EQUIPMENT PERFORMANCE AND ACCURACY		
<b>4. DESCRIPTIVE NOTES (Type of report and inclusive dates)</b> Final Report: August 1966 to October 1967		
<b>5. AUTHOR(S) (Last name, first name, initial)</b> Rentz, Peter E.		
<b>6. REPORT DATE</b> May 1968	<b>7a. TOTAL NO. OF PAGES</b> 221	<b>7b. NO. OF REFS</b> 92
<b>8a. CONTRACT OR GRANT NO.</b> AF33(615)-67-C-1033 <b>b. PROJECT NO.</b> 1367 <b>c. Task No.</b> 136716 <b>d.</b>	<b>9a. ORIGINATOR'S REPORT NUMBER(S)</b> AFFDL-TR-68-52, Part II <b>9b. OTHER REPORT NO(S) (Any other numbers that may be assigned this report)</b> MAC 610-01B	
<b>10. AVAILABILITY/LIMITATION NOTICES</b> This document is subject to special export controls and each transmittal to foreign governments or foreign nationals may be made only with prior approval of the Air Force Flight Dynamics Laboratory, FDTR, Wright-Patterson AFB, Ohio 45433.		
<b>11. SUPPLEMENTARY NOTES</b> None	<b>12. SPONSORING MILITARY ACTIVITY</b> Air Force Flight Dynamics Laboratory (FDTR), Wright-Patterson AFB, Ohio	
<b>13. ABSTRACT</b> <p style="text-align: justify;">                             This report discusses the principles of operation and the various machine errors of airborne flight loads measuring equipment. The categories of equipment covered are angle of attack sensors, gyroscopes, accelerometers, strain gages, pressure transducers, signal conditioning equipment, and magnetic tape recorders. Machine errors are classified as being either intrinsic, environmentally induced, or attributable to usage or application. The errors are further classified in accordance with their effect on the measured data. The principles of operation and errors are expressed either with mathematical formulae or by indicating the state-of-the-art performance. Methods for minimizing both the errors and the effect of the errors are indicated.                         </p>		

DD FORM 1473  
1 JAN 64

Unclassified

Security Classification



Unclassified

Security Classification

14.	KEY WORDS	LINK A		LINK B		LINK C	
		ROLE	WT	ROLE	WT	ROLE	WT
	Transducers Recorders Flight Loads Measuring Apparatus						

**INSTRUCTIONS**

1. **ORIGINATING ACTIVITY:** Enter the name and address of the contractor, subcontractor, grantee, Department of Defense activity or other organization (*corporate author*) issuing the report.
- 2a. **REPORT SECURITY CLASSIFICATION:** Enter the overall security classification of the report. Indicate whether "Restricted Data" is included. Marking is to be in accordance with appropriate security regulations.
- 2b. **GROUP:** Automatic downgrading is specified in DoD Directive 5200.10 and Armed Forces Industrial Manual. Enter the group number. Also, when applicable, show that optional markings have been used for Group 3 and Group 4 as authorized.
3. **REPORT TITLE:** Enter the complete report title in all capital letters. Titles in all cases should be unclassified. If a meaningful title cannot be selected without classification, show title classification in all capitals in parenthesis immediately following the title.
4. **DESCRIPTIVE NOTES:** If appropriate, enter the type of report, e.g., interim, progress, summary, annual, or final. Give the inclusive dates when a specific reporting period is covered.
5. **AUTHOR(S):** Enter the name(s) of author(s) as shown on or in the report. Enter last name, first name, middle initial. If military, show rank and branch of service. The name of the principal author is an absolute minimum requirement.
6. **REPORT DATE:** Enter the date of the report as day, month, year, or month, year. If more than one date appears on the report, use date of publication.
- 7a. **TOTAL NUMBER OF PAGES:** The total page count should follow normal pagination procedures; i.e., enter the number of pages containing information.
- 7b. **NUMBER OF REFERENCES:** Enter the total number of references cited in the report.
- 8a. **CONTRACT OR GRANT NUMBER:** If appropriate, enter the applicable number of the contract or grant under which the report was written.
- 8b, 8c, & 8d. **PROJECT NUMBER:** Enter the appropriate military department identification, such as project number, subproject number, system numbers, task number, etc.
- 9a. **ORIGINATOR'S REPORT NUMBER(S):** Enter the official report number by which the document will be identified and controlled by the originating activity. This number must be unique to this report.
- 9b. **OTHER REPORT NUMBER(S):** If the report has been assigned any other report numbers (*either by the originator or by the sponsor*), also enter this number(s).
10. **AVAILABILITY/LIMITATION NOTICES:** Enter any limitations on further dissemination of the report, other than those

imposed by security classification, using standard statements such as:

- (1) "Qualified requesters may obtain copies of this report from DDC."
- (2) "Foreign announcement and dissemination of this report by DDC is not authorized."
- (3) "U. S. Government agencies may obtain copies of this report directly from DDC. Other qualified DDC users shall request through \_\_\_\_\_."
- (4) "U. S. military agencies may obtain copies of this report directly from DDC. Other qualified users shall request through \_\_\_\_\_."
- (5) "All distribution of this report is controlled. Qualified DDC users shall request through \_\_\_\_\_."

If the report has been furnished to the Office of Technical Services, Department of Commerce, for sale to the public, indicate this fact and enter the price, if known.

11. **SUPPLEMENTARY NOTES:** Use for additional explanatory notes.
12. **SPONSORING MILITARY ACTIVITY:** Enter the name of the departmental project office or laboratory sponsoring (*paying for*) the research and development. Include address.
13. **ABSTRACT:** Enter an abstract giving a brief and factual summary of the document indicative of the report, even though it may also appear elsewhere in the body of the technical report. If additional space is required, a continuation sheet shall be attached.

It is highly desirable that the abstract of classified reports be unclassified. Each paragraph of the abstract shall end with an indication of the military security classification of the information in the paragraph, represented as (TS), (S), (C), or (U).

There is no limitation on the length of the abstract. However, the suggested length is from 150 to 225 words.

14. **KEY WORDS:** Key words are technically meaningful terms or short phrases that characterize a report and may be used as index entries for cataloging the report. Key words must be selected so that no security classification is required. Identifiers, such as equipment model designation, trade name, military project code name, geographic location, may be used as key words but will be followed by an indication of technical context. The assignment of links, rules, and weights is optional.

Unclassified

Security Classification